Exploration of Quark Matter and QCD Phases at Collider Energies

- introduction and perspective
- The quark-gluon plasma and Lattice QCD
- The ALICE experiment: historical remarks
- A brief synopsis of very selected results
- Hadron production and the QCD phase boundary
- Charmonia and deconfinement
- Outlook

53rd Int. Winter Meeting on Nuclear Physics
Bormio, Italy
Jan. 27, 2015

Peter Braun-Munzinger

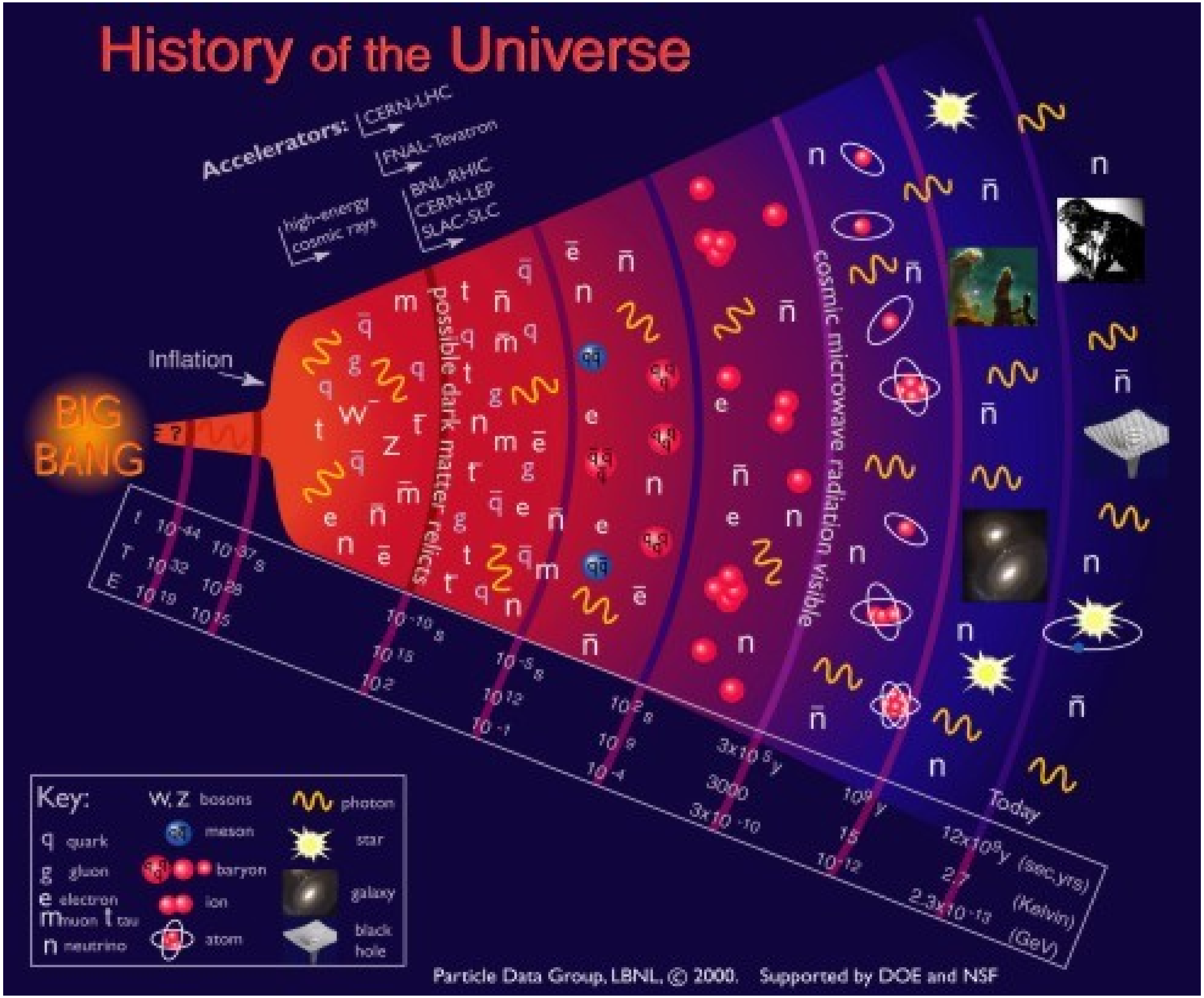
History of the Universe
Accelerators:
CERN-LHC
FNAL-Tevatron
BNL-RHIC
CERN-LEP
SLAC-SLC
high-energy cosmic rays
Inflation
BIG BANG
possible dark matter relics
cosmic microwave radiation visible
t 10-44 10-37 s
T 1032 1028
E 1019 1015
10-10 s
1015
102
10-5 s
1012
10-1
102 s
109
10-4
3x105 y
3000
3x10-10
109 y
15
10-12
Today
12x109 y (sec,yrs)
2.7 (Kelvin)
2.3x10-13 (GeV)
Key:
q quark
g gluon
e electron
m muon t tau
n neutrino
W, Z bosons
meson
baryon
ion
atom
photon
star
galaxy
black hole
Particle Data Group, LBNL, © 2000. Supported by DOE and NSF

The phase diagram of quantum chromodynamics

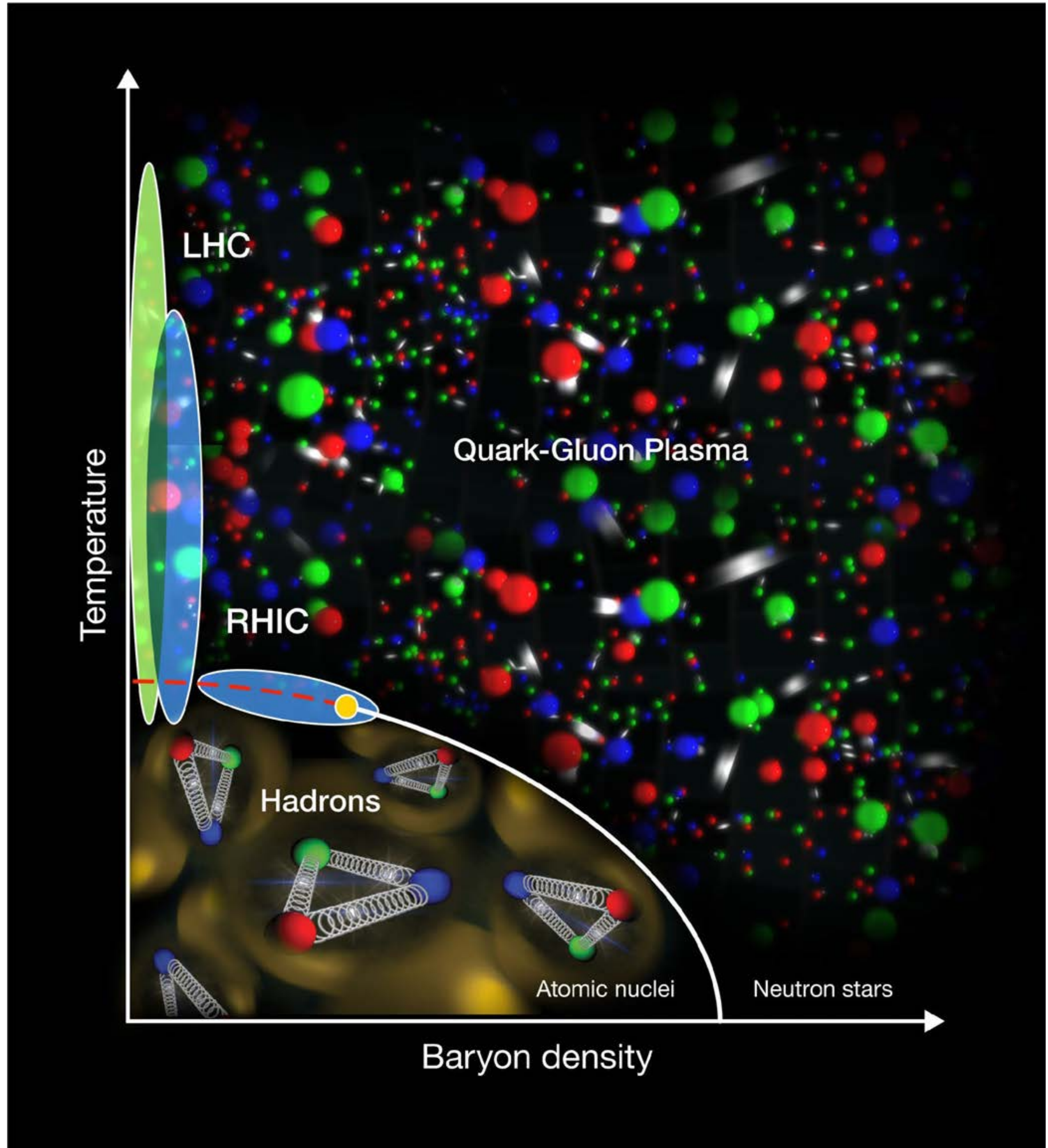

The equation of state of hot QCD matter – a chiral (cross over) phase transition between hadron gas and the QGP

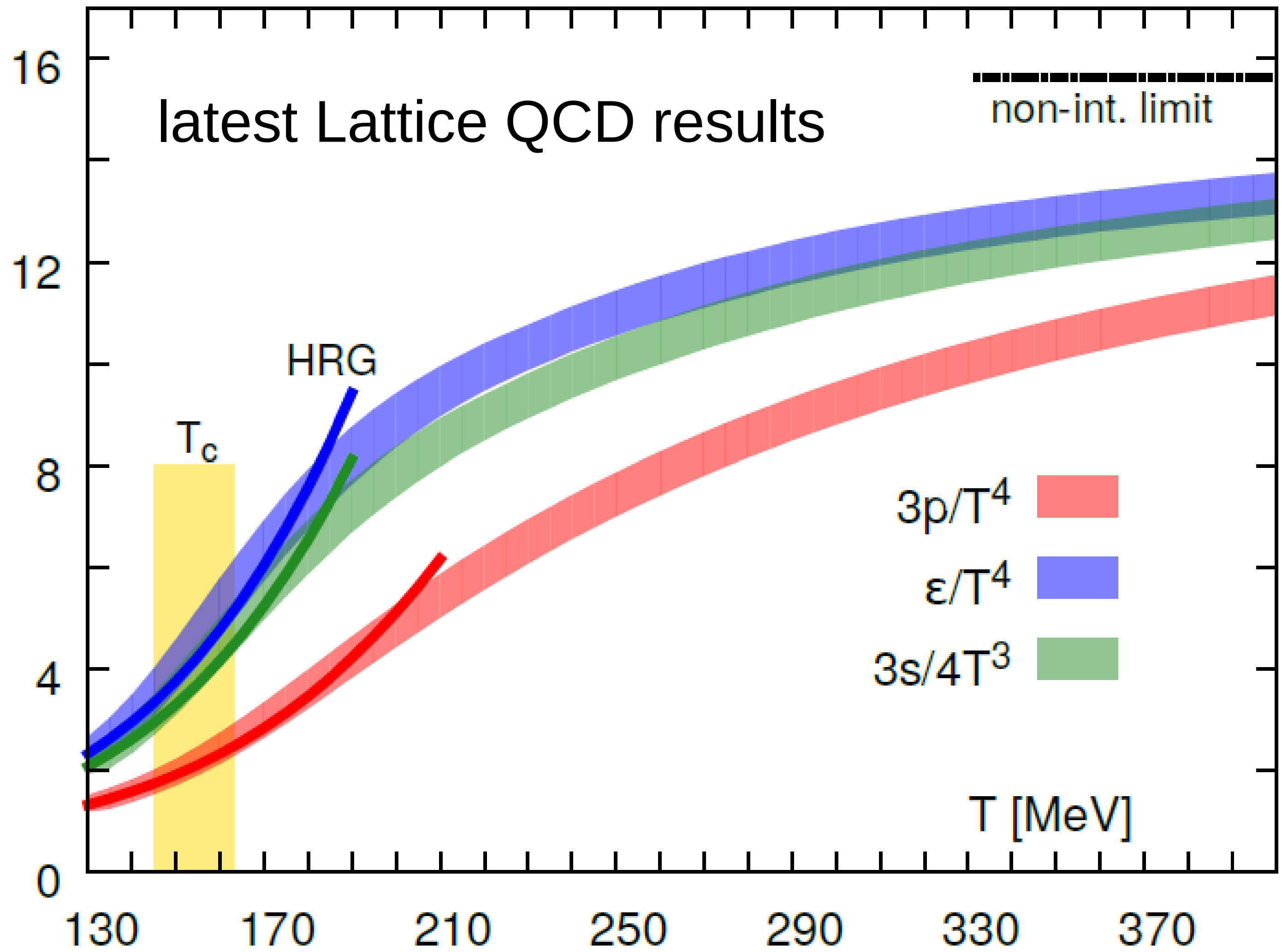

critical region: T_c = (154 ± 9) MeV ε_{crit} = (340 ± 45) MeV/fm^3

HOTQCD coll., Phys.Rev. D90 (2014) 9, 094503

Evolution of the Early Universe and the QCD phase Diagram

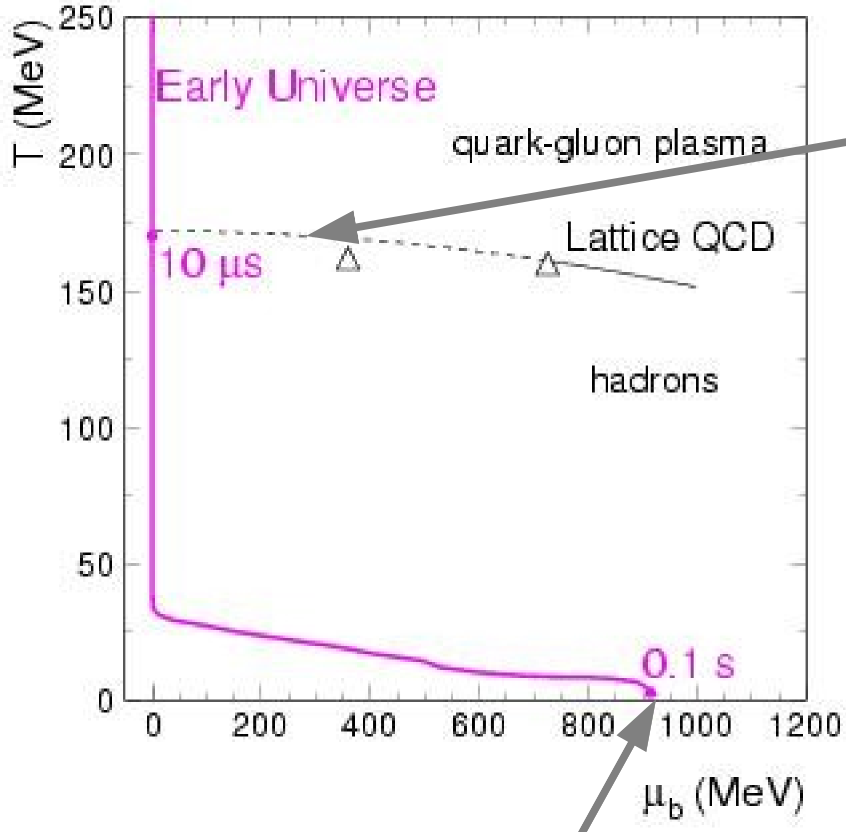

QCD Phase Boundary

Homogeneous Universe in Equilibrium, this matter can only be investigated in nuclear collisions

- Charge neutrality
- Net lepton number = net baryon number
- Constant entropy/baryon

neutrinos decouple and light nuclei begin to be formed

The Quark-Gluon Plasma formed in Nuclear Collisions at very high Energy

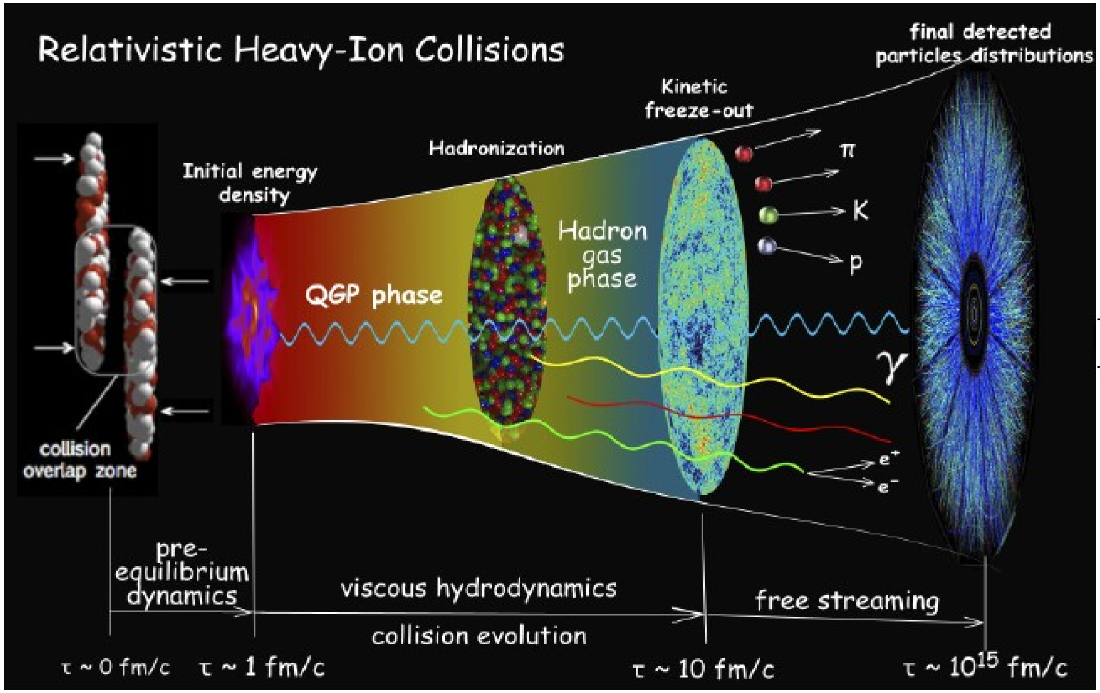

Paul Sorensen and Chun Shen

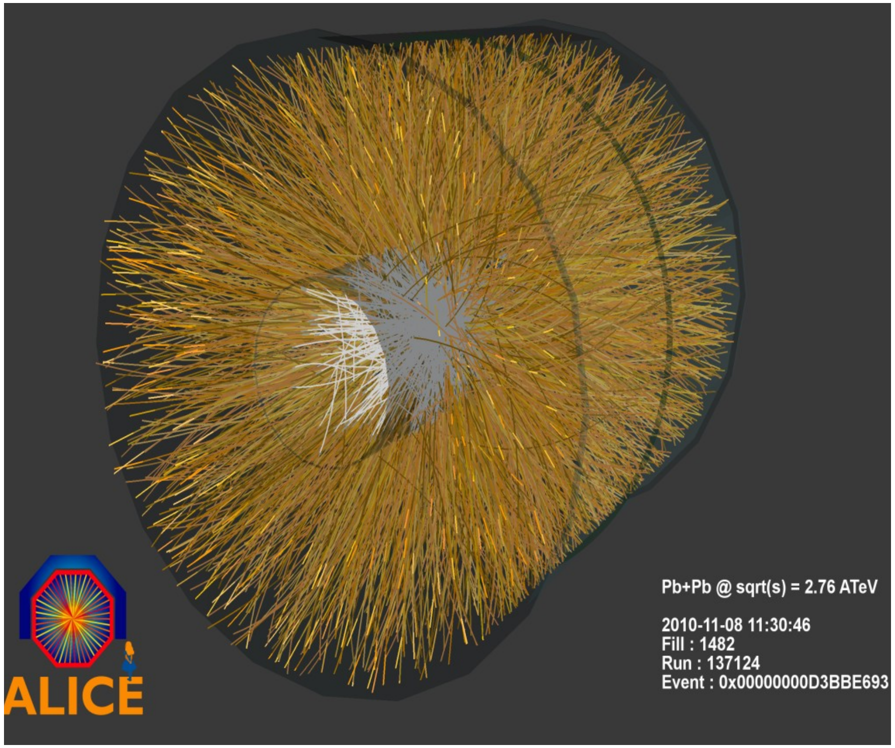

How to create QGP in the laboratory?

Compression,
Expansion and
freeze-out

1

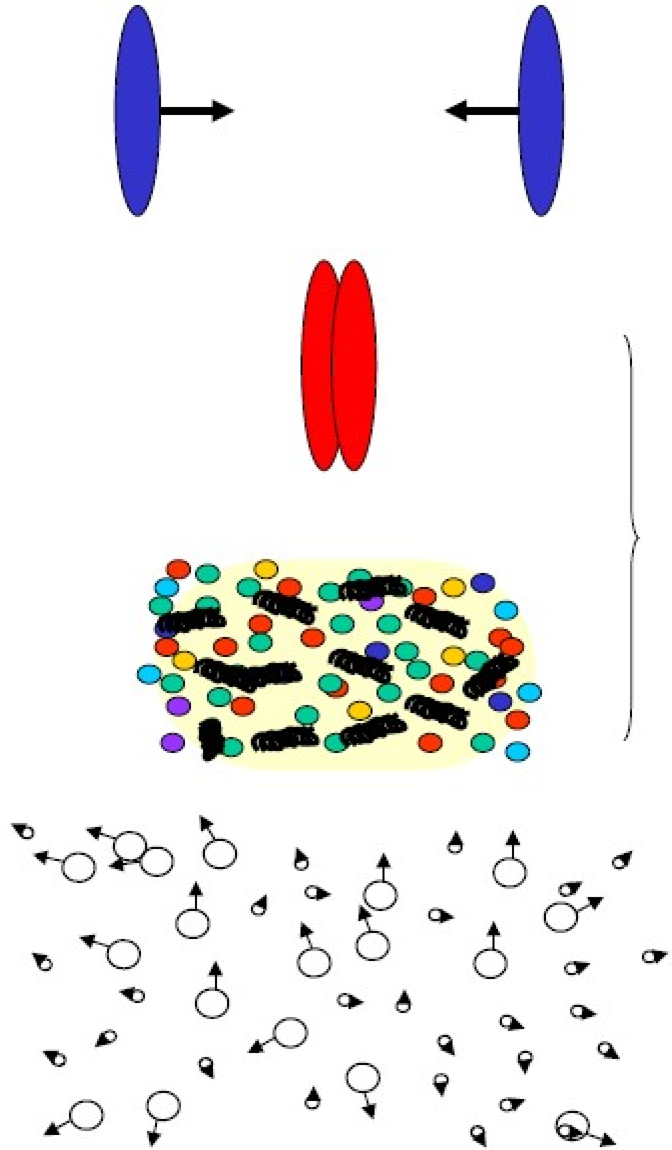

Normal nuclear matter
$\rho_0 = 0.17\ /\mathrm{fm}^3$
$\varepsilon_0 = 0.16\ \mathrm{GeV/fm}^3$

Quark-Gluon Matter
Quark-Gluon Plasma

QGP reached
$\rho = 1.2\ /\mathrm{fm}^3$
$\varepsilon = 3\ \mathrm{GeV/fm}^3$

Free streaming particles

Time

The Large Hadron Collider (LHC)

27 km long, 8 sectors

1232 **dipole** magnets (15m, 30 tonnes each) to bend the beams

Cooled with **120 tonnes of He at 1.9 K**

pp: 2808 bunches/ring, each 1.15×10^{11} protons (8 min filling time)

Design luminosity: **10^{34} cm^{-2}s^{-1}**

PbPb: 592 bunches/ring, each 7×10^{7} Pb ions

Design luminosity: 10^{27} cm^{-2}s^{-1}

Transverse r.m.s beam size: **16 μm**, r.m.s. bunch length: 7.5 cm

Beam kinetic energy: 362 MJ per beam (1 MJ melts 2 kg copper)

Total stored electromagnetic energy: **8.5 GJ** (dipole magnets only)

The ALICE experiment at the CERN LHC

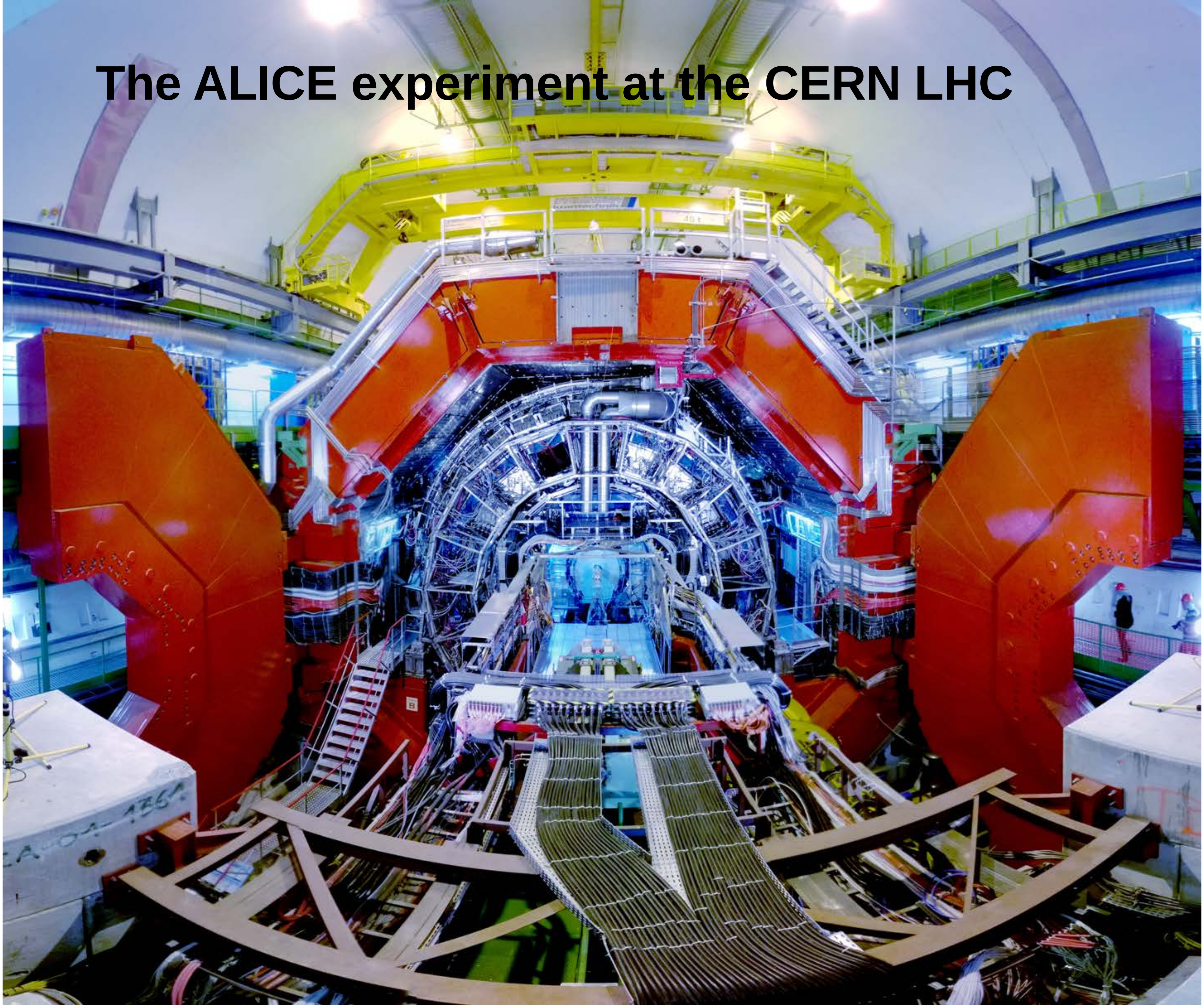

ALICE at the LHC

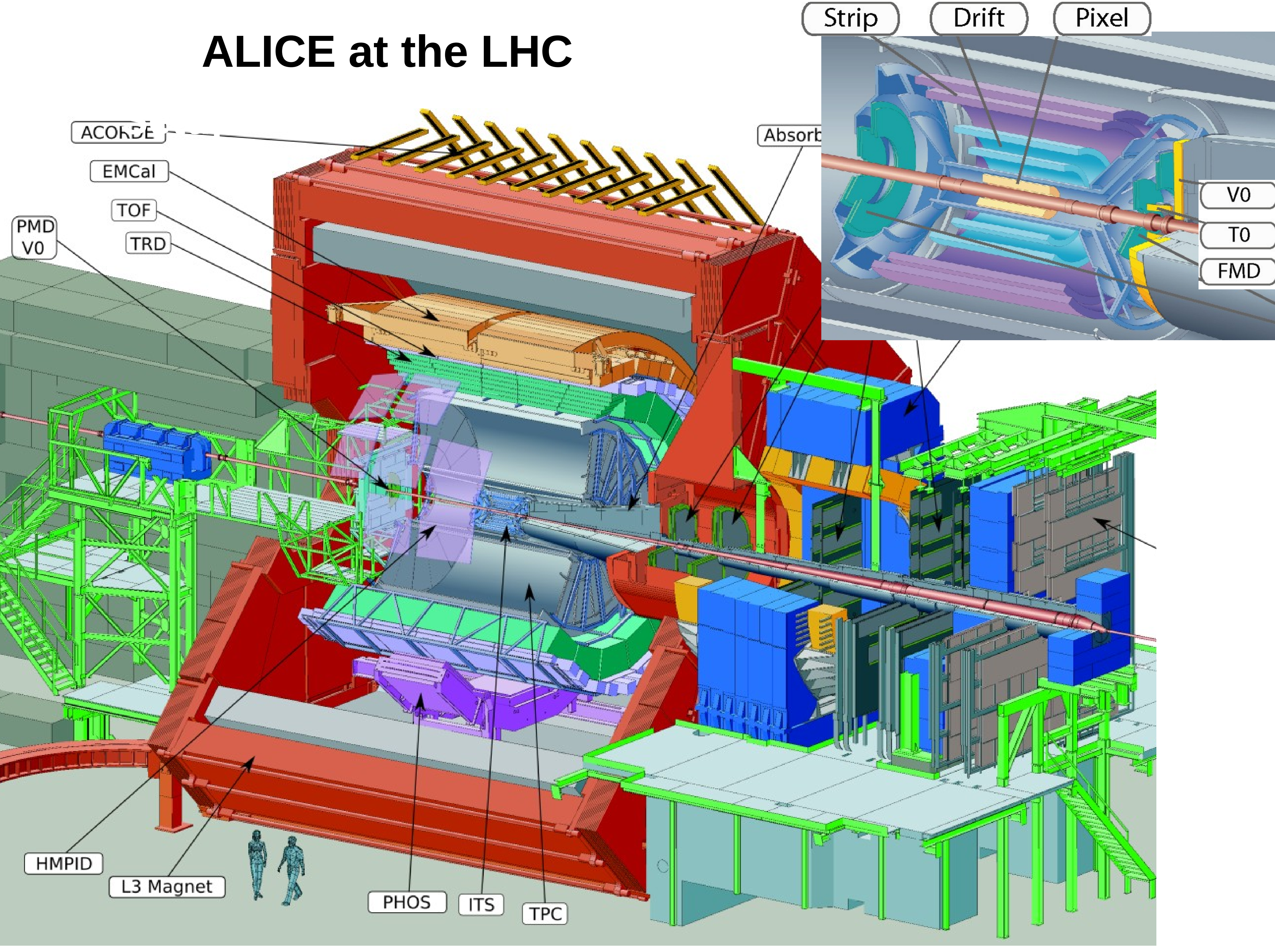

the TPC (Time Projection Chamber) - 3D reconstruction of up to 15 000 tracks of charged particles per event

with 95 m^3 the largest TPC ever

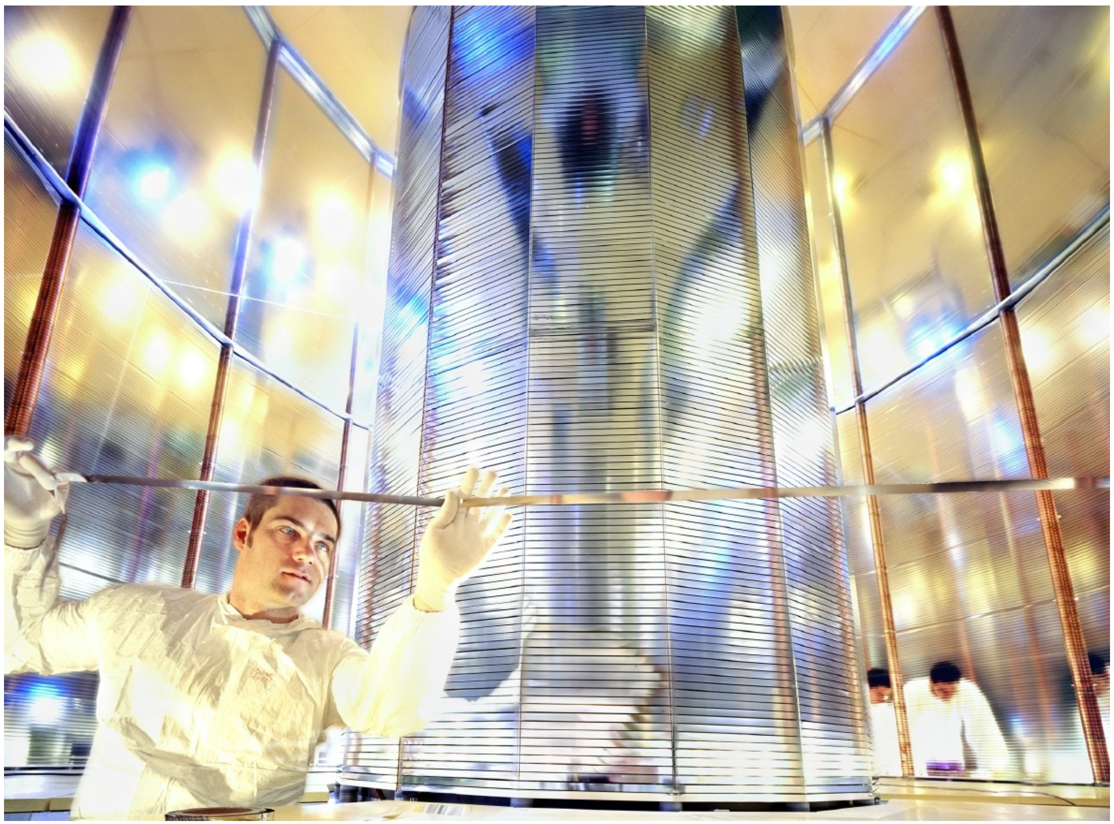

560 million read-out pixels!

precision better than 500 μm in all 3 dim.

180 space and charge points per track

The interior of the TPC, 2004

first PbPb collisions at LHC at √s = 2.76 A TeV

setup for ion collisions: November 4
first collisions with stable beams:
November 8 until Dec 6

Run1: 3 data taking campaigns
pp, pPb, Pb—Pb
> 80 publications

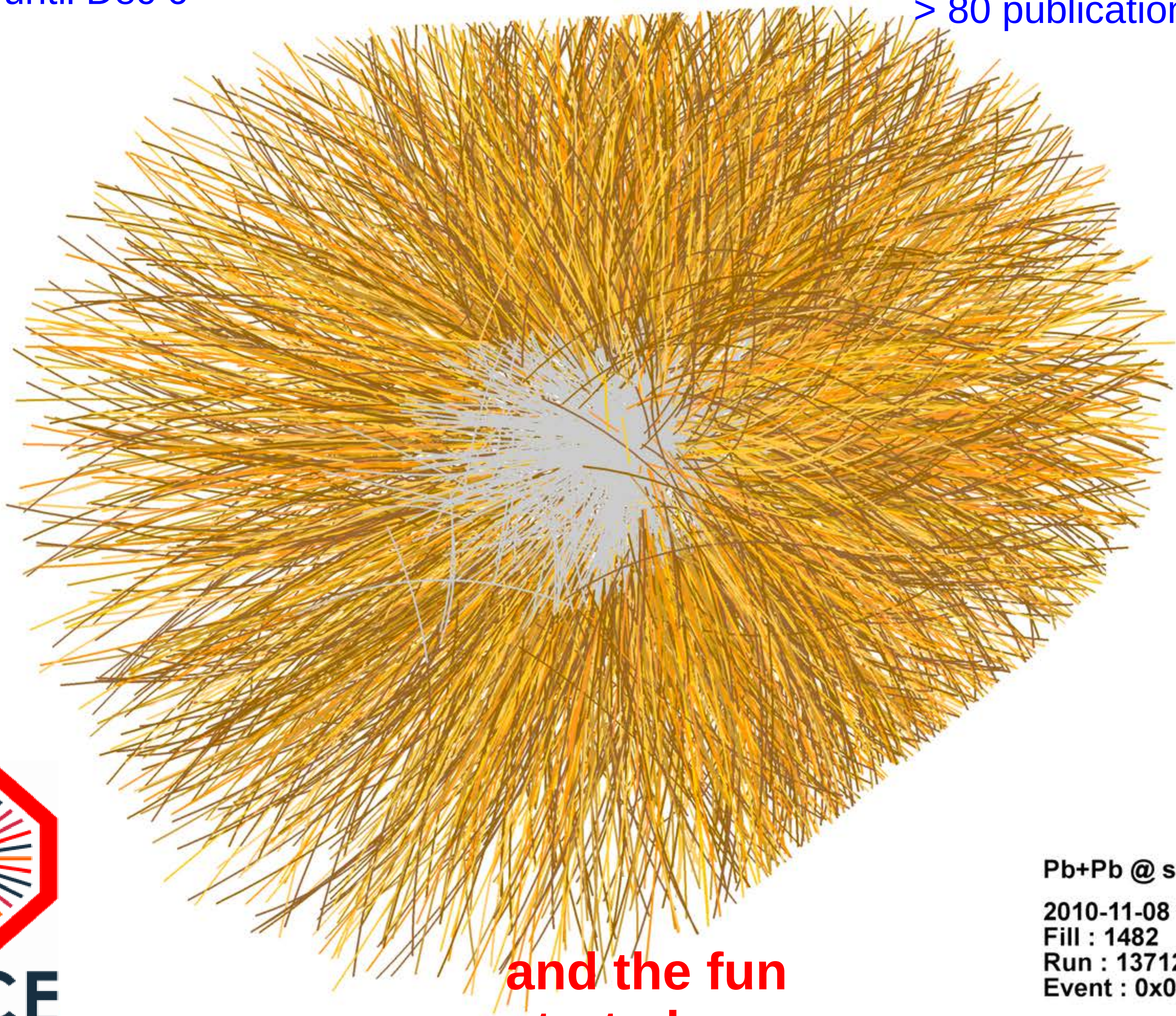

and the fun started

Pb+Pb @ sqrt(s) = 2.76 ATeV
2010-11-08 11:30:46
Fill : 1482
Run : 137124
Event : 0x00000000D3BBE693

ALICE

A synopsis of very selected results

hydrodynamic expansion of fireball

fireball expands collectively like an ideal fluid

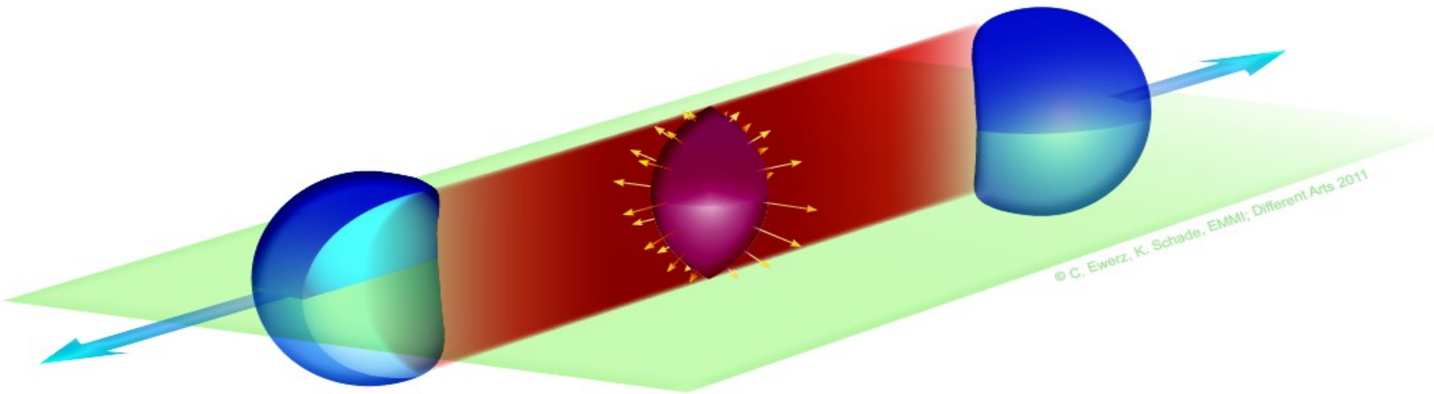

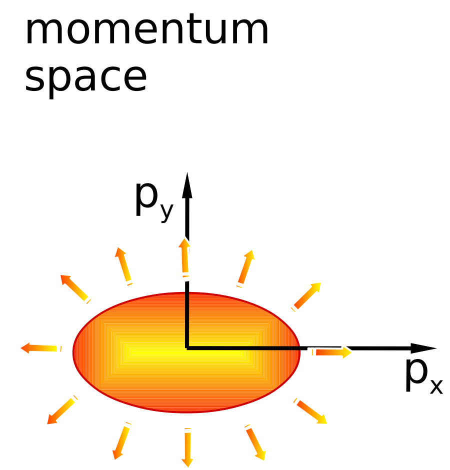

$$dN/d\phi = 1 + 2\,V_2\cos 2\,(\phi - \psi) + \ldots$$

hydrodynamic flow characterized by azimuthal anisotropy coeffient v_2

+ higher orders

Elliptic Flow in PbPb Collisions at $\sqrt{s}_{NN}$ = 2.76 TeV

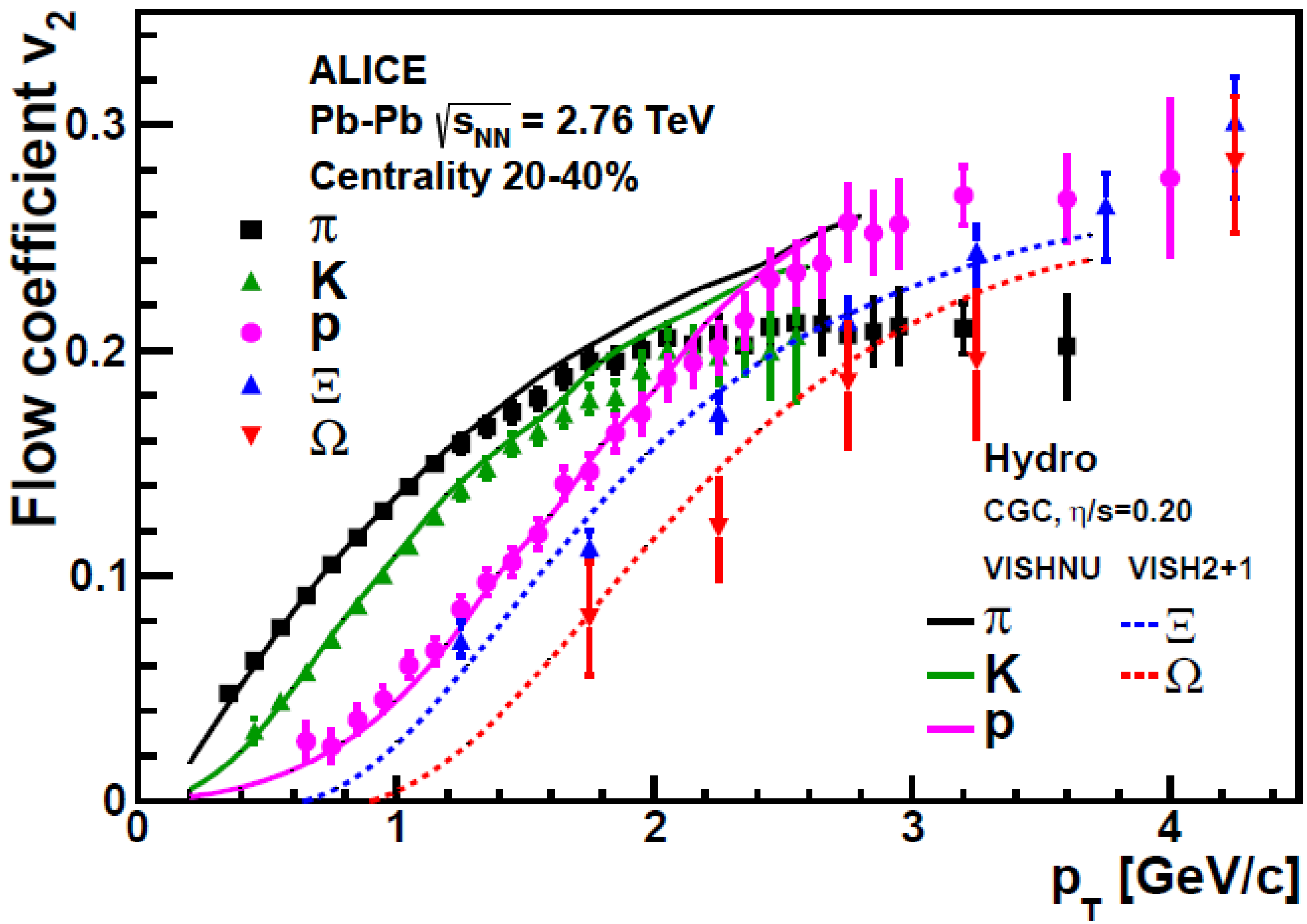

rapidly rising v_2 with p_t and mass ordering are typical features of hydrodyn. expansion

nearly ideal (non-dissipative) hydrodynamics reproduces data, system fairly strongly coupled arXiv:1405.4632 ALICE coll.

phi meson and proton transverse momentum spectra

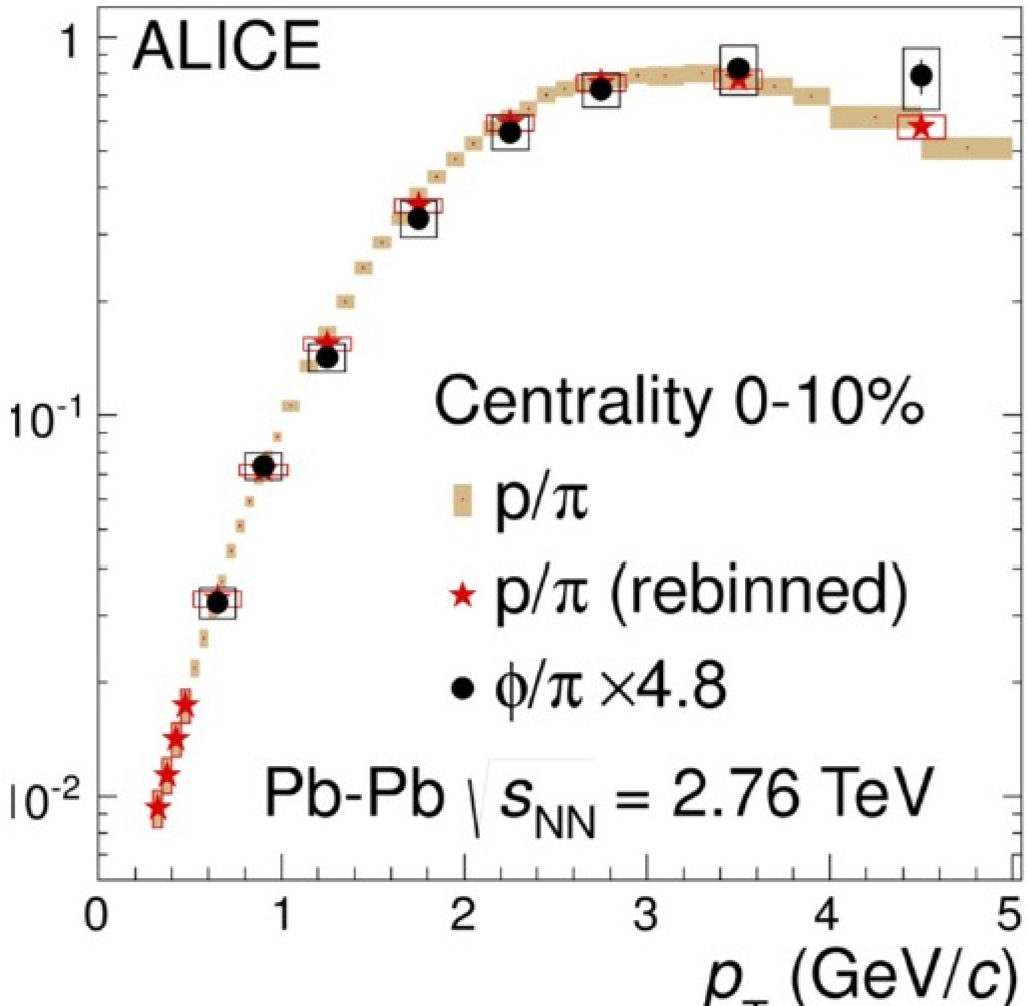

… depend only on particle mass, not quark content. Strong sign of hydrodynamic flow. **Apparent 'constituent quark scaling' is not observed**. Not consistent with hydrodynamic behavior anyway...

Fireball at LHC energy has much large size and lives longer than at lower energies

volume and lifetime
from Hanbury-Brown/Twiss
analysis

fireball volume at freeze-out
is about 5 x larger than
volume of a Pb nucleus

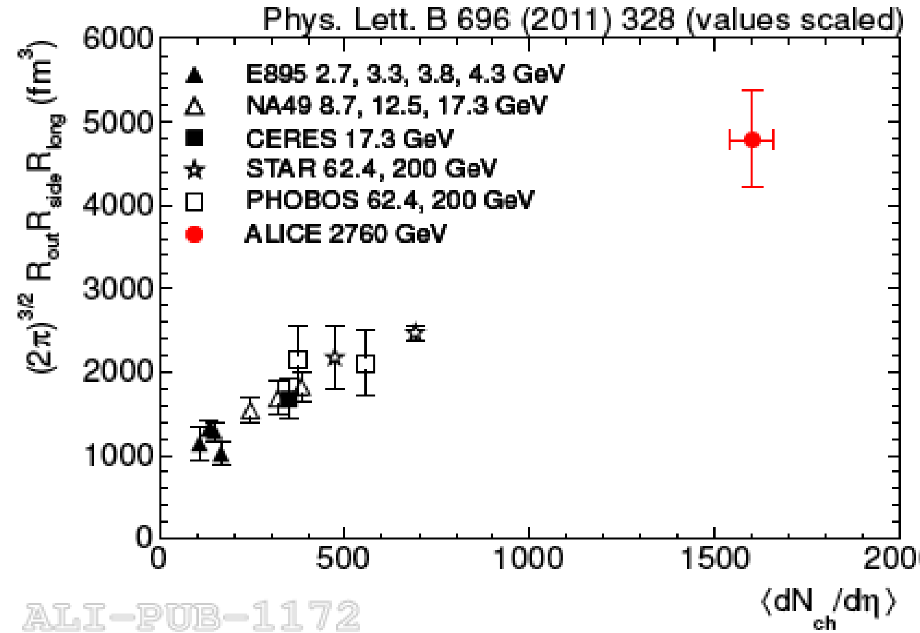

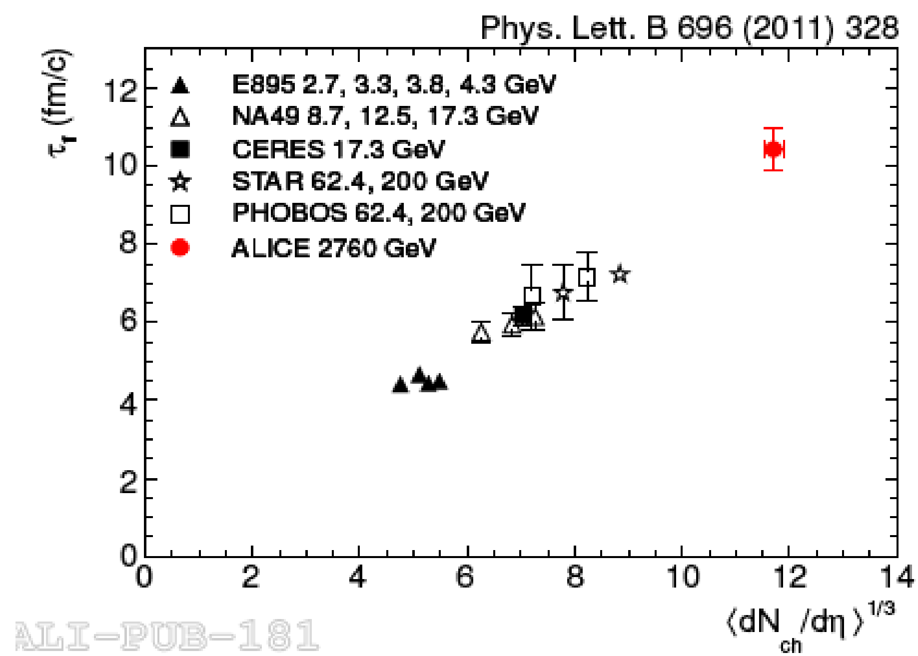

The fireball is opaque to high energy partons (quarks and gluons)

Jets of hard partons as probe of the hot medium

- Hard parton scattering observed via leading particles
- Expect strong $\Delta\varphi=\pi$ azimuthal correlations

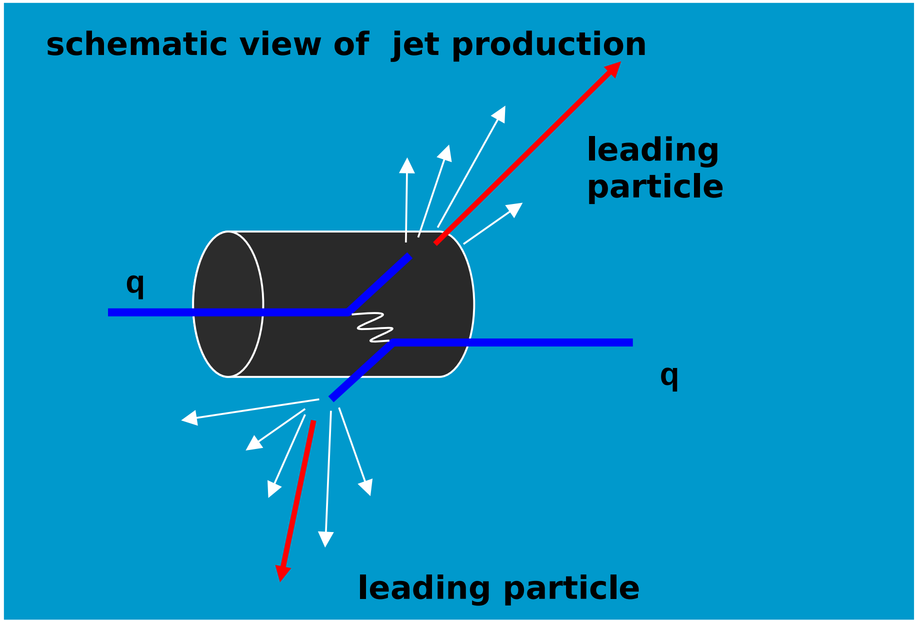

However, the scattered partons may loose energy (~ several GeV/fm) in the colored medium

$\rightarrow$ momentum reduction (fewer high p_T particles in jet)
$\rightarrow$ no jet partner on other side

Jet Quenching

The nuclear modification factor R_AA

The R_{AA} function:

$$R_{AA}(b) = \frac{\frac{\mathrm{d}^2 N^{AA}}{\mathrm{d}p_t^2 \mathrm{d}y}}{N_{coll}^{AA}(b) \cdot \frac{\mathrm{d}^2 N^{NN}}{\mathrm{d}p_t^2 \mathrm{d}y}}$$

if hard scattering only:

$$R_{AA}(b) = 1$$

Qualitative expectations

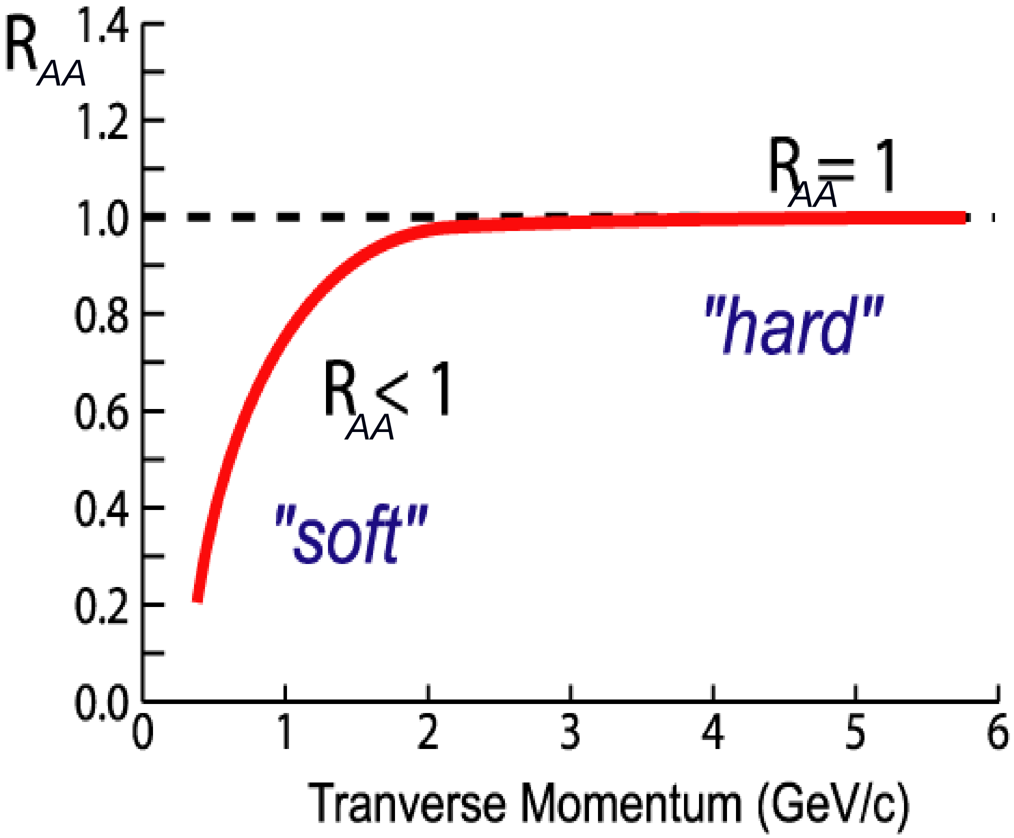

no medium effects:

R_{AA} < 1 in regime of soft physics

R_{AA} = 1 at high-p_T where hard scattering dominates

Suppression:

R_{AA} << 1 at high-p_T

Synopsis of Energy Loss measurements for Strongly Interacting Hard Probes

no suppression in pPb, QGP opaque for high energy partons

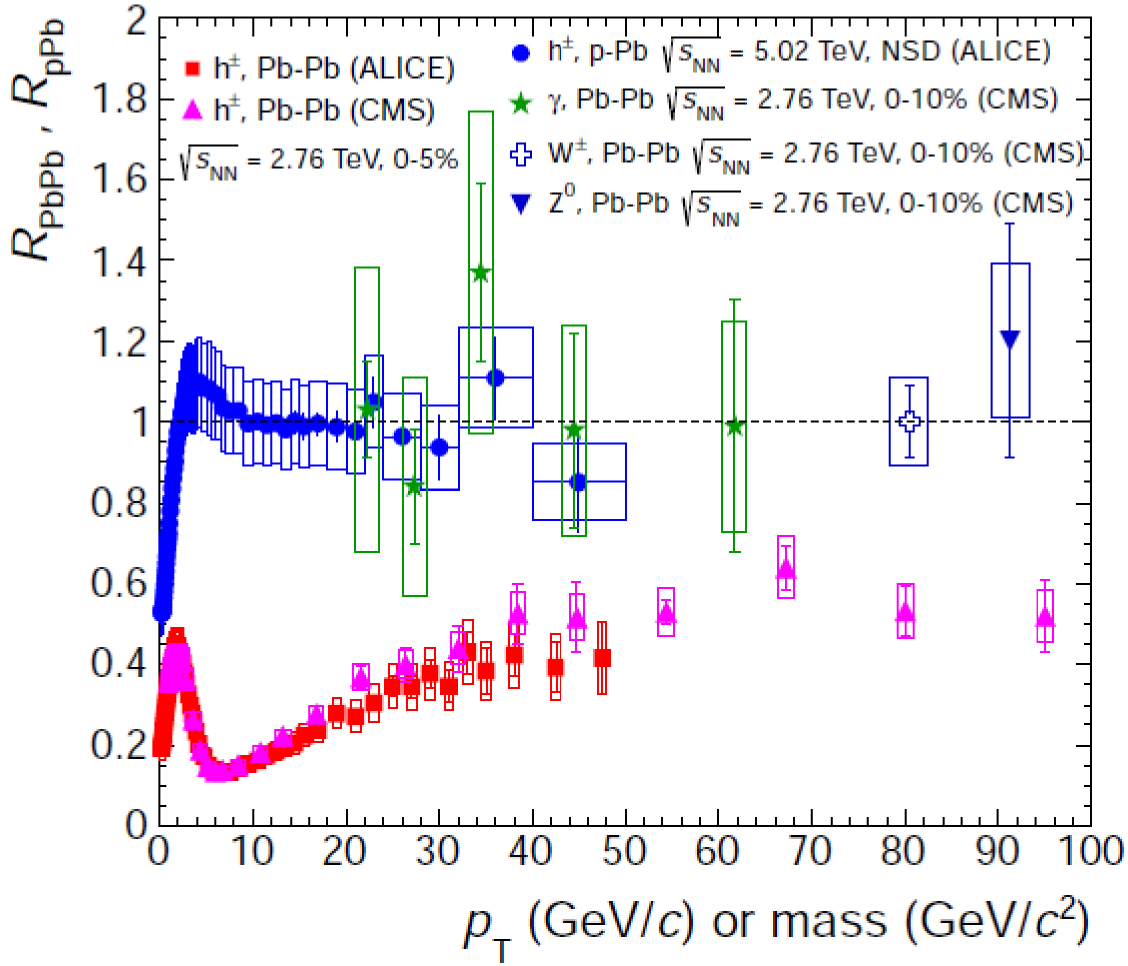

Alice coll.,

arXiv:1405.2737

photons, Z and W scale with number of binary collisions in PbPb – not affected by medium

→ demonstrates that charged particle suppression is medium effect: energy loss in QGP

Hadron production and the QCD Phase Boundary

Quark-gluon plasma and hadron yields in central nuclear collisions

QCD implies duality between (quarks and gluons) – hadrons

Hadron gas is equilibrated state of all known hadrons

QGP is equilibrated state of deconfined quarks and gluons

at a critical temperature T_c a hadronic system converts to QGP

consequence:

QGP in central nuclear collisions if:

1. all hadrons in equilibrium state at common temperature T
2. as function of cm energy the hadron state must reach a limiting temperature T_{lim}
3. all hadron yields must agree with predictions using the full QCD partition function at the QCD critical temperature $T_c = T_{lim}$

The hadron mass spectrum and lattice QCD

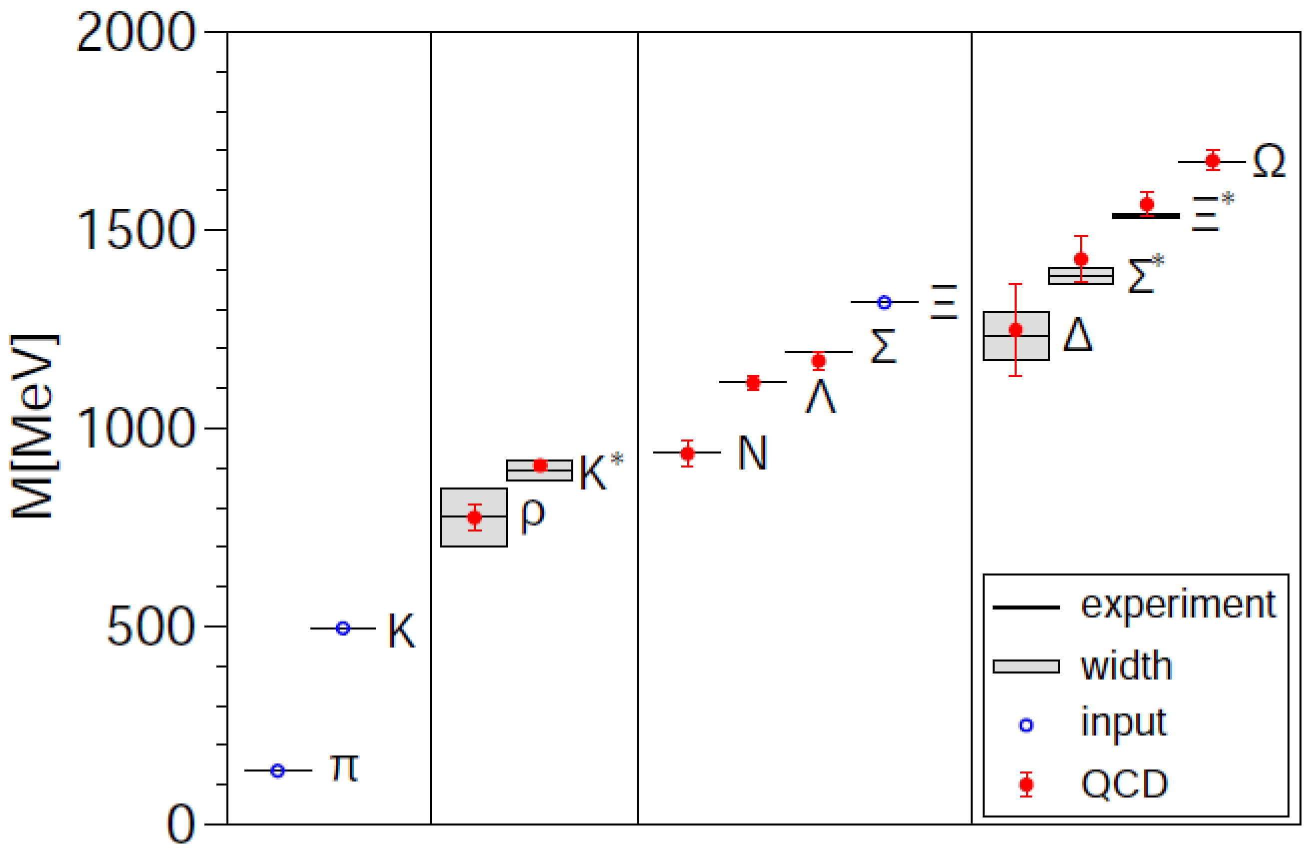

S. Duerr et al., Science 322 (2008) 1224-1227

Equilibration at the phase boundary

- Statistical model analysis of (u,d,s) hadron production: an important test of equilibration of quark matter near the phase boundary,   **no equilibrium → no QGP matter**

- No (strangeness) equilibration in hadronic phase

- Present understanding: multi-hadron collisions near phase boundary bring hadrons close to equilibrium – supported by success of statistical model analysis

- This implies little energy dependence above RHIC energy

- Analysis of hadron production → determination of T_c

pbm, Stachel, Wetterich,
Phys.Lett. B596 (2004) 61-69

At what energy is phase boundary reached?

Thermal model of particle production and QCD

Partition function Z(T,V) contains sum over the full hadronic mass spectrum and is fully calculable in QCD

For each particle i, the statistical operator is:

$$\ln Z_i = \frac{V g_i}{2\pi^2} \int_0^\infty \pm p^2 \mathrm{d}p \ln[1 \pm \exp(-(E_i - \mu_i)/T)]$$

Particle densities are then calculated according to:

$$n_i = N_i/V = -\frac{T}{V}\frac{\partial \ln Z_i}{\partial \mu} = \frac{g_i}{2\pi^2} \int_0^\infty \frac{p^2 \mathrm{d}p}{\exp[(E_i - \mu_i)/T] \pm 1}$$

From analysis of all available nuclear collision data we now know the energy dependence of the parameters T, mu_b, and V over an energy range from threshold to LHC energy and can confidently extrapolate to even higher energies

In practice, we use the full experimental hadronic mass spectrum from the PDG compilation to compute the 'primordial yield'

Comparison with measured hadron yields needs evaluation of all strong decays

Excellent description of LHC data

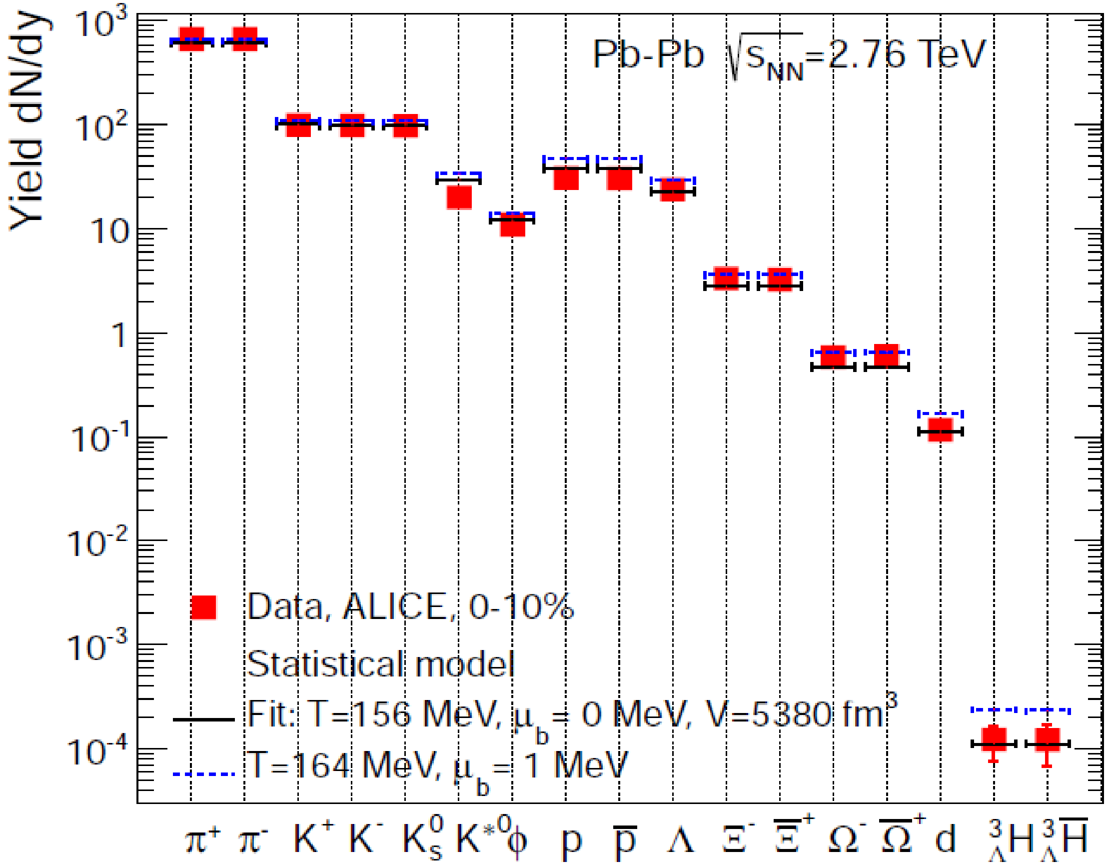

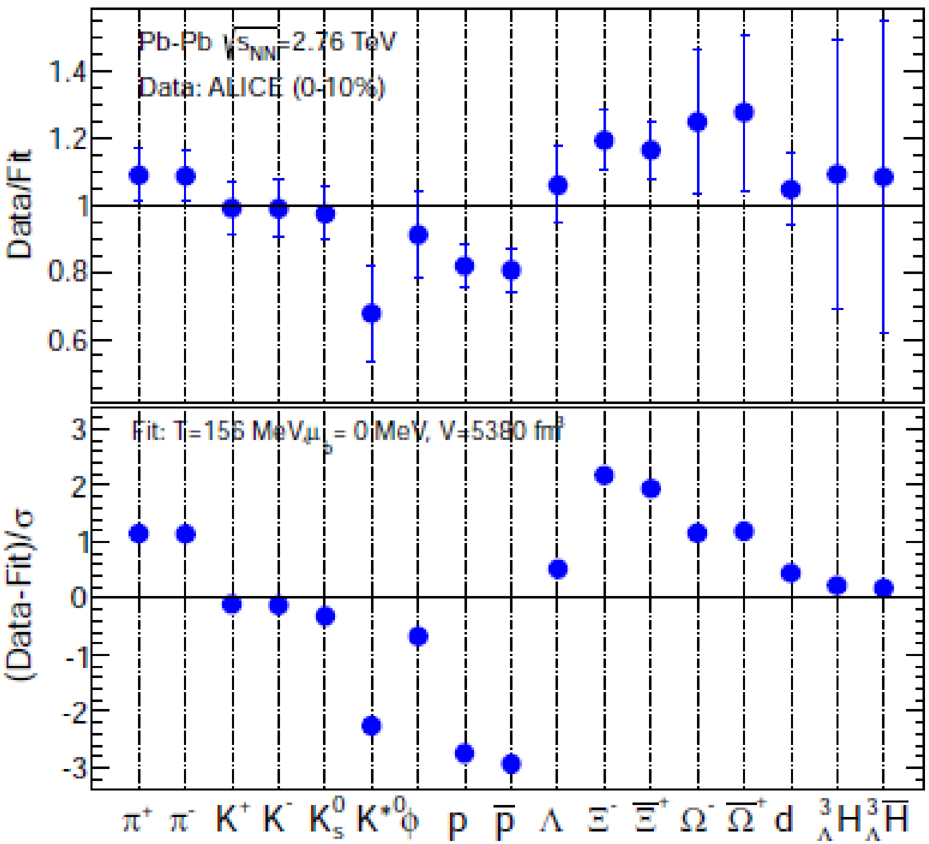

proton discrepancy 2.8 sigma

fit includes loosely bound systems such as deuteron and hypertriton
hypertriton is bound by only 100 keV, it is the **ultimate halo nucleus,**
produced at T=156 MeV. Close to an Efimov state.

Energy dependence of temperature and baryo-chemical potential

energy range from SPS down to threshold

is phase boundary ever reached for $\sqrt{s_{NN}}$ < 10 GeV?

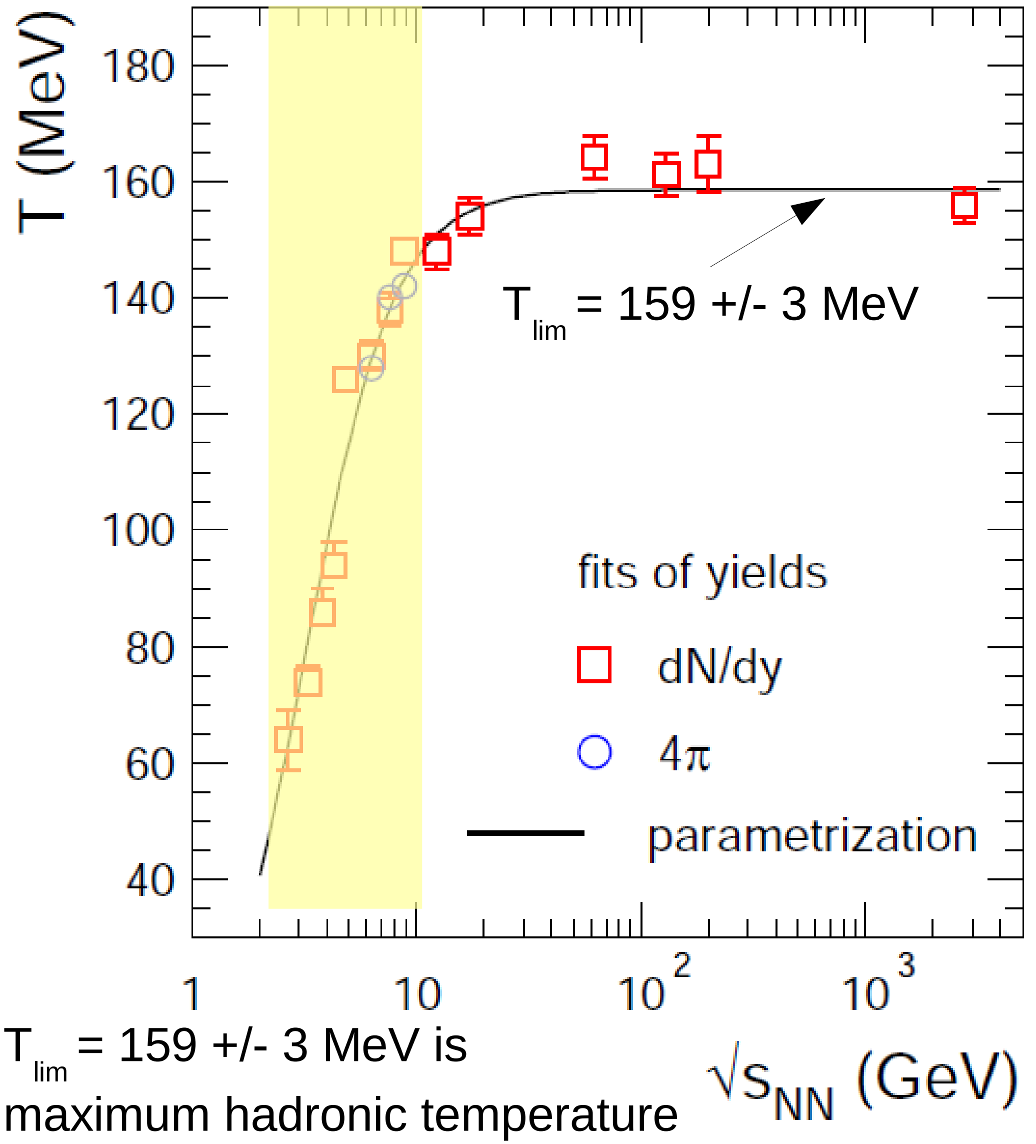

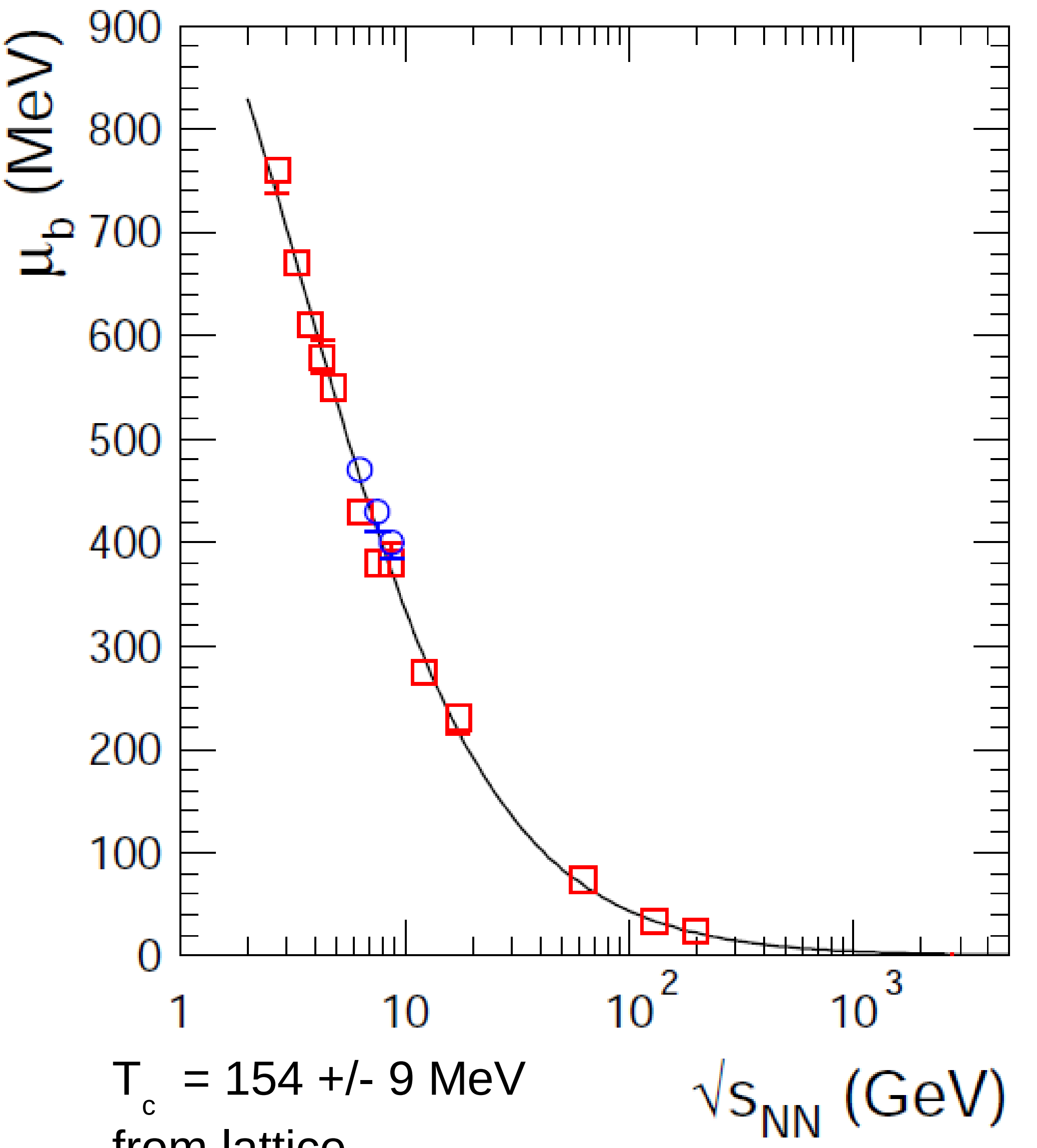

T_{lim} = 159 +/- 3 MeV is maximum hadronic temperature

T_c = 154 +/- 9 MeV from lattice

Mass dependence of primordial and total yield compared to LHC data

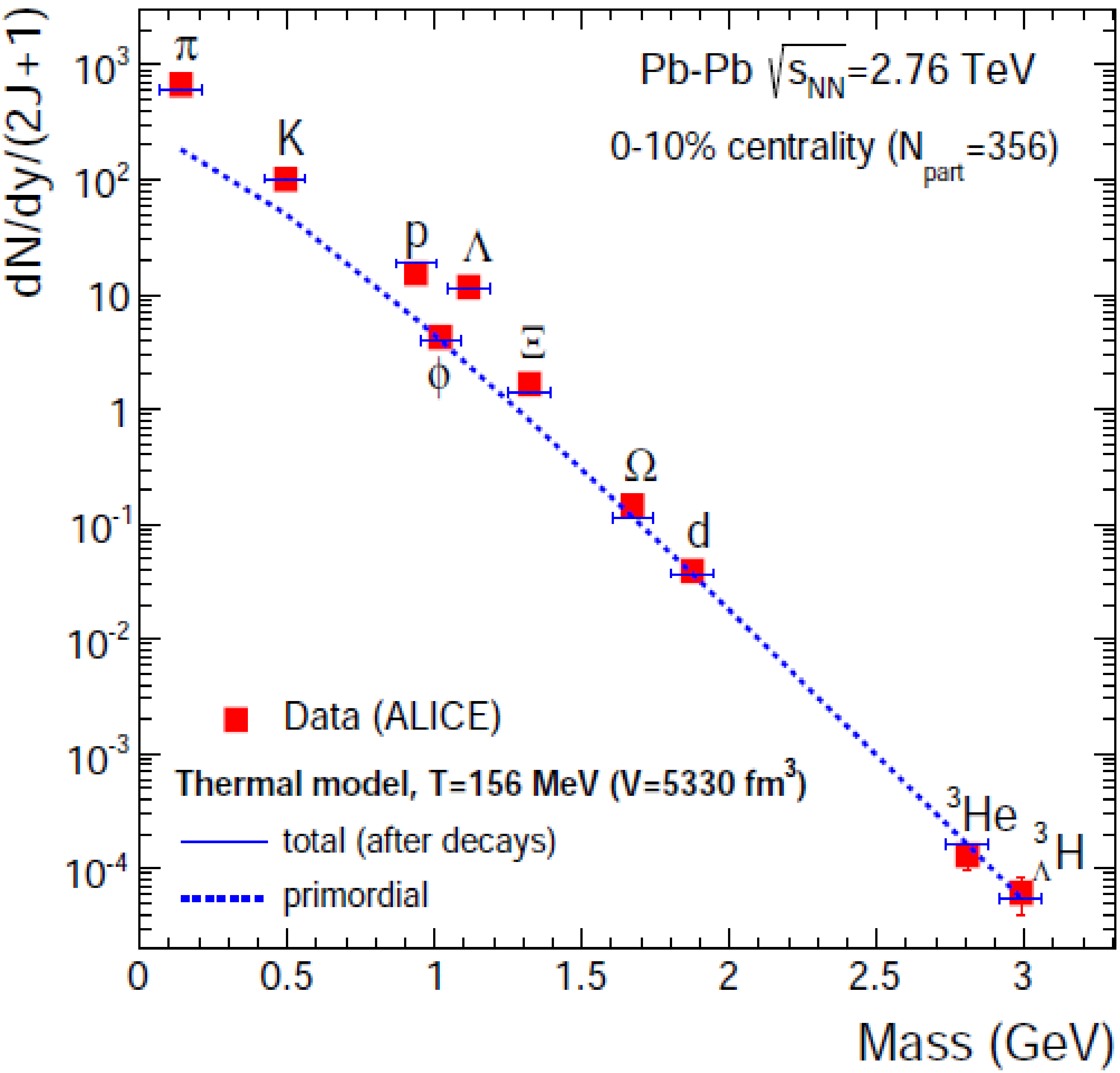

… and also including anti-alphas

agreement over 9 orders of magnitude with QCD statistical operator prediction

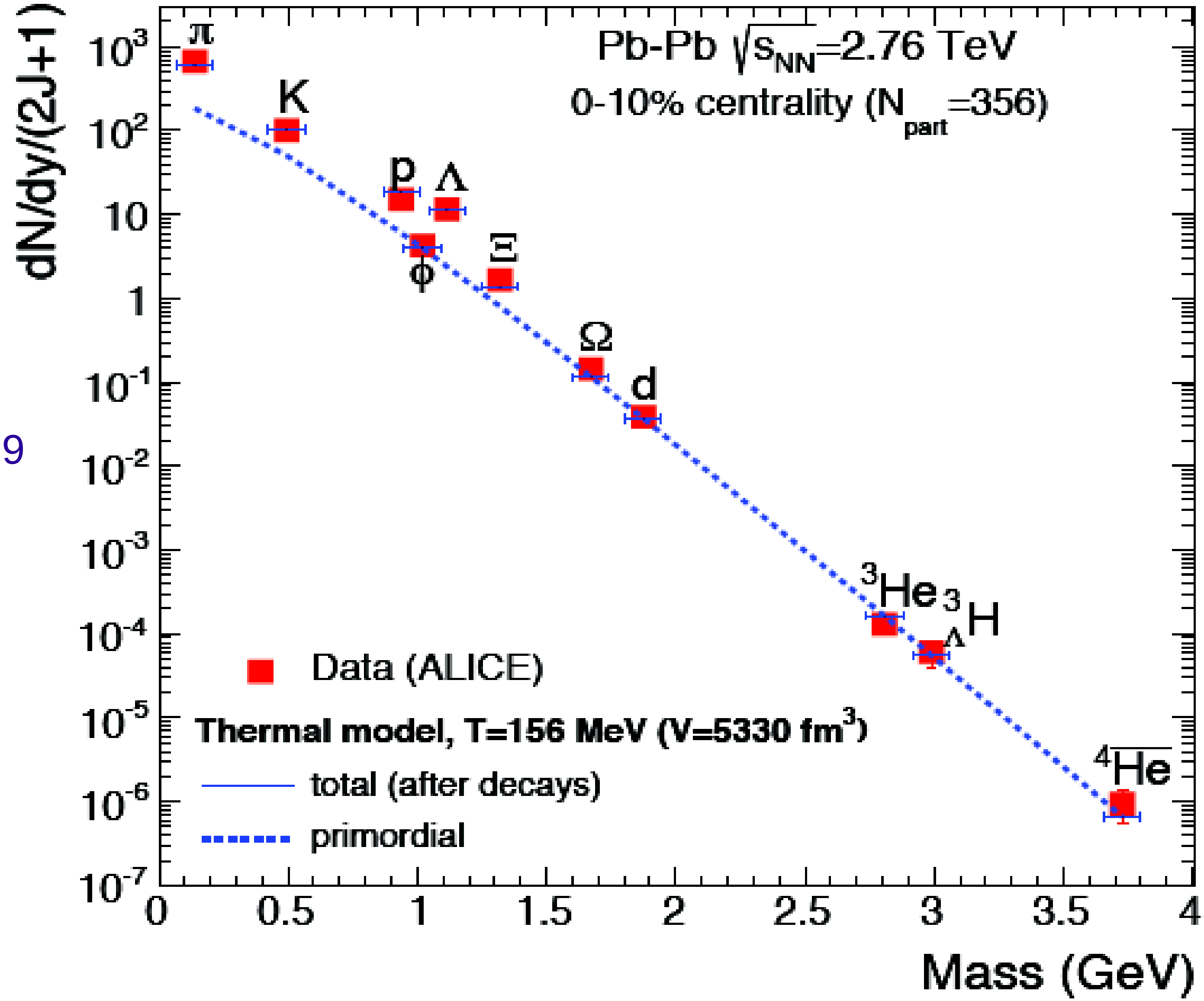

yield of light nuclei predicted in: pbm, J. Stachel, J.Phys. G28 (2002) 1971-1976,
J.Phys. G21 (1995) L17-L20

The thermal model and loosely bound, fragile objects

successful description of production yields for d, d_bar, 3He hypertriton, …
implies no entropy production after chemical freeze-out

hypertriton Lambda separation energy is 130 keV << T_chem = 156 MeV

size of hypertriton: about 10 fm, 'ultimate halo nucleus'

use relativistic nuclear collision data and thermal model predictions to search for exotic objects

A. Andronic, P. Braun-Munzinger, J. Stachel, H. Stoecker, Production of light nuclei, hypernuclei and their antiparticles in relativistic nuclear collisions, Phys. Lett. B697 (2011) 203, arXiv:1010.2995 [nucl-th].

energy dependence of d/p ratio and thermal model prediction

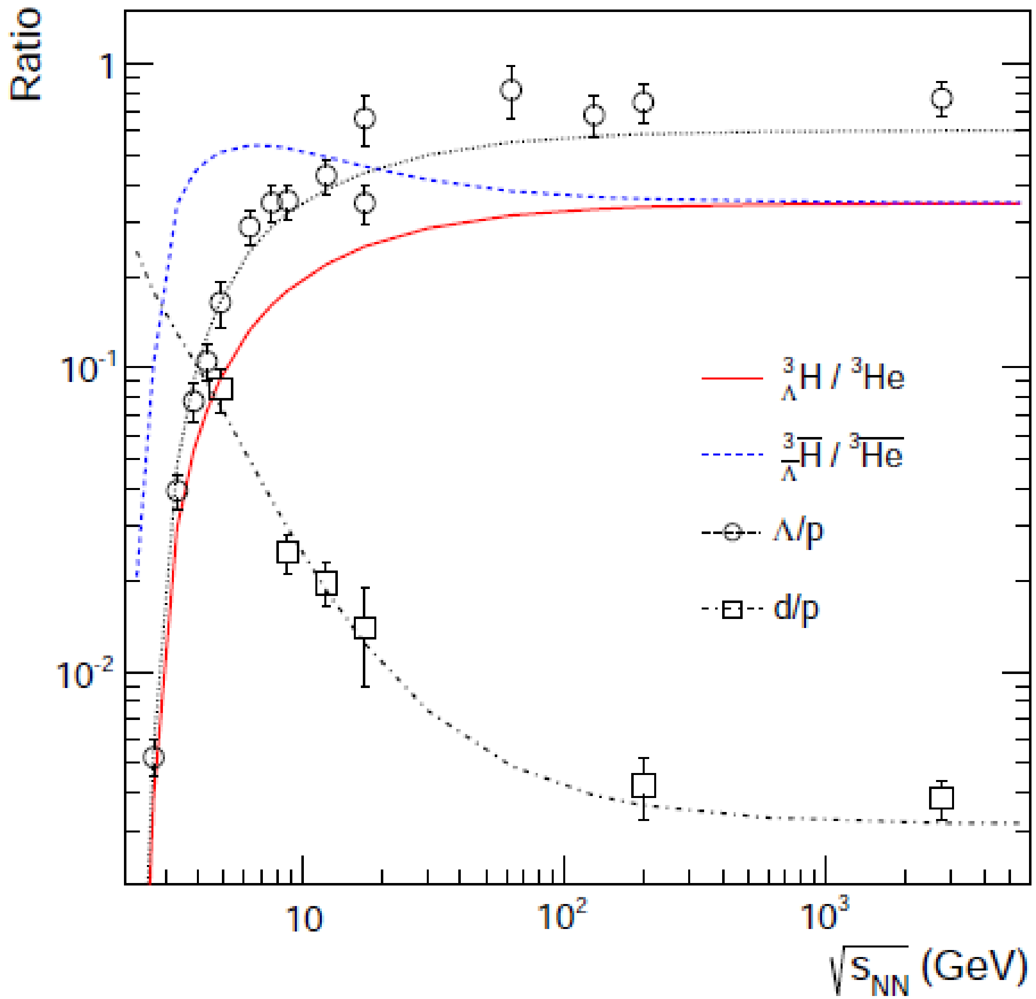

agreement between thermal model calculations and data from Bevalac/SIS18 to LHC energy

A. Andronic, P. Braun-Munzinger, J. Stachel, H. Stoecker, Phys. Lett. B697 (2011) 203, arXiv:1010.2995 [nucl-th].

The QGP Phase Diagram and Hadron Production Data

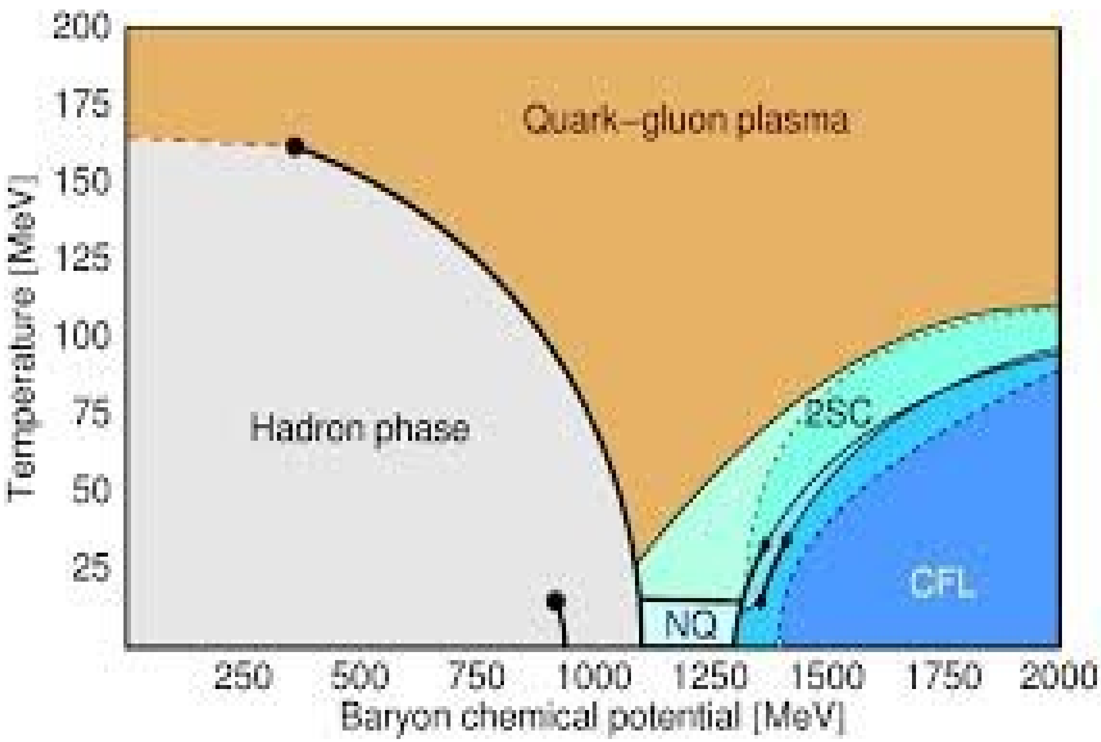

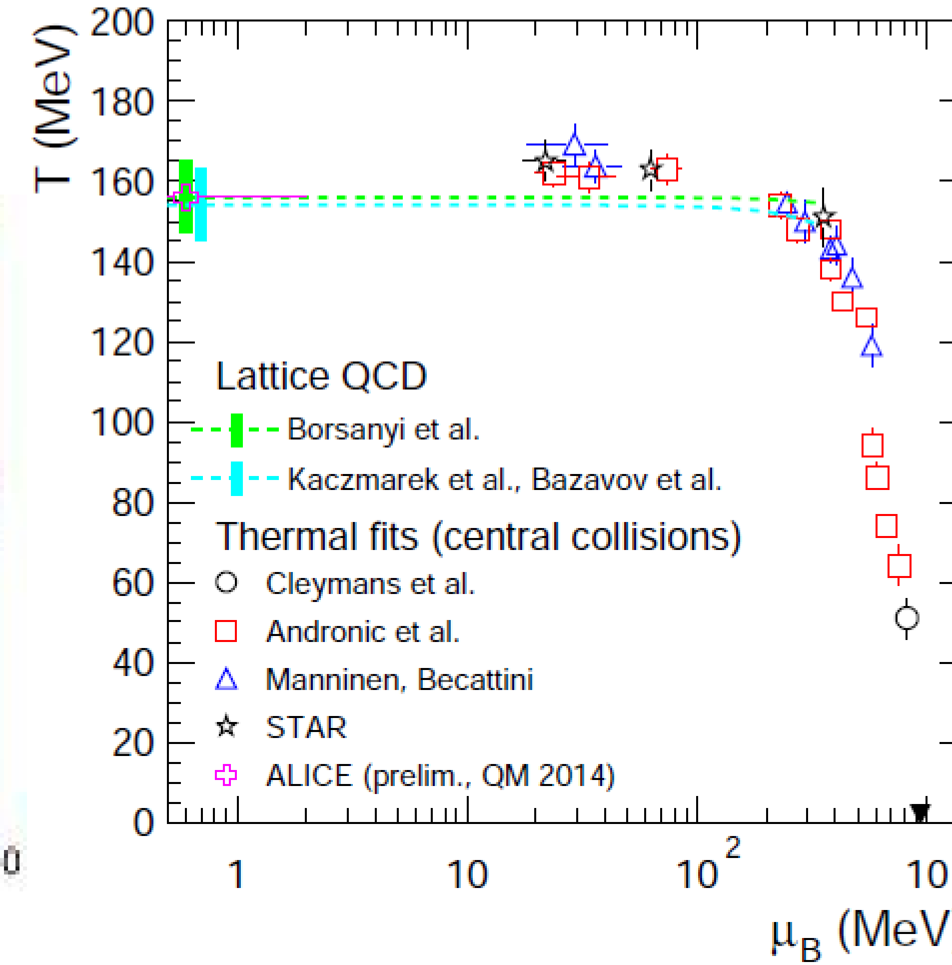

Summary I

overall the LHC data provide strong support for chemical freeze-out driven by the phase transition at T_c = 156 MeV

the full QCD statistical operator is encoded in the nuclear collision data on hadron multiplicities

energy dependence of hadron yields provides strong connection to fundamental QCD prediction of hadronic and quark-gluon matter at high temperature

success to describe also yields of loosely bound states provides strong evidence for isentropic expansion after chemical freeze-out

Charmonium as a probe for the properties of the QGP

the original idea: (Matsui and Satz 1986) implant charmonia into the QGP and observe their modification, in terms of suppressed production in nucleus-nucleus collisions with or without plasma formation – sequential melting

new insight (pbm, Stachel 2000) QGP screens all charmonia, but charmonium production takes place at the phase boundary, enhanced production at colliders – signal for deconfined, thermalized charm quarks production probability scales with $N(_{ccbar})^2$

recent reviews: L. Kluberg and H. Satz, arXiv:0901.3831

pbm and J. Stachel, arXiv:0901.2500

both published in Landoldt-Boernstein Review, R. Stock, editor, Springer 2010

n.b. at collider energies there is a complete separation of time scales

$t_{coll} << t_{QGP} < t_{Jpsi}$

implanting charmonia into QGP is an inappropriate notion

this issue was already anticipated by Blaizot and Ollitrault in 1988

color screening removes bound states

vacuum QGP

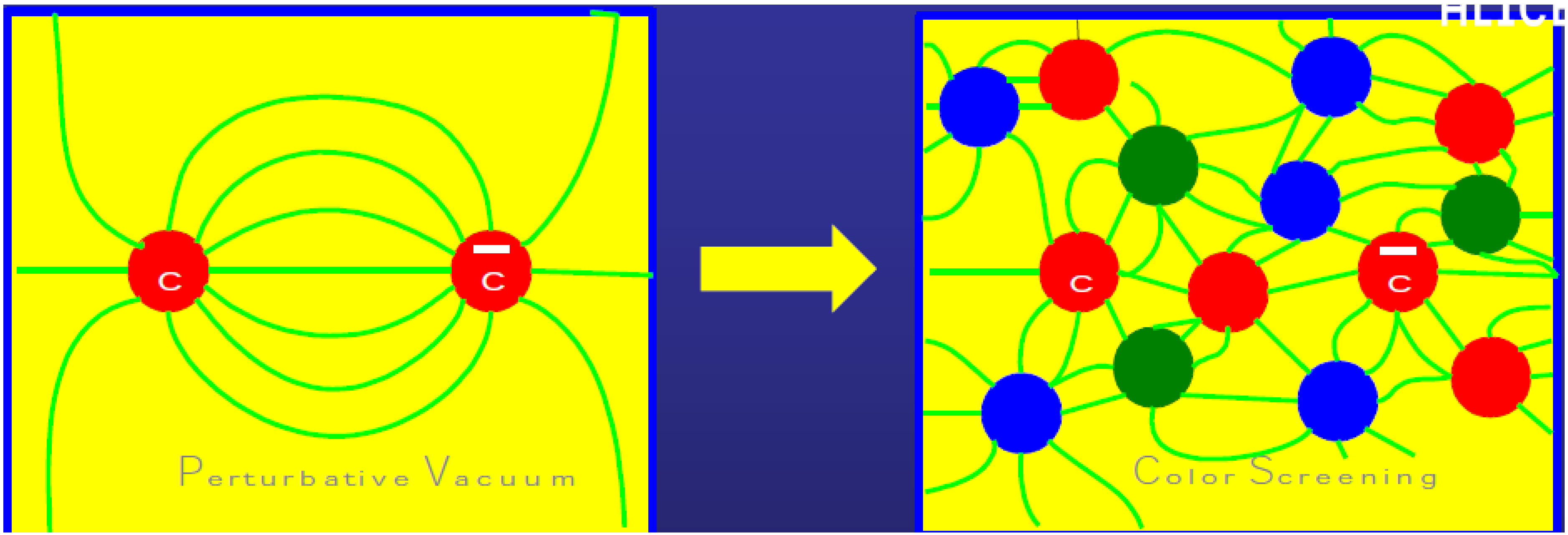

Will this happen at T_c or only when deep inside the QGP?

quarkonium as a probe for deconfinement at the LHC
the statistical (re-)generation picture

P. Braun-Munzinger, J. Stachel, The Quest for the Quark-Gluon Plasma, Nature **448** Issue 7151, (2007) 302-309.

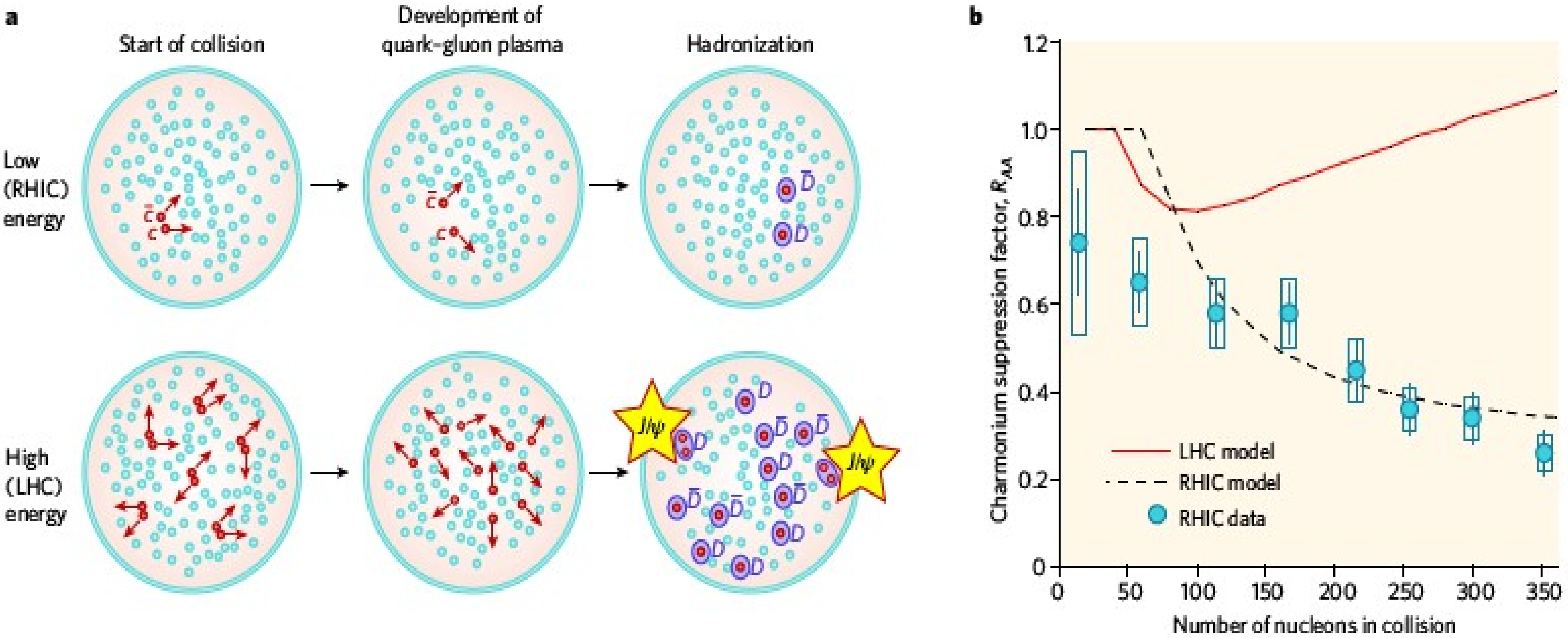

charmonium enhancement as fingerprint of color screening and deconfinement at LHC energy

pbm, Stachel, Phys. Lett. B490 (2000) 196
Andronic, pbm, Redlich, Stachel, Phys. Lett. B652 (2007) 659

decision on regeneration vs sequential suppression from LHC data

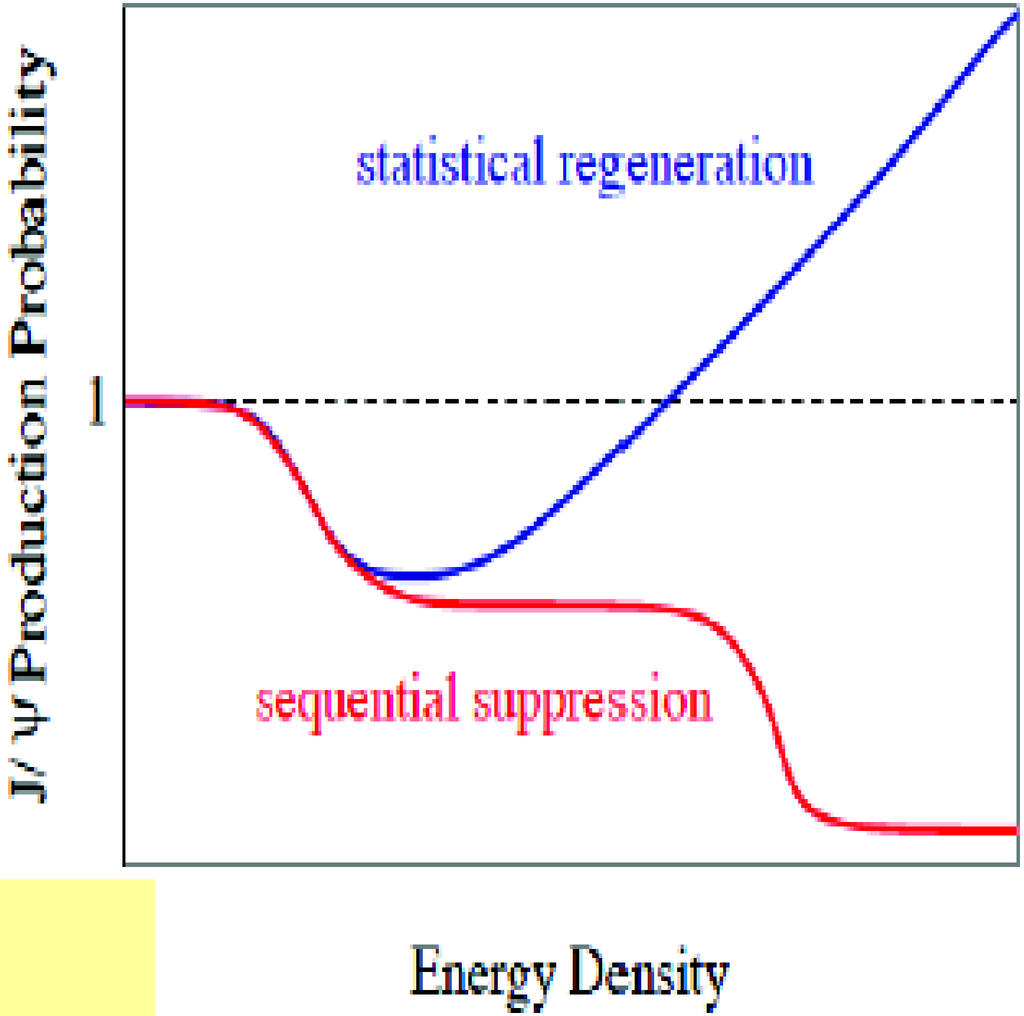

Picture:
H. Satz 2009

SPS RHIC LHC

Tracking accuracy
J/psi measurement in ultra-peripheral Pb-Pb collisions

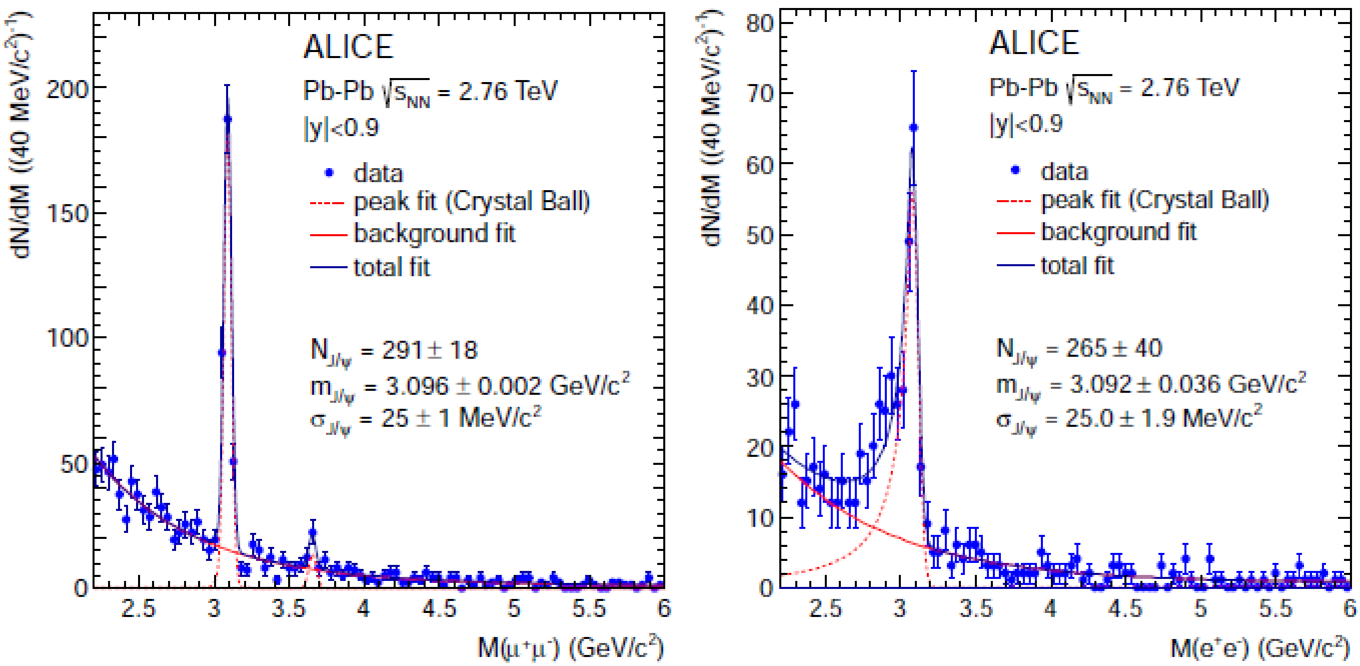

less suppression when increasing the energy density

midrapidity forward rapidity

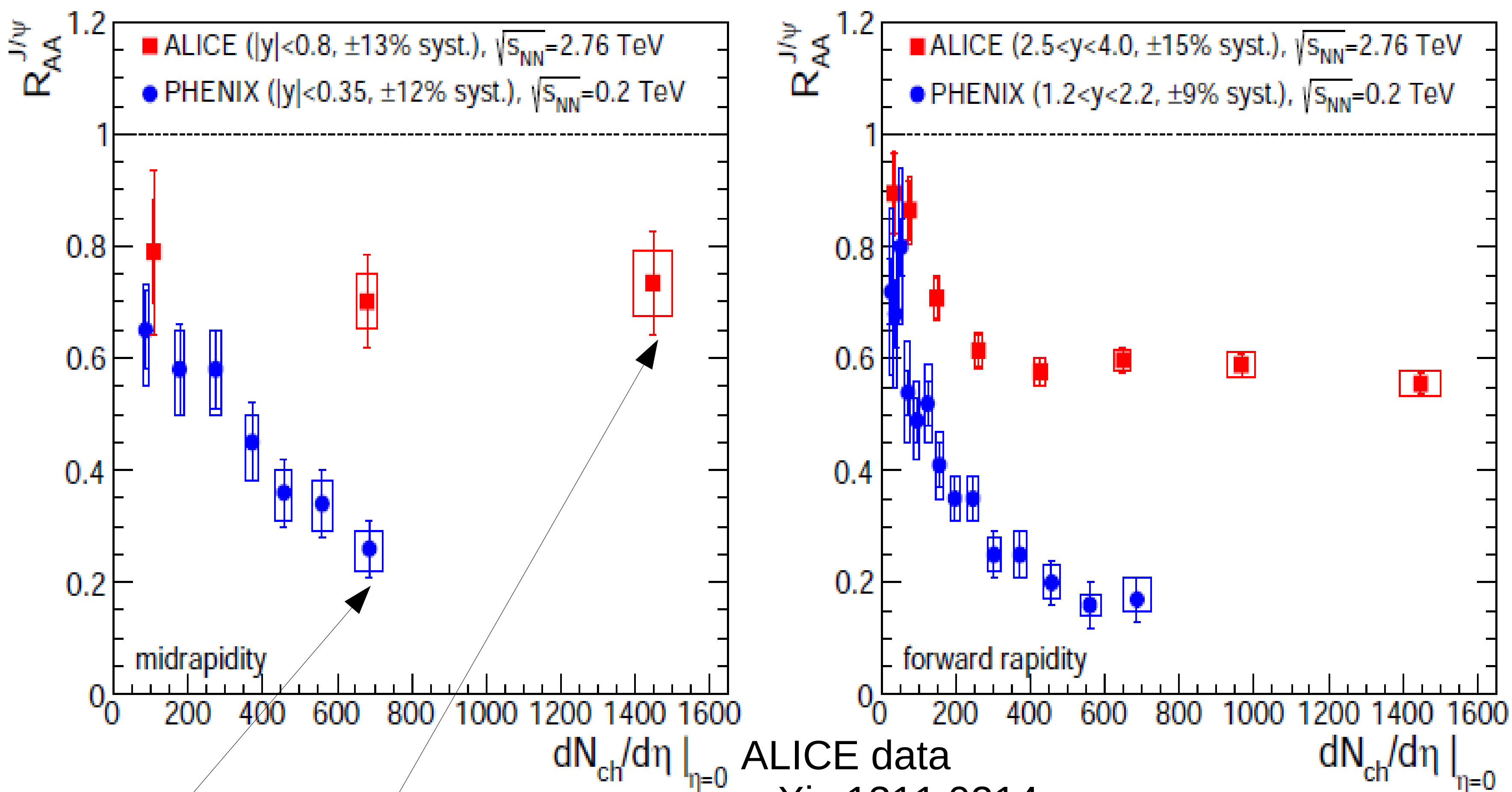

ALICE data
arXiv:1311.0214
PLB, in print

from here to here more than factor of 2 increase in energy density, but R_{AA} increases by more than a factor of 3

2007 prediction impressively confirmed by LHC data

Rapidity dependence

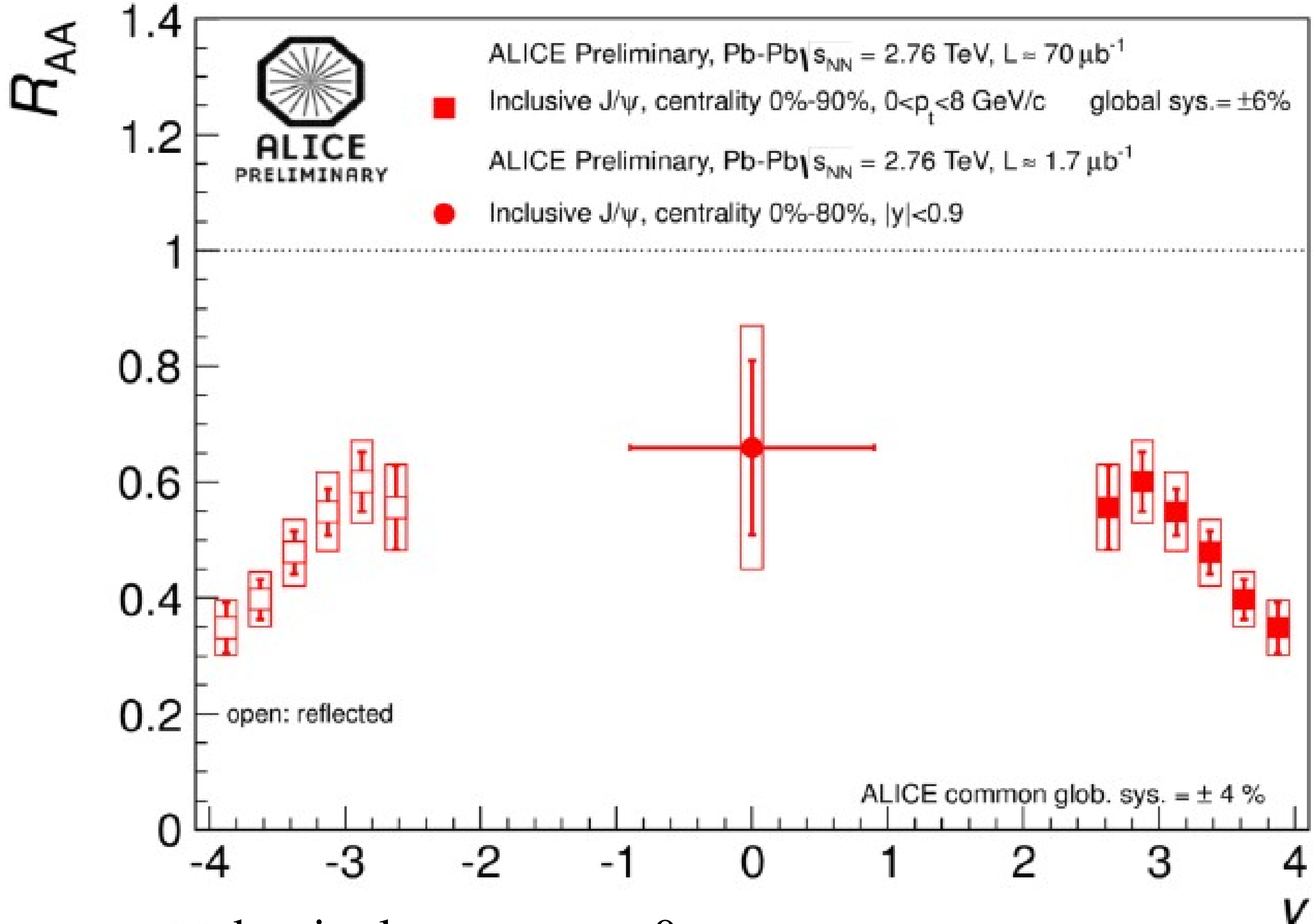

note: energy density largest at y = 0

statistical hadronization model
all J/psi production at the phase boundary

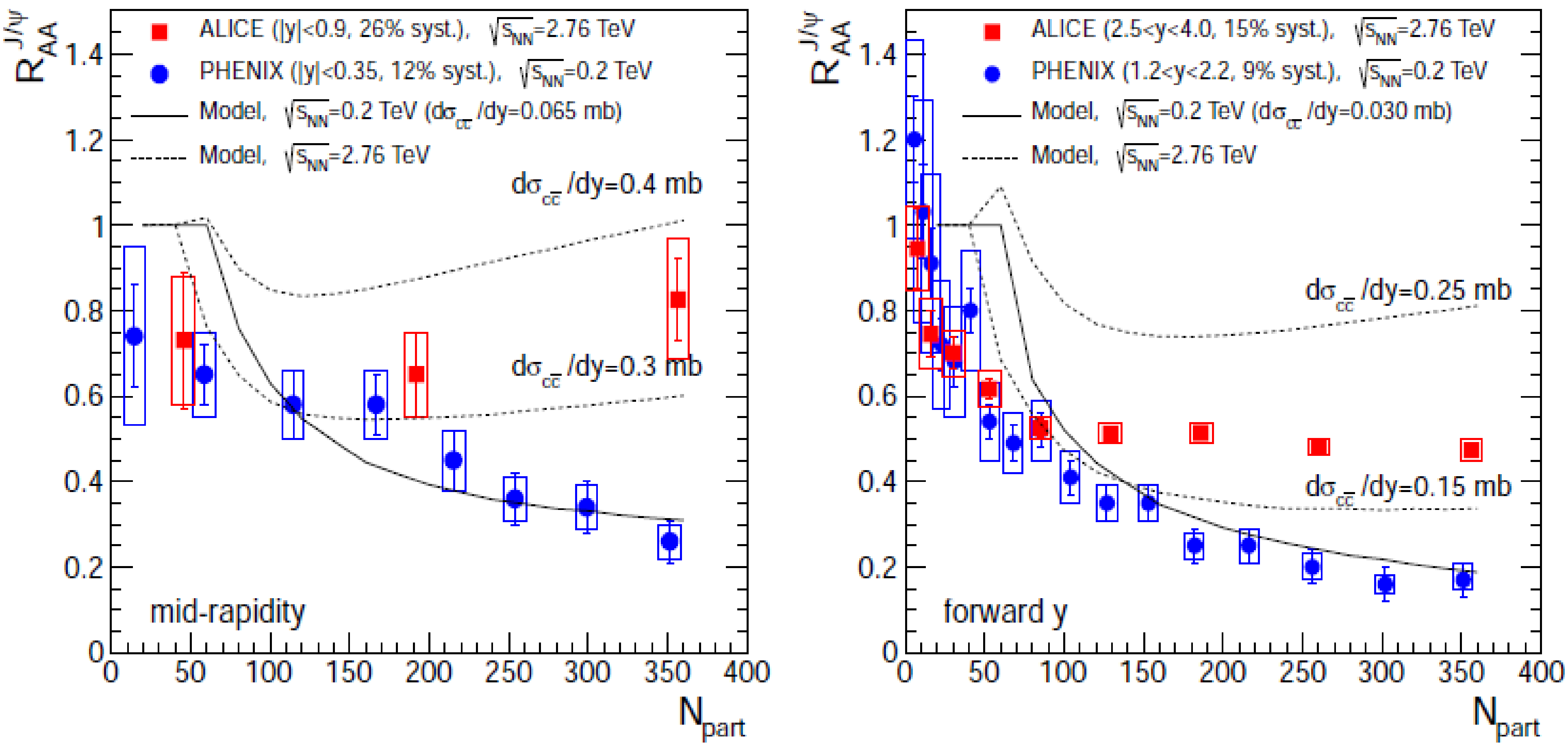

ALICE data and evolution from RHIC to LHC energy
described quantitatively

back to J/psi data – what about spectra and hydrodynamic flow of charm and charmonia?

if charmonia are produced via statistical hadronization of charm quarks at the phase boundary, then:

- charm quarks should be in thermal equilibrium
  - low pt enhancement
  - flow of charm quarks
  - flow of charmonia

Comparison of transverse momentum spectra at RHIC and LHC

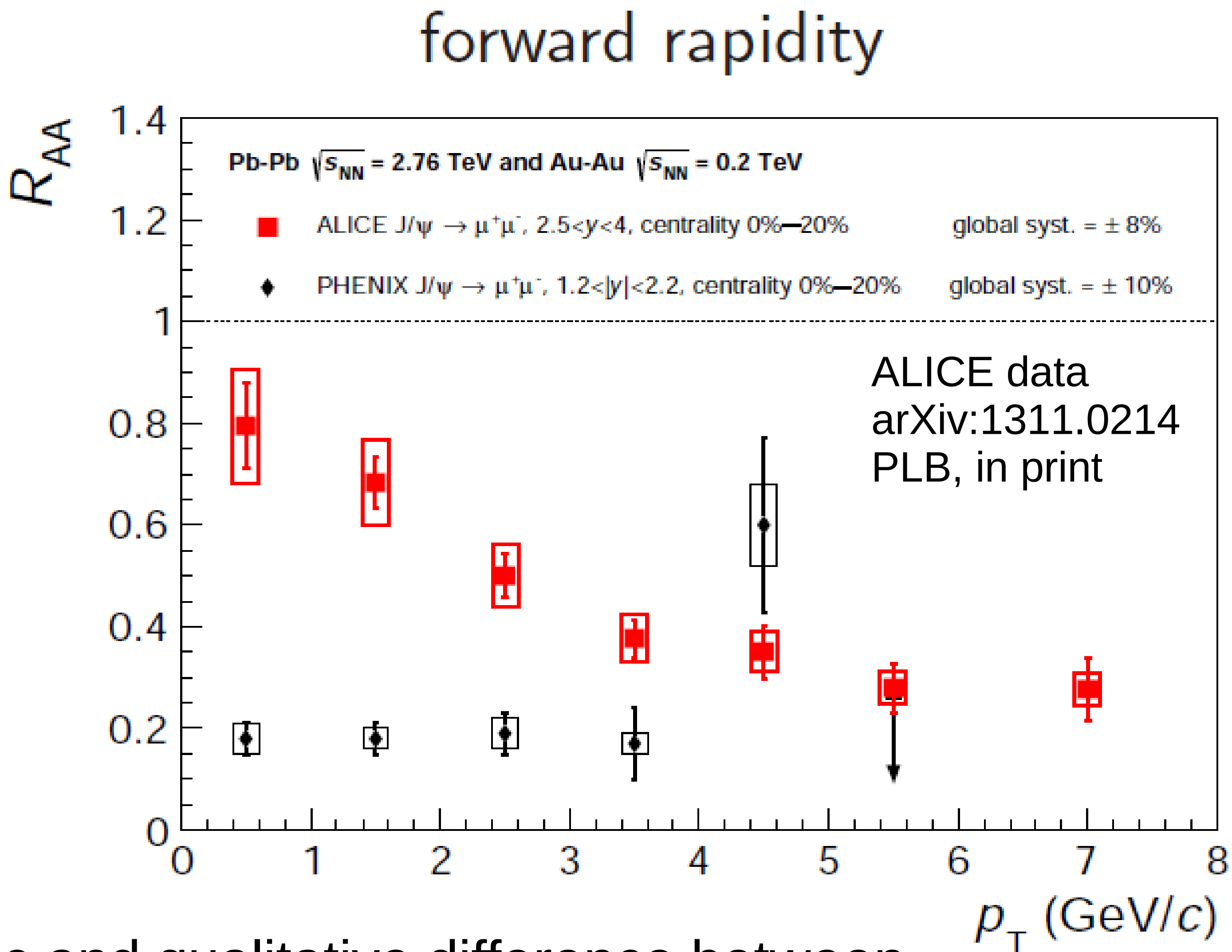

dramatic and qualitative difference between RHIC and LHC results

comparison with (re-)generation models

midrapidity

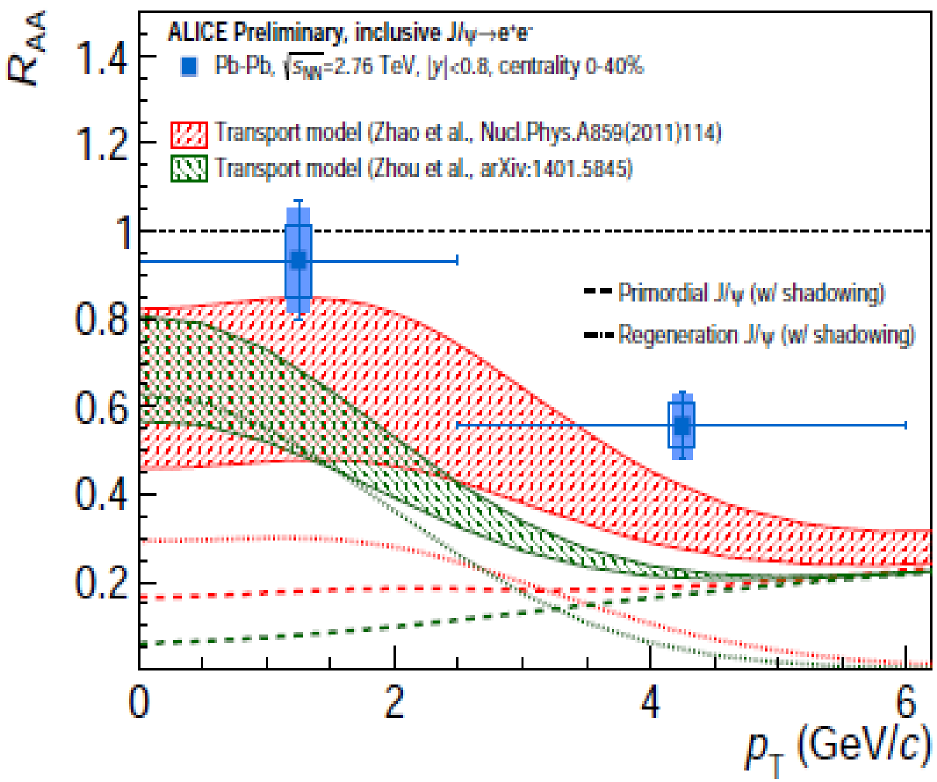

forward rapidity

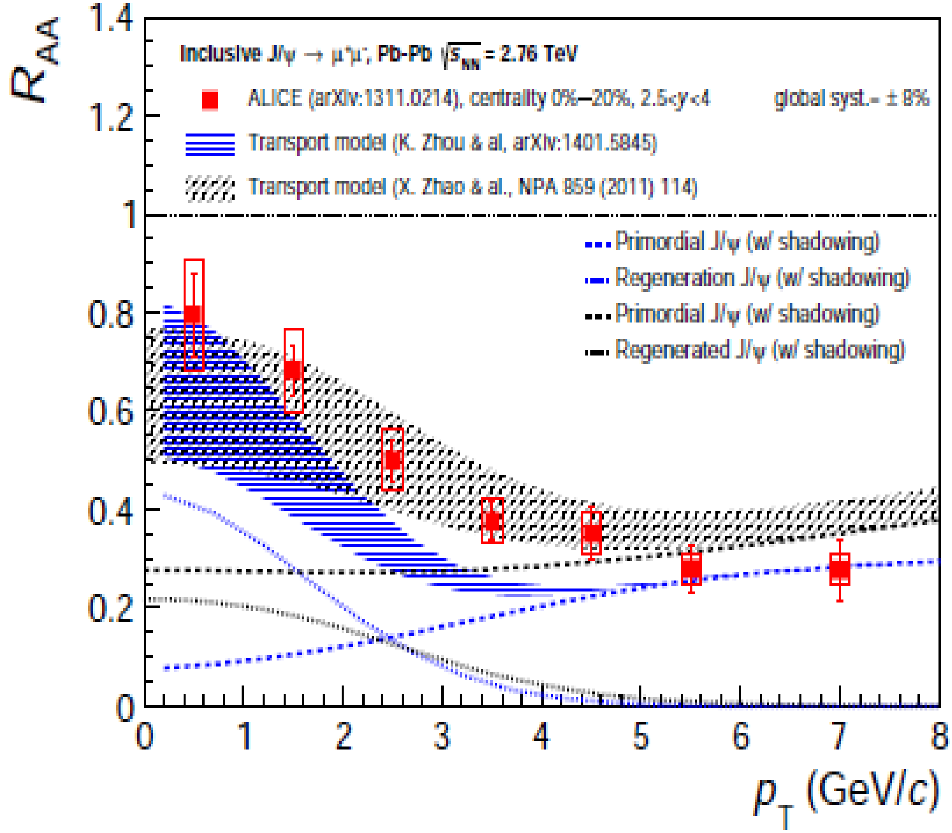

good agreement lends further strong support to the 'full color screening and late J/psi production' picture

analysis of transverse momentum spectra

arXiv:1309.7520v1 [nucl-th] 29 Sep 2013

Zhou, Xu, Zhuang

at LHC energy, mostly (re-) generation of charmonium, p_t distribution exhibits features of strong energy loss and approach to thermalization for charm quarks

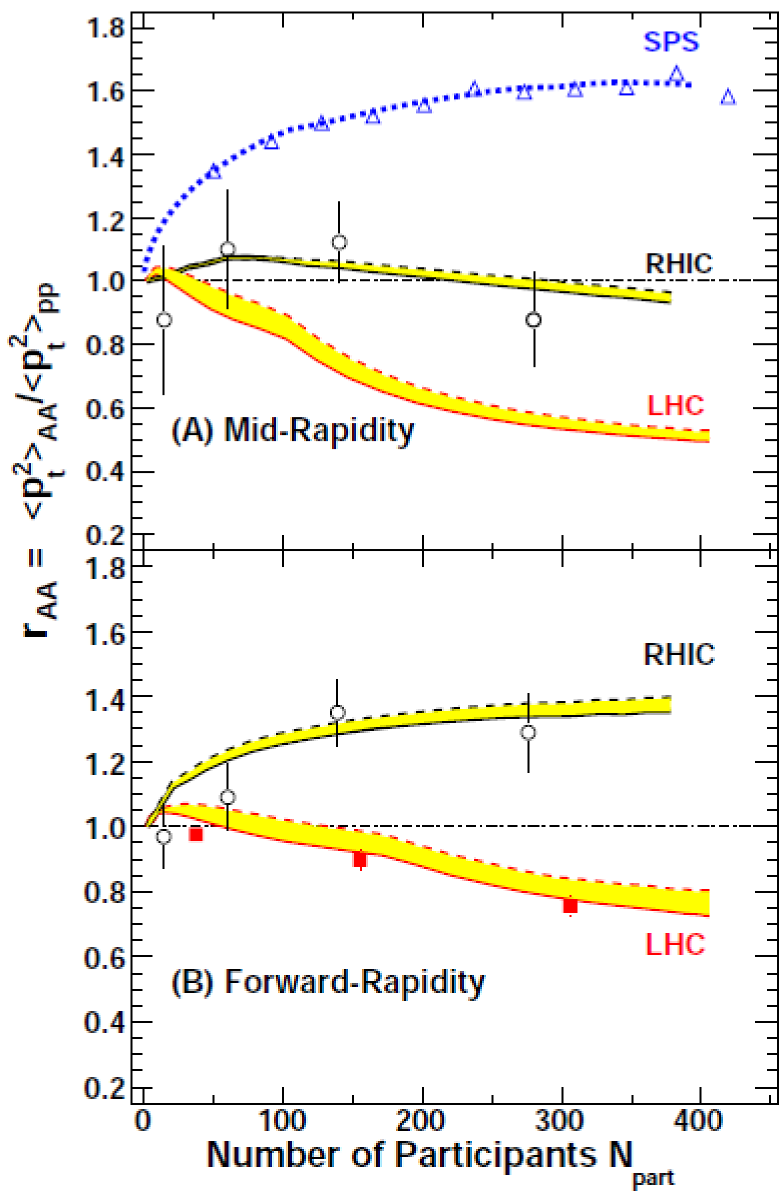

J/psi flow compared to models including (re-) generation

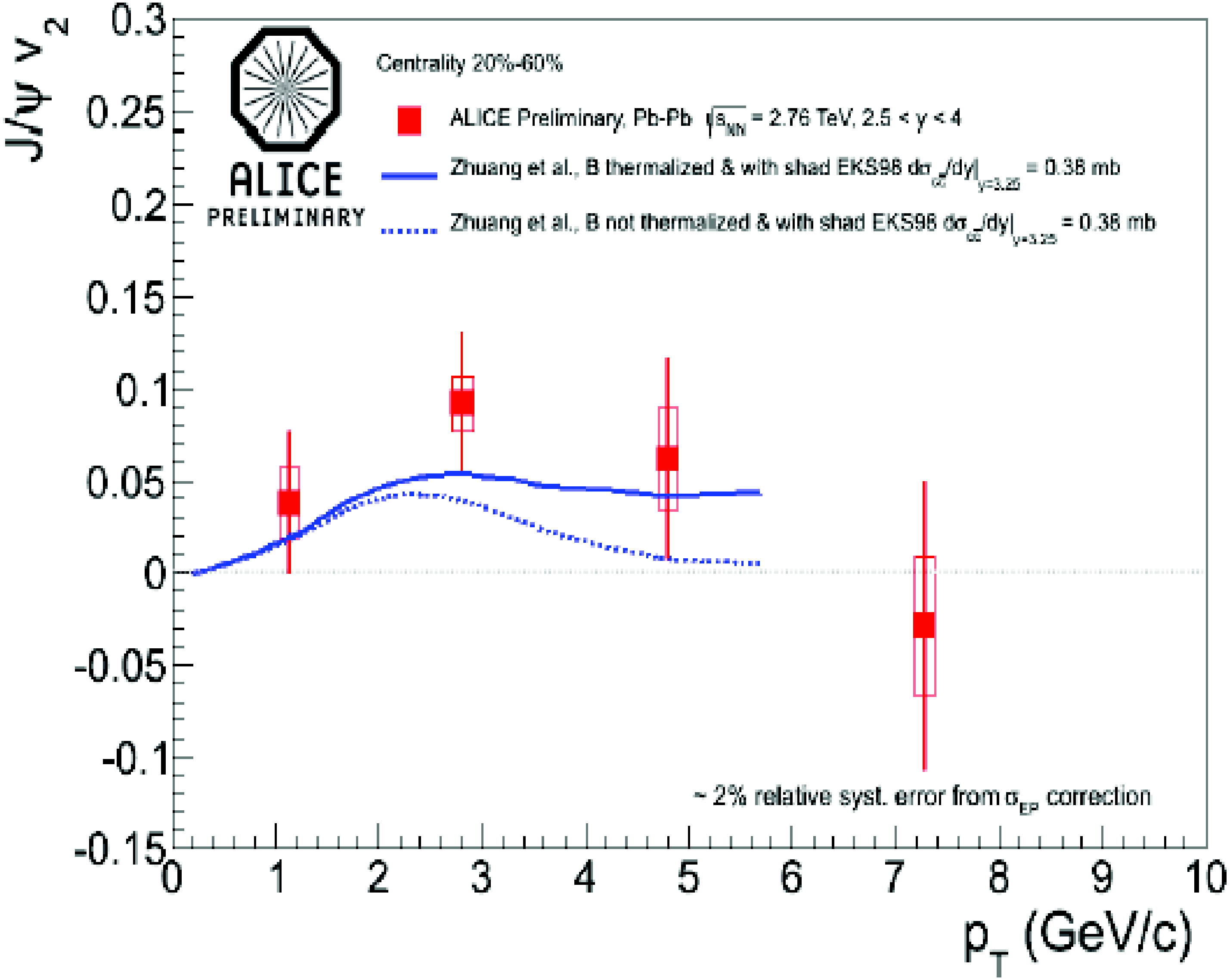

hydrodynamic flow of J/psi consistent with (re-)generation

Charmonium production at LHC energy: deconfinement,and color screening

- Charmonia formed at the phase boundary → full color screening at T_c
- Debye screening length < 0.4 fm near T_c
- Combination of uncorrelated charm quarks into J/psi → deconfinement

statistical hadronization picture of charmonium production provides most direct way towards information on the degree of deconfinement reached as well as on color screening and the question of bound states in the QGP

Debye mass, LQCD, and J/psi data

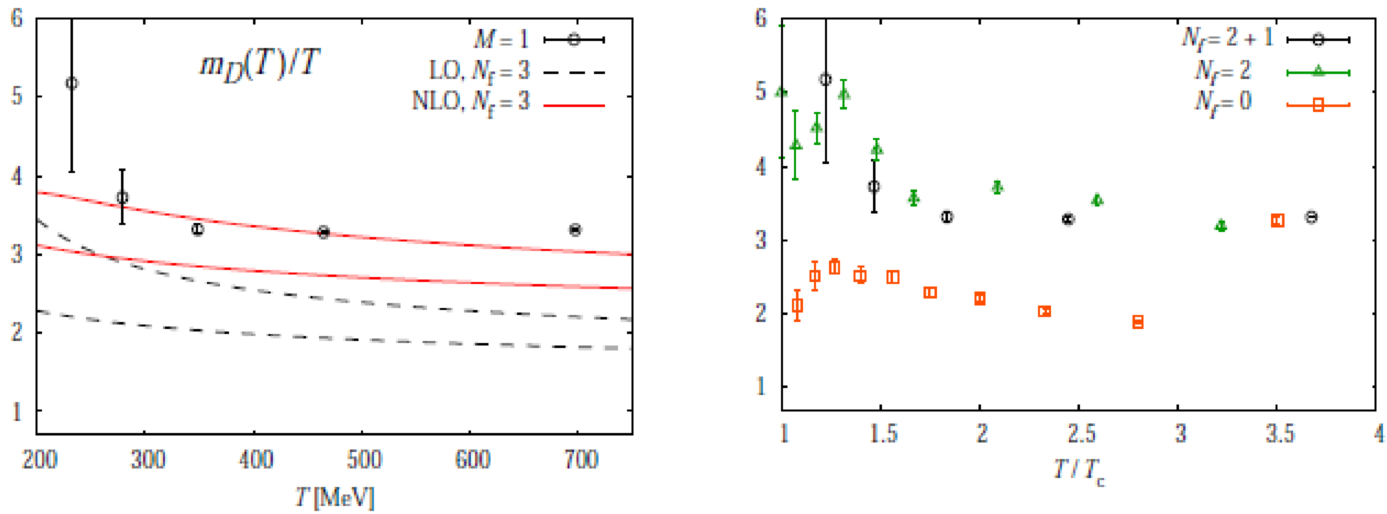

Fig. 6. (Left) The Debye screening mass on the lattice in the color-singlet channel together with that calculated in the leading-order (LO) and next-to-leading-order (NLO) perturbation theory shown by dashed-black and solid-red lines, respectively. The bottom (top) line expresses a result at $\mu = \pi T$ ($3\pi T$), where μ is the renormalization point. (Right) Flavor dependence of the Debye screening masses. We assume the pseudo-critical temperature for $2+1$-flavor QCD as $T_c \sim 190$ MeV.

arXiv:1112.2756 WHOT-QCD Coll.

from J/psi data and statistical hadronization analysis:

$m_{Debye}/T > 3.3$

at T = 0.15 GeV

J/psi data on color screening at the phase boundary are close to predictions from Lattice QCD

The bottomonium puzzle (I)

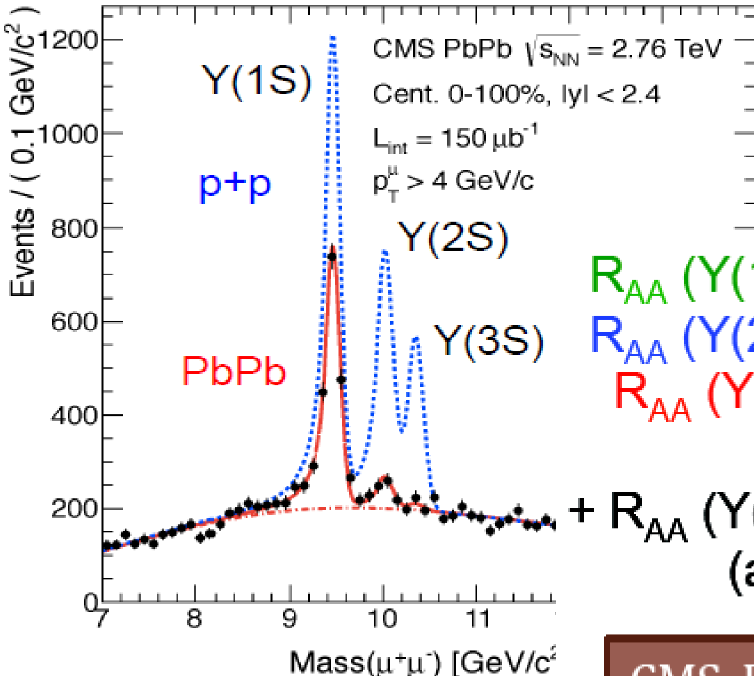

R_{AA} (Υ(1S)) = 0.56 ± 0.08 ± 0.07
R_{AA} (Υ(2S)) = 0.12 ± 0.04 ± 0.02
R_{AA} (Υ(3S)) < 0.10 @ 95% CL

+ R_{AA} (Υ(1S)) = 0.30 ± 0.05 ± 0.04
(at forward rapidity)

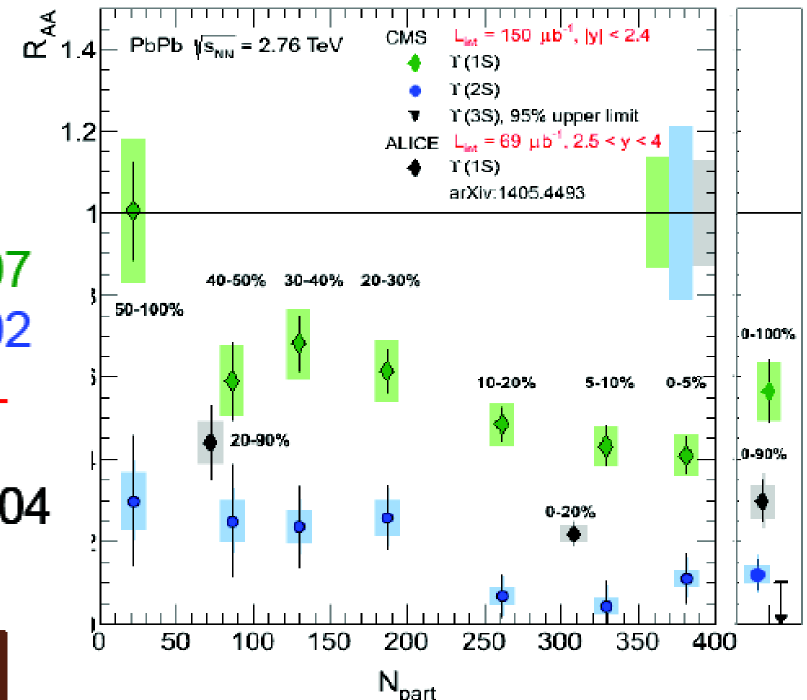

CMS, PRL109 (2012) 222301
ALICE, PLB738 (2014) 361

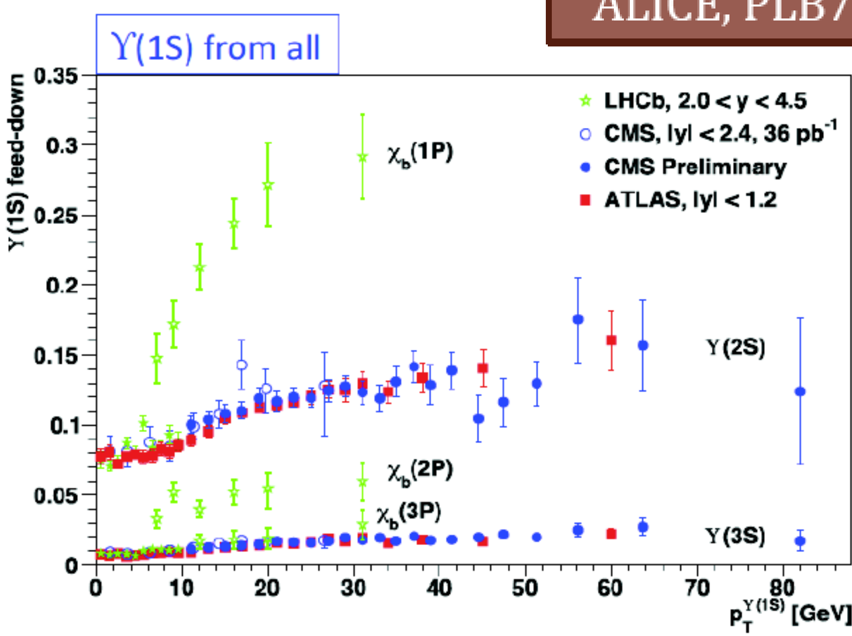

New results from LHCb: feeding into Υ(1s) only about 30% → Υ(1s) for pp suppression not due to reduced feeding in Pb—Pb collisions

The bottomonium puzzle (II)

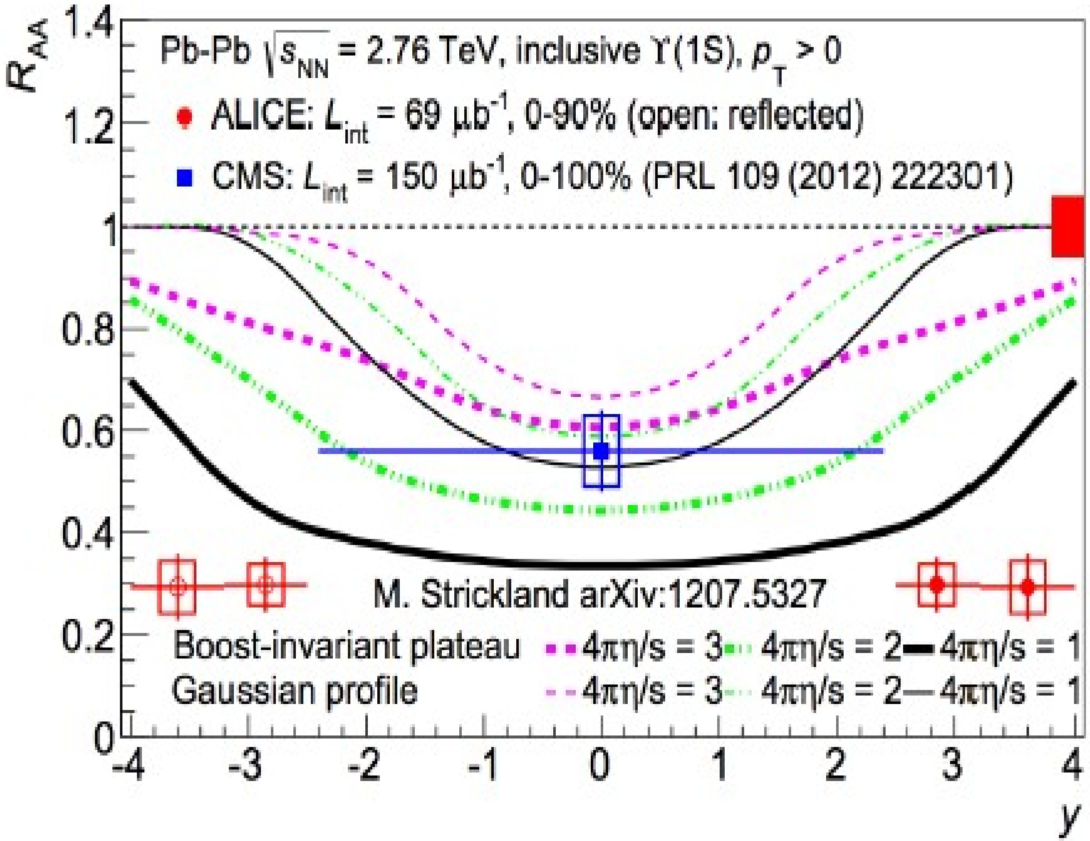

Rapidity distribution of RAA for Y(1s) is peaked at y=0, not consistent with suppression scenarios

Measurements at large rapidity (ALICE muon arm) are crucial!

summary II

- charmonium production – a fingerprint for deconfined quarks and gluons

- evidence for energy loss and flow of charm quarks --> thermalization
- charmonium generation at the phase boundary – a new process
- first indications for this from psi'/(J/psi) SPS and J/psi RHIC data
- evolution from RHIC to LHC described quantitatively
- charmonium enhancement at LHC – J/psi color-screened at T_c
  charm quarks deconfined in QGP

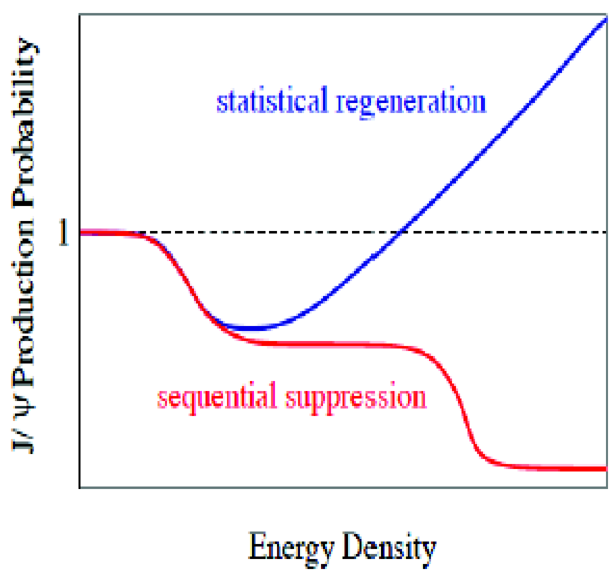

cartoon Helmut Satz, 2009 SPS RHIC LHC

outlook

Run2 at the LHC will commence in April 2015

LHC close to full design energy $\sqrt{s} = 13$ TeV for pp
$\sqrt{s_{NN}} = 5.1$ TeV for Pb—Pb

Pb-Pb interaction rate 20 kHz (factor 4 increase compared to Run1)

ALICE detector adapted to new running conditions

Plan for order of magnitude increase in data at higher energy and significantly improved precision

Run 3: upgrade overview

- **The ALICE upgrade strategy is outlined in the Letter Of Intent**
  - CERN-LHCC-2012-012 ; LHCC-I-022
  - http://cds.cern.ch/record/1475243
- **Operate ALICE at high luminosity ($\mathcal{L}$=6x10^{-27} cm^{-2}s^{-1}) and record all minimum bias events**
  - 50 kHz in Pb-Pb collisions → 100 x larger than the current read-out rate
  - 5 overlapping events in TPC drift volume → TPC can not run in triggered mode
- **The TPC upgrade is described in a Technical Design Report**

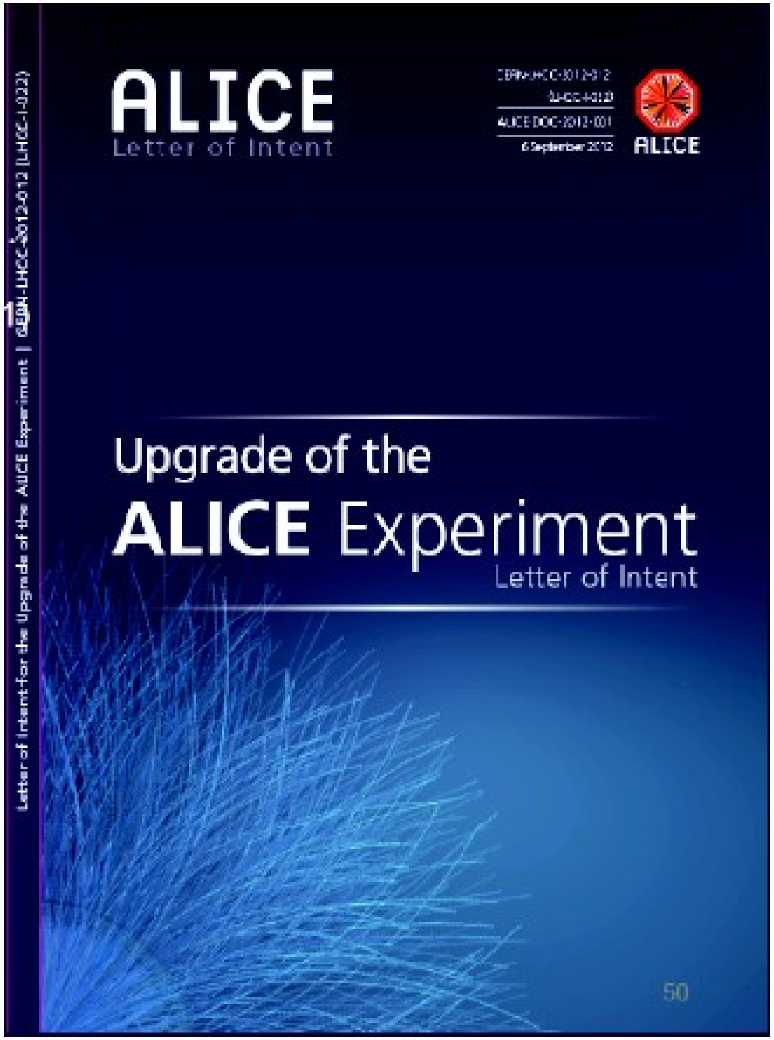

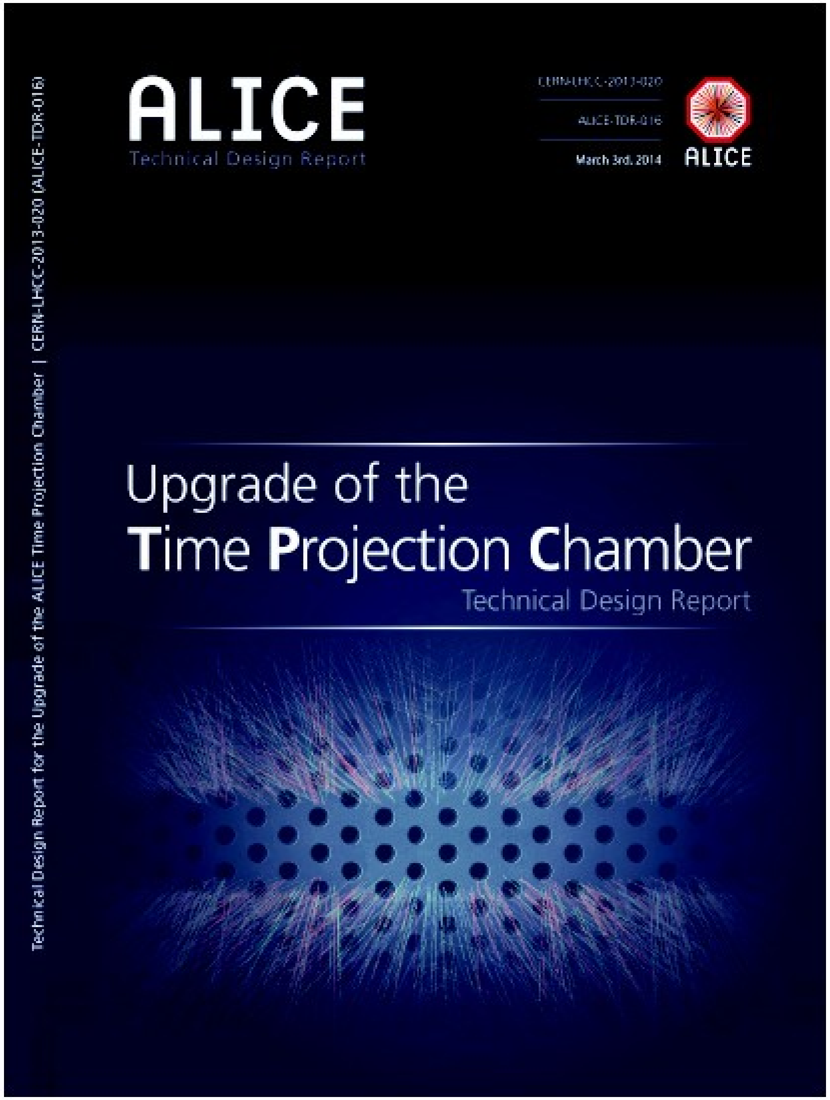

ALICE

UNDER APPROVAL PROCESS BY ALICE

CERN-LHCC-2014-XXX
1st November 2014

Technical Design Report for the Muon Forward Tracker

The ALICE Collaboration*

Abstract

The ALICE physics program after LS2 is mostly devoted to high precision measurements of hard probes (heavy-flavour hadrons, quarkonia, photons and jets). The approved strategy of the associated upgrade programme is reported in the ALICE Letter of Intend [1, 2]. The present Technical Design Report describes the Muon Forward Tracker (MFT). The MFT will allow ALICE to extend the precision measurements of the QGP fundamental properties towards the forward rapidity region. The MFT will substantially improve the present performance of the MUON spectrometer and eliminate its limitations on the measurement of open charm, open beauty, charmonium and low mass vector mesons. The MFT consists of two half-cones containing 5 detection half-disks placed along the beams axis between -460 mm to -768 mm away from the average position of the ALICE interaction point. The MFT acceptance coverage in pseudo-rapidity is $-3.6 < \eta < -2.5$. The basic detection element is a silicon pixel sensor, developed by the ALICE pixel groups for both ITS and MFT. The 896 silicon pixel sensors of the MFT will be assembled, using the same technology as the one used for the ITS assembly, on 280 ladders of 1, 2, 3, 4 or 5 sensors each. A read-out electronics, common to both ITS and MFT, is developped jointly by the two projects.

*see list of authors in App. A

Additional slides

The thermal model and loosely bound, fragile objects

successful description of production yields for d, d_bar, 3He hypertriton, …
implies no entropy production after chemical freeze-out

hypertriton binding energy is 130 keV << T_chem = 156 MeV

use relativistic nuclear collision data and thermal model predictions to search for exotic objects

A. Andronic, P. Braun-Munzinger, J. Stachel, H. Stoecker, Production of light nuclei, hypernuclei and their antiparticles in relativistic nuclear collisions, Phys. Lett. B697 (2011) 203, arXiv:1010.2995 [nucl-th].

see also Pal and Greiner, Phys. Rev. C87 (2013) 034608

The thermal model and loosely bound, fragile objects

successful description of production yields for d, d_bar, 3He hypertriton, …
implies no entropy production after chemical freeze-out

hypertriton binding energy is 130 keV << T_chem = 156 MeV

use relativistic nuclear collision data and thermal model predictions to search for exotic objects

A. Andronic, P. Braun-Munzinger, J. Stachel, H. Stoecker, Production of light nuclei, hypernuclei and their antiparticles in relativistic nuclear collisions, Phys. Lett. B697 (2011) 203, arXiv:1010.2995 [nucl-th].

see also Pal and Greiner, Phys. Rev. C87 (2013) 034608

Some historical context on cluster production in relativistic nuclear collisions

P.J. Siemens and J.I. Kapusta, Phys. Rev. Lett. 43 (1979) 1486.

here the provocative statement was made that cluster formation probability is determined by the entropy of the fireball in its compressed state, i.e. for example:
entropy/baryon is proportional to -ln(d/p)

ENTROPY AND CLUSTER PRODUCTION IN NUCLEAR COLLISIONS

László P. CSERNAI* and Joseph I. KAPUSTA

PHYSICS REPORTS (Review Section of Physics Letters) 131, No. 4 (1986) 223–318.

Very concise summary, including an elucidation of the relation between thermal fireball model and coalescence model

The 'snowball in hell' story

Production of strange clusters and strange matter in nucleus-nucleus collisions at the AGS

P. Braun-Munzinger, J. Stachel (SUNY, Stony Brook). Dec 1994. 9 pp.

Published in J.Phys. G21 (1995) L17-L20

In conclusion, the fireball model based on thermal and chemical equilibrium describes cluster formation well, where measured. It gives results similar in magnitude to the predictions of the coalescence model developed recently [6] to estimate production probabilities for light nuclear fragments (p, d, t, α ...) and for for strange hadronic clusters (such as the H dibaryon) in Au-Au collisions at the AGS. Predicted yields for production of strange matter with baryon number larger than 10 are well below current experimental sensitivities.

Thermal vs coalescence model predictions for the production of loosely bound objects in central Au—Au collisions

A.J. Baltz, C.B. Dover, et al.,
Phys. Lett. B315 (1994) 7

	Thermal Model		
Particles	T=.120 GeV	T=.140 GeV	Coalescence Model
d	15	19	11.7
t+^{3}He	1.5	3.0	0.8
α	0.02	0.067	0.018
H_0	0.09	0.15	0.07
${}^{5}_{\Lambda\Lambda}\mathrm{H}$	$3.5 \cdot 10^{-5}$	$2.3 \cdot 10^{-4}$	$4 \cdot 10^{-4}$
${}^{6}_{\Lambda\Lambda}\mathrm{He}$	$7.2 \cdot 10^{-7}$	$7.6 \cdot 10^{-6}$	$1.6 \cdot 10^{-5}$
${}^{7}_{\Xi^0\Lambda\Lambda}\mathrm{He}$	$4.0 \cdot 10^{-10}$	$9.6 \cdot 10^{-9}$	$4 \cdot 10^{-8}$
${}^{10}_{1}\mathrm{St}^{-8}$	$1.6 \cdot 10^{-14}$	$7.3 \cdot 10^{-13}$	
${}^{12}_{1}\mathrm{St}^{-9}$	$1.6 \cdot 10^{-17}$	$1.7 \cdot 10^{-15}$	
${}^{14}_{1}\mathrm{St}^{-11}$	$6.2 \cdot 10^{-21}$	$1.4 \cdot 10^{-18}$	
${}^{16}_{2}\mathrm{St}^{-13}$	$2.4 \cdot 10^{-24}$	$1.2 \cdot 10^{-21}$	
${}^{20}_{2}\mathrm{St}^{-16}$	$9.6 \cdot 10^{-31}$	$2.3 \cdot 10^{-27}$	

P. Braun-Munzinger, J. Stachel, J. Phys. G **28** (2002) 1971 [arXiv:nucl-th/0112051]

J.Phys. G21 (1995)
L17-L20

deuterons and anti-deuterons also well described at AGS energy

14.6 A GeV/c central Si + Au collisions and GC statistical model

P. Braun-Munzinger, J. Stachel, J.P. Wessels, N. Xu, PLB 1994

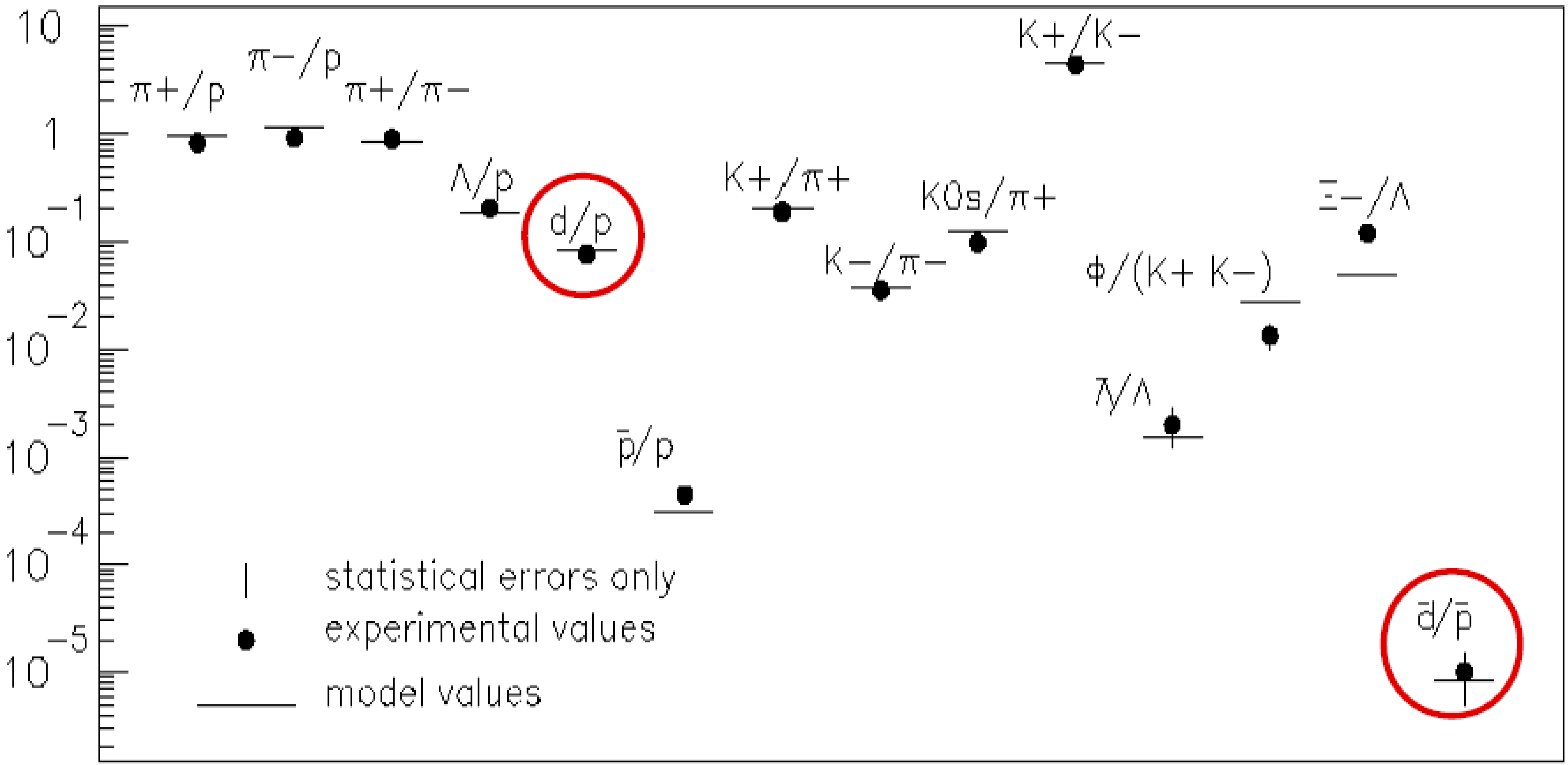

dynamic range: 9 orders of magnitude! No deviation

Thermal model and production of light nuclei at AGS energy

<u>data cover 10 oom!</u>
addition of every nucleon
-> penalty factor $R_p = 48$
but data are at very low pt
use m-dependent slopes following
systematics up to deuteron
-> $R_p = 26$

<u>GC statistical model:</u>

$R_p \approx \exp[(m_n \pm \mu_b)/T]$
for T=124 MeV and μ_b= 537 MeV
$R_p = 24$ good agreement
also good for **antideuterons**:
data: $R_p = 2 \pm 1 \cdot 10^5$ SM: $1.3 \cdot 10^5$

P. Braun-Munzinger, J. Stachel,
J. Phys. G28 (2002) 1971

E864 Coll., Phys. Rev. C61 (2000) 064908

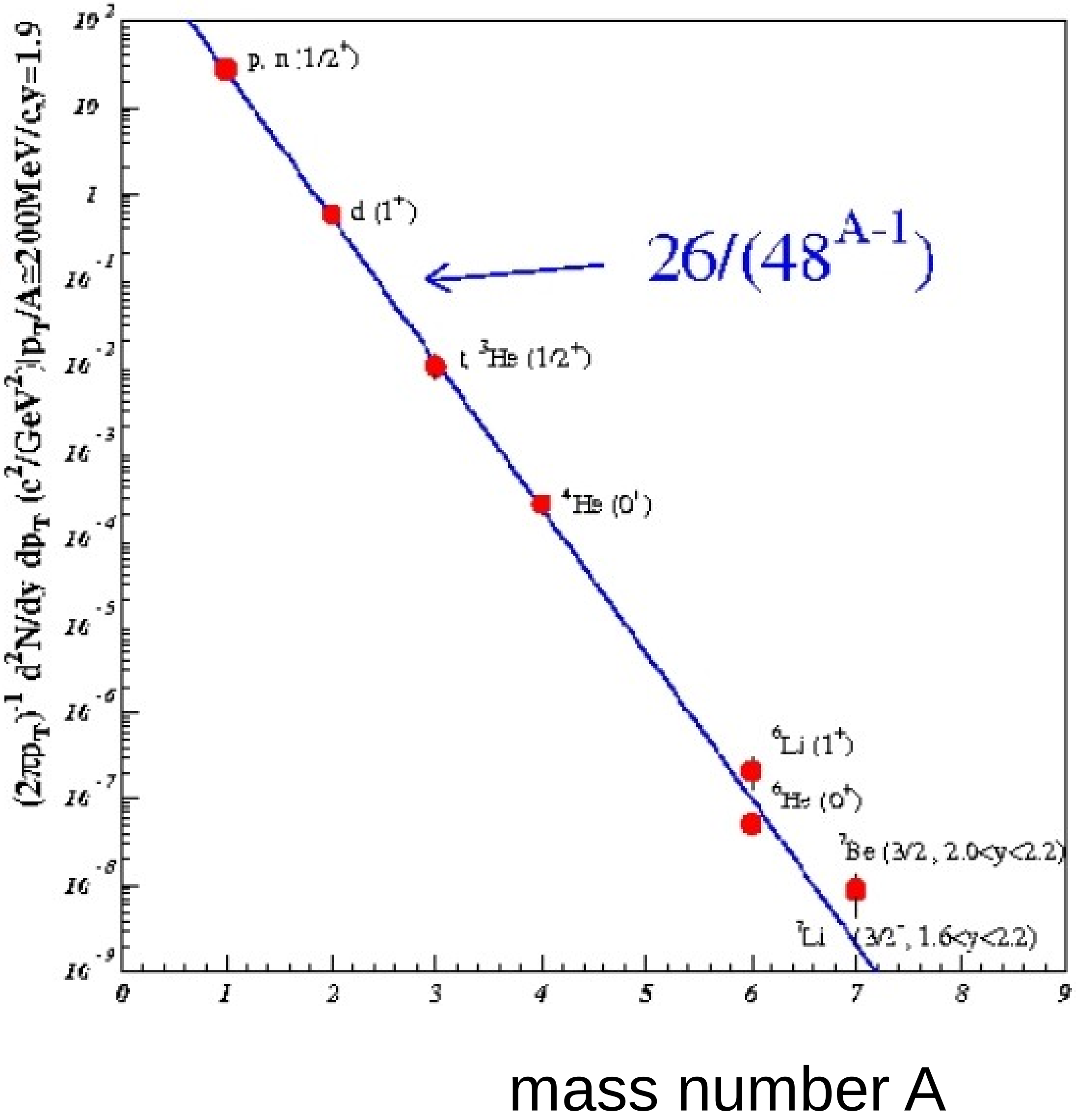

Production of light anti-nuclei at LHC energy

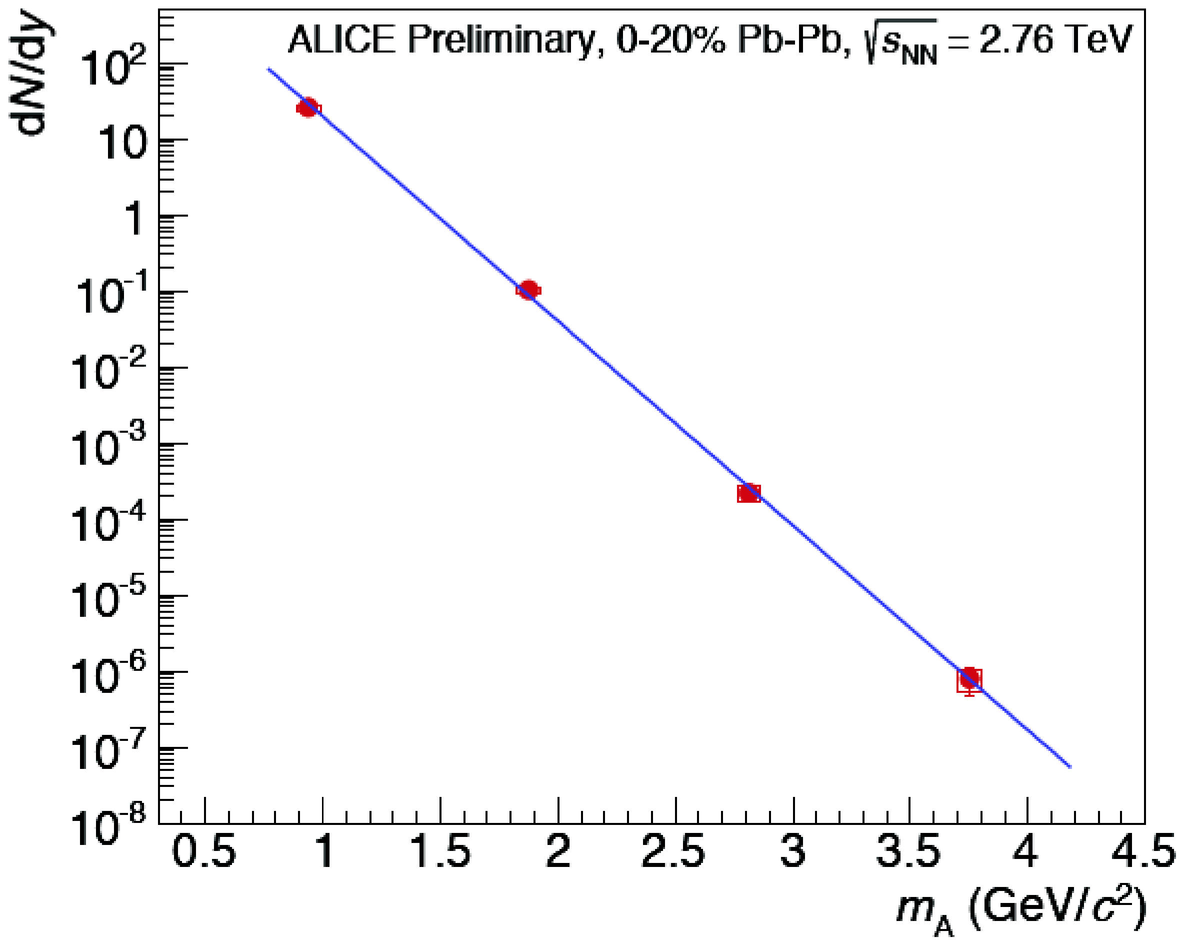

penalty factor exp{-m/T} ≈ 330

Cluster production and entropy

S = s V = -const ln(d/p)

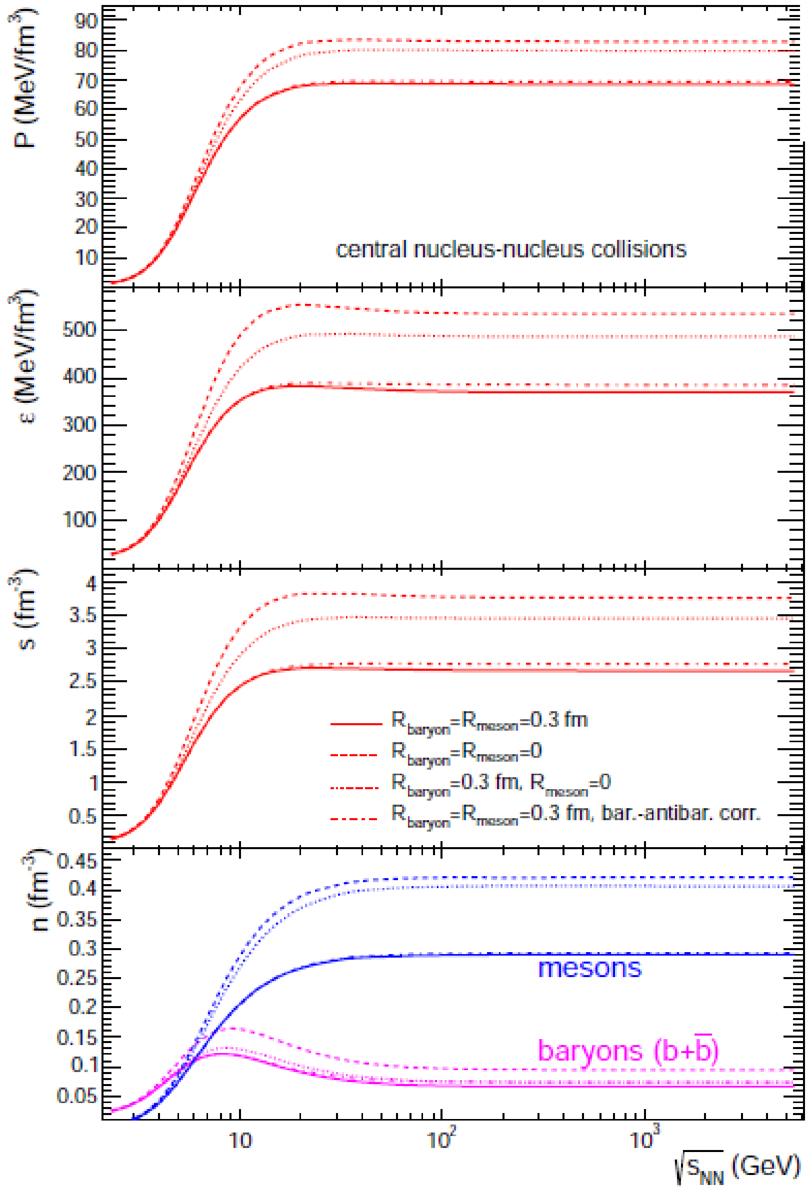

Interacting hadron resonance gas meets lattice QCD

arXiv:1201.0693

A. Andronic[a,b], P. Braun-Munzinger[a,c,d,e], J. Stachel[f], M. Winn[f]

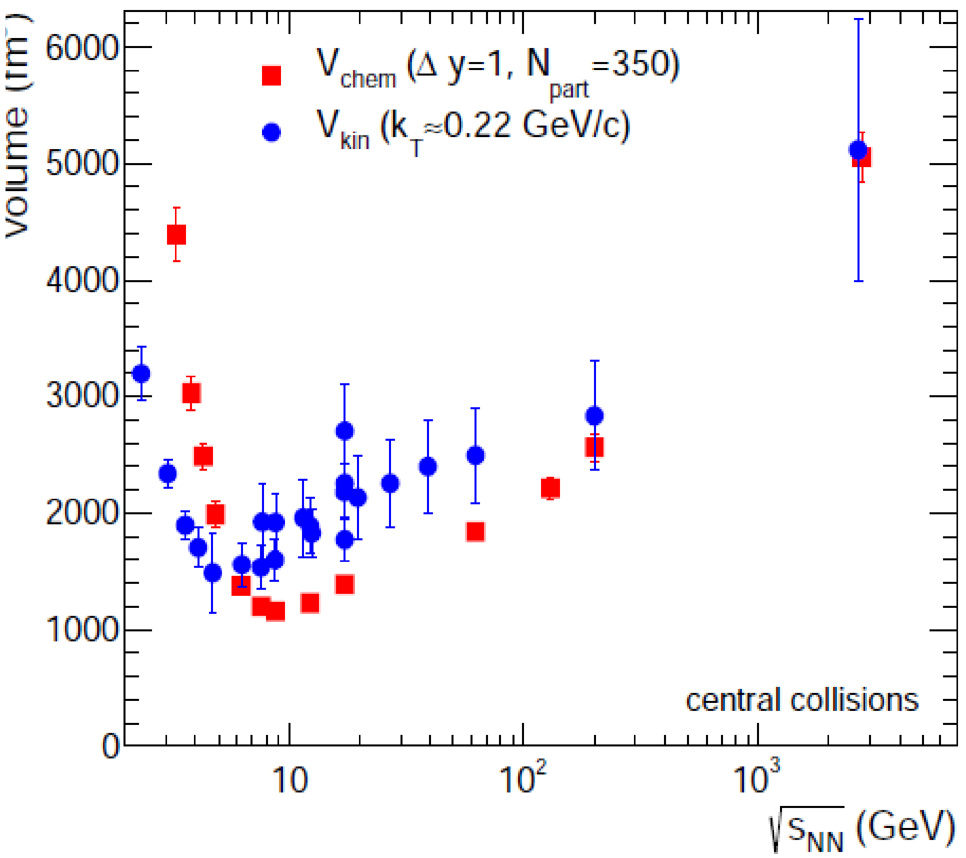

energy dependence of d/p ratio and thermal model prediction

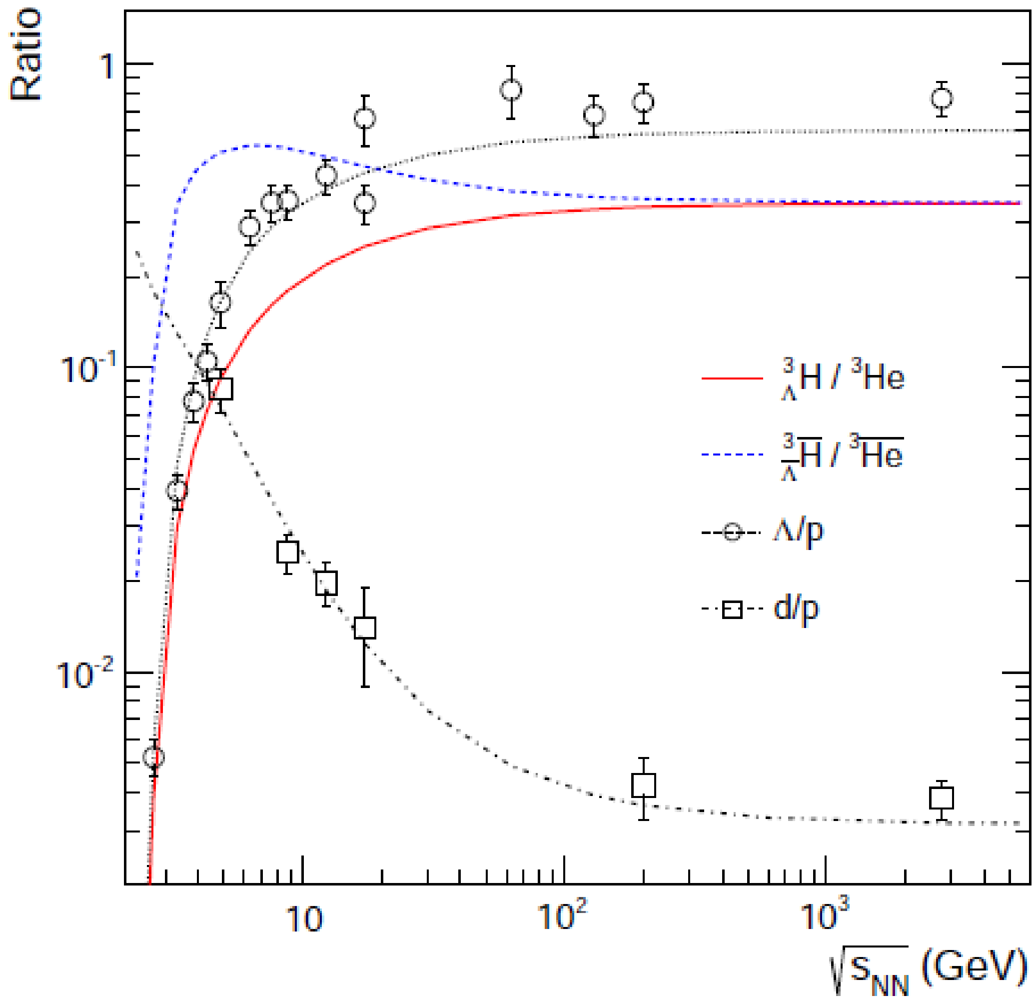

agreement between thermal model calculations and data from Bevalac/SIS18 to LHC energy

A. Andronic, P. Braun-Munzinger, J. Stachel, H. Stoecker, Phys. Lett. B697 (2011) 203, arXiv:1010.2995 [nucl-th].

loosely bound objects are formed at chemical freeze-out very near the phase boundary

implies that chemical freeze-out is followed by an isentropic expansion

no appreciable annihilation in the hadronic phase

loosely bound objects are formed at chemical freeze-out very near the phase boundary

implies that chemical freeze-out is followed by an isentropic expansion

no appreciable annihilation in the hadronic phase

The size of loosely bound molecular objects

Examples: deuteron, hypertriton, XYZ 'charmonium states, molecules near Feshbach resonances in cold quantum gases

Quantum mechanics predicts that a bound state that is sufficiently close to a 2-body threshold and that couples to that threshold through a short-range S-wave interaction has universal properties that depend only on its binding energy. Such a bound state is necessarily a loosely-bound molecule in which the constituents are almost always separated by more than the range. One of the universal predictions is that the root-mean-square (rms) separation of the constituents is $(4\mu E_X)^{-1/2}$, where E_X is the binding energy of the resonance and μ is the reduced mass of the two constituents. As the binding energy is tuned to zero, the size of the molecule increases without bound. A classic example of a loosely-bound S-wave molecule is the deuteron, which is a bound state of the proton and neutron with binding energy 2.2 MeV. The proton and neutron are correctly predicted to have a large rms separation of about 3.1 fm.

Artoisenet and Braaten, arXiv:1007.2868

The deuteron as a loosely bound object

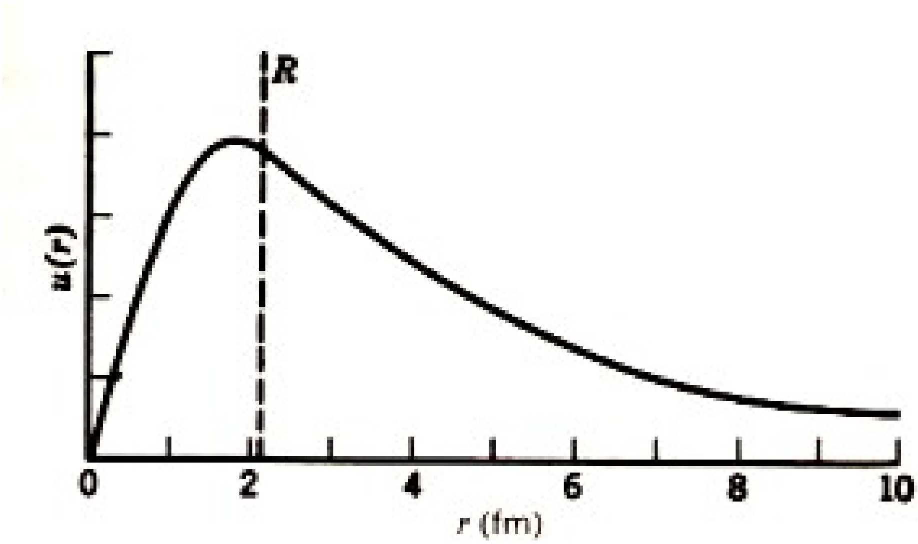

Mass = 1875 MeV
B.E. = 2.23 MeV
rms radius = 3 fm > range of potential

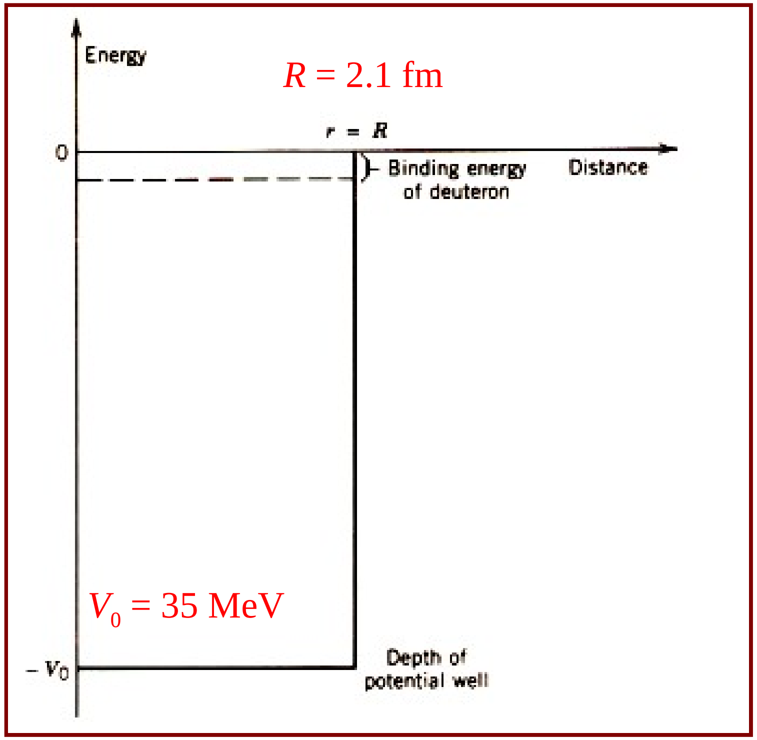

The Hypertriton

mass = 2.990 MeV

B.E. = 0.13 MeV

molecular structure: (p+n) + Lambda

hypertriton is (very close to) an 'Efimov' state

2-body threshold: (p+p+n) + pi- = ^{3}He + pi-

rms radius = (4 B.E. M_{red})$^{-1/2}$ = 10.3 fm = rms separation between d and Lambda

in that sense: hypertriton = (p n Lambda) = (d Lambda) is the ultimate halo state

yet production yield is fixed at 156 MeV temperature (about 1000 x E.B.)

The X(3872)

mass is below threshold of (D^{*0} D^0_{bar}) by (0.42 +/- 0.39) MeV

$D^{*0}\bar{D}^0 + D^0\bar{D}^{*0}$

rms separation = 3.5 – 18.3 fm   structure:

should be able to predict the X(3872) production probability in pp collisions at LHC energy with an accuracy of about 30%, uncertainty is due to not very precisely known number of charm quarks

result ready shortly

where are we?

since QM2012, discrepancy between protons and thermal fit went from 7 sigma to 2.9 (2.7) sigma

T went from 152 to 156.5 MeV

fit without protons yields slighty higher T = 158 MeV, driven by hyperons

where are we?

since QM2012, discrepancy between protons and thermal fit went from 7 sigma to 2.9 (2.7) sigma

T went from 152 to 156.5 MeV

fit without protons yields slighty higher T = 158 MeV, driven by hyperons

important note: corrections for weak decays

All ALICE data do not contain hadrons from weak decays of hyperons and strange mesons – correction done in hardware via ITS inner tracker

The RHIC data contain varying degrees of such weak decay hadrons. This was on average corrected for in previous analyses.

in light of high precision LHC data the corrections done at RHIC may need to be revisited.

treatment of weak decays

fraction of yield from weak decays

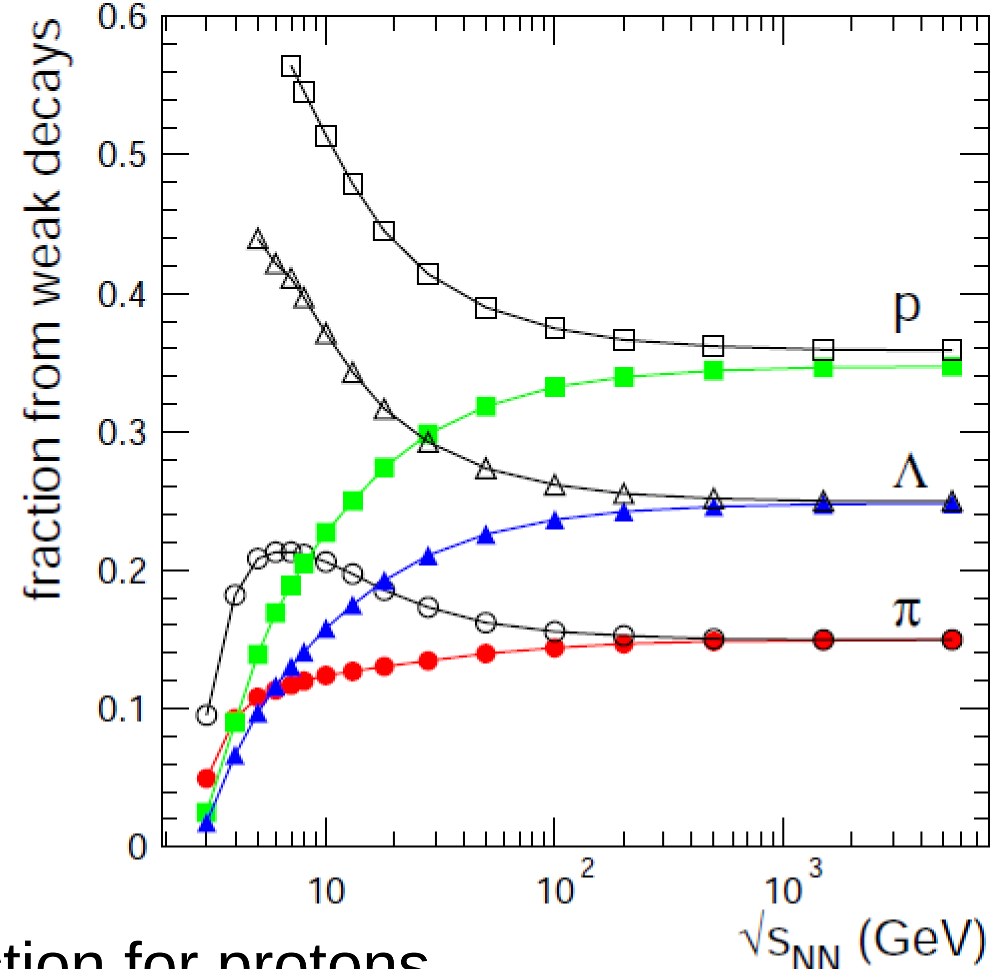

biggest correction for protons
done in hardware (vertex cut) at ALICE
software corrections at all lower energies

Re-evaluation of fits at RHIC energies – special emphasis on corrections for weak decays

Note: corrections for protons and pions from weak decays of hyperons depend in detail on experimental conditions

RHIC hadron data all measured without application of Si vertex detectors

In the following, corrections were applied as specified by the different RHIC experiments

Au+Au central at 200 GeV, all experiments combined

T = 162 Me'

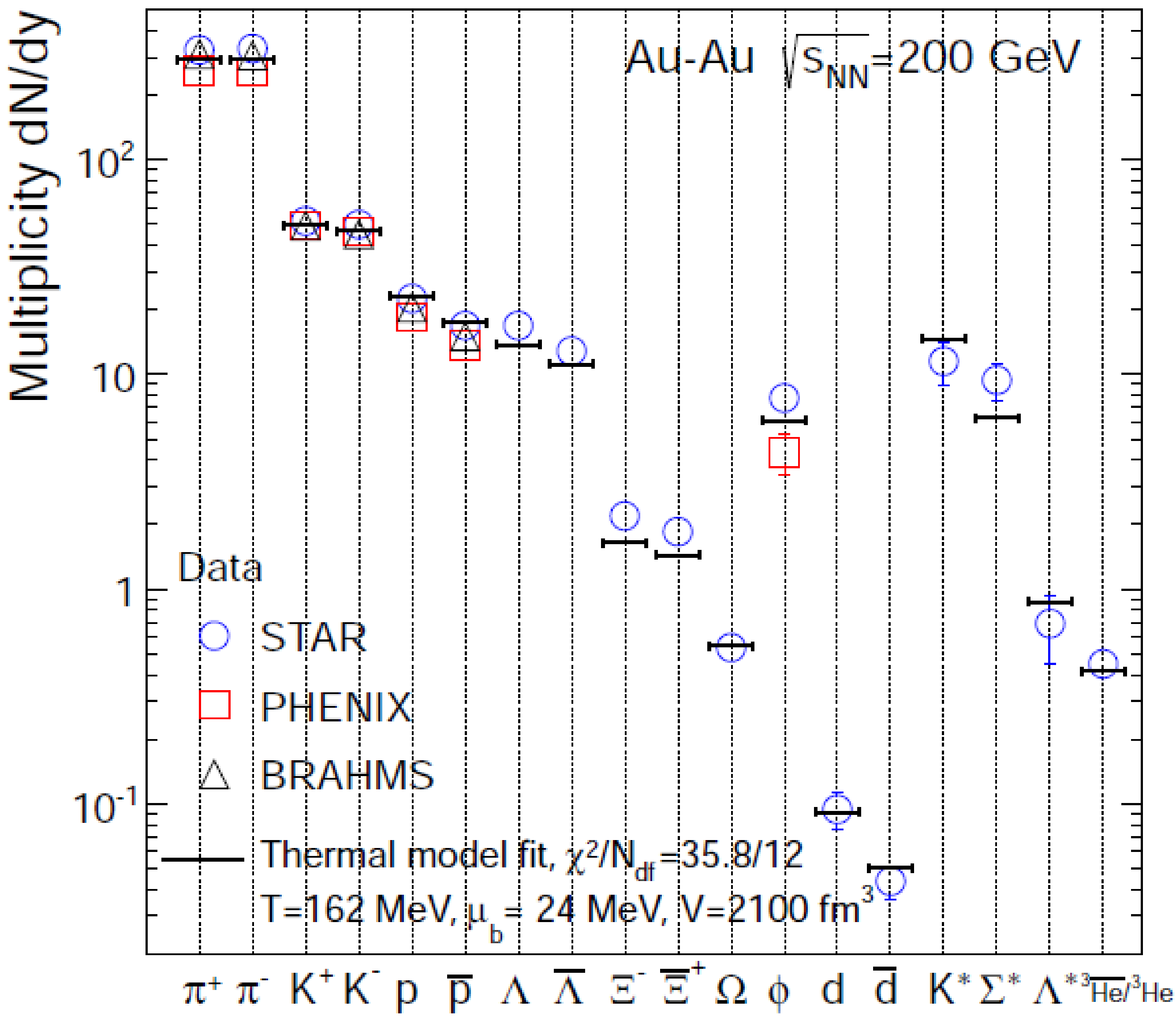

could it be weak decays from charm?

weak decays from charmed hadrons are included in the ALICE data sample

at LHC energy, cross sections for charm hadrons is increased by more than an order of magnitude compared to RHC

first results including charm and beauty hadrons indicate changes of less than 3%, mostly for kaons

not likely an explanation

could it be incomplete hadron resonance spectrum?

Note: because of baryon conservation, adding more baryon resonances will decrease in the model the p/pi ratio

An N* will decay dominantly into 1 N + a number (depending on the N* mass) of pions

Same effect seen in
K/pi ratio because of strangeness conservation

A. Andronic, P. Braun-Munzinger, J. Stachel, Thermal hadron production in relativistic nuclear collisions: the sigma meson, the horn, and the QCD phase transition, Phys. Lett. **B673** (2009) 142, erratum ibid. **B678** (2009) 516, arXiv:0812.1186.

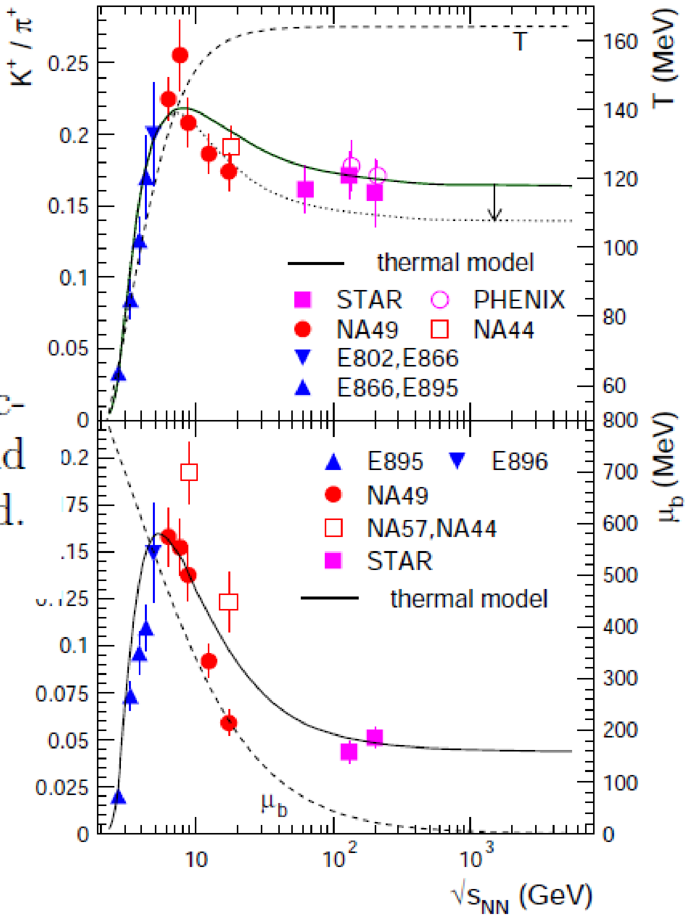

could it be proton annihilation in the hadronic

F. Becattini et al., Phys. Rev. C85 (2012) 044921 and arXiv: 1212.2431

- need to incorporate detailed balance, 5pi → p p_bar not included in current Monte Carlo codes (RQMD)

- taking detailed balance into account reduces effect strongly, see Rapp and Shuryak 1998

- see also W. Cassing, Nucl. Phys. A700 (2002) 618 and recent reanalysis, by Pan and Pratt, arXiv:

- agreement with hyperon data would imply strongly reduced hyperon annihilation cross section with anti-baryons → no evidence for that

centrality dependence of proton/pion ratio

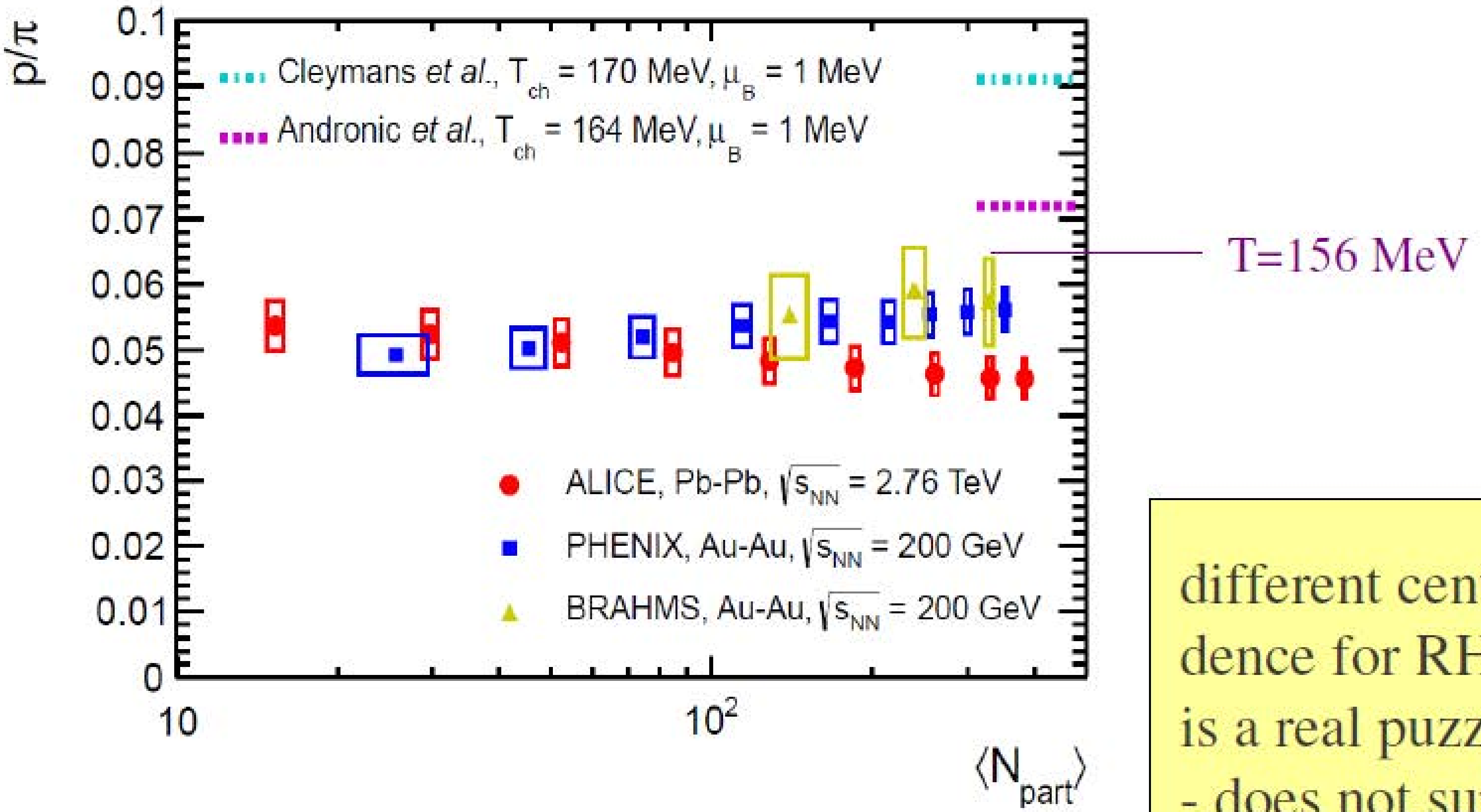

different centrality dependence for RHIC and LHC is a real puzzle
- does not support annihilation picture
- is it real? physics origin?

the 'proton anomaly' and production of light nuclei

can the measurement of d, t, 3He and 4He settle the issue?
what about hypertriton?

important to realize: production yield of deuterons is fixed at $T = T_{chem} = 156$ MeV even if $E_B(d) = 2.23$ MeV!

entropy/baryon is proportional to $-\ln(d/p)$ and is conserved after T_{chem}

good agreement with LHC d and hyper-triton yield implies: there is no shortage of protons and neutrons at chemical freeze-out, inconsistent with annihilation scenario

Nuclear collisions, open and hidden charm hadrons, and QCD

Hadrons containing charm quarks can also be described provided open charm cross section is known

Recent ALICE data imply Debye screening near T_c for charmonium and deconfined heavy quarks, see talk by Johanna Stachel

Could it be that increasing number of charm quarks changes (lowers) T_c?
An issue for the FCC!

Quarkonium Properties and Debye Screening

state	J/ψ	χ_c	ψ'	Υ	χ_b	Υ'	χ_b'	Υ''
mass [GeV]	3.10	3.53	3.68	9.46	9.99	10.02	10.26	10.36
ΔE [GeV]	0.64	0.20	0.05	1.10	0.67	0.54	0.31	0.20
ΔM [GeV]	0.02	-0.03	0.03	0.06	-0.06	-0.06	-0.08	-0.07
radius [fm]	0.25	0.36	0.45	0.14	0.22	0.28	0.34	0.39

table from H. Satz, J. Phys. G32 (2006) R25

In the QGP, the screening radius $r_{Debye}(T)$ decreases with increasing T. If $r_{Debye}(T) < r_{charmonium}$ the system becomes unbound $\rightarrow$ suppression compared to charmonium production without QGP. The screening radius can be computed using potential models or solving QCD on the lattice.

Charmonium production at LHC energy: deconfinement,and color screening

- Charmonia formed at the phase boundary → full color screening at T_c

- Debye screening length < 0.4 fm near T_c

- Combination of uncorrelated charm quarks into J/psi → deconfinement

statistical hadronization picture of charmonium production provides
most direct way towards information on the degree of deconfinement reached
as well as on
color screening and the question of bound states in the QGP

Debye mass, LQCD, and J/psi data

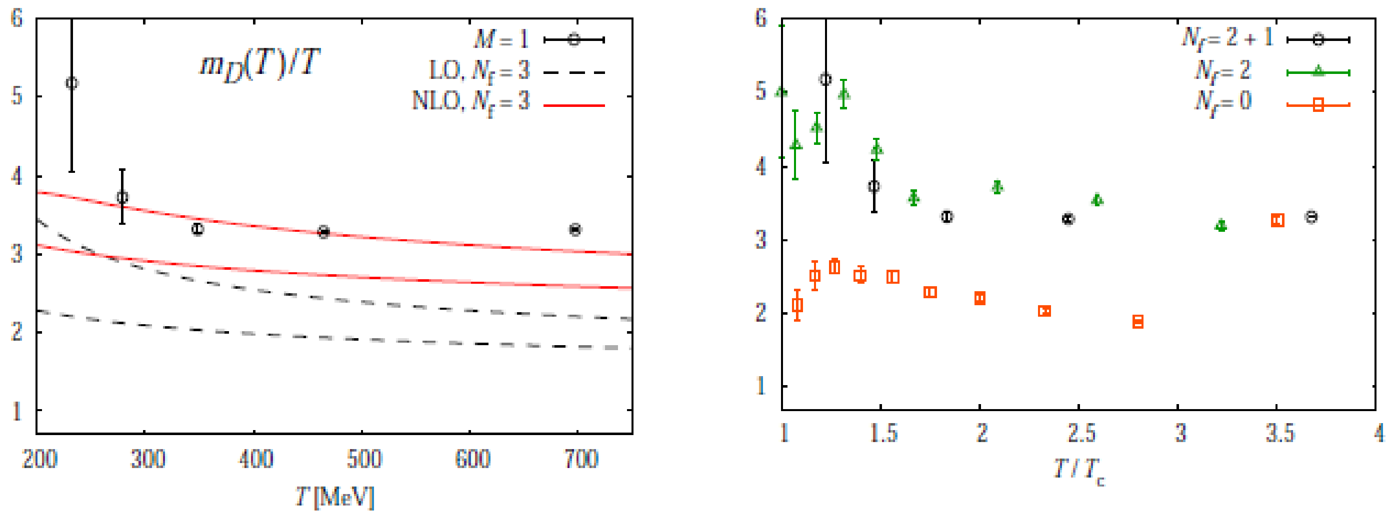

Fig. 6. (Left) The Debye screening mass on the lattice in the color-singlet channel together with that calculated in the leading-order (LO) and next-to-leading-order (NLO) perturbation theory shown by dashed-black and solid-red lines, respectively. The bottom (top) line expresses a result at $\mu = \pi T$ $(3\pi T)$, where μ is the renormalization point. (Right) Flavor dependence of the Debye screening masses. We assume the pseudo-critical temperature for $2+1$-flavor QCD as $T_c \sim 190$ MeV.

arXiv:1112.2756 WHOT-QCD Coll.

from J/psi data and statistical hadronization analysis: $m_{Debye}/T > 3.3$

at T = 0.15 GeV

energy dependence of d/p ratio and thermal model prediction

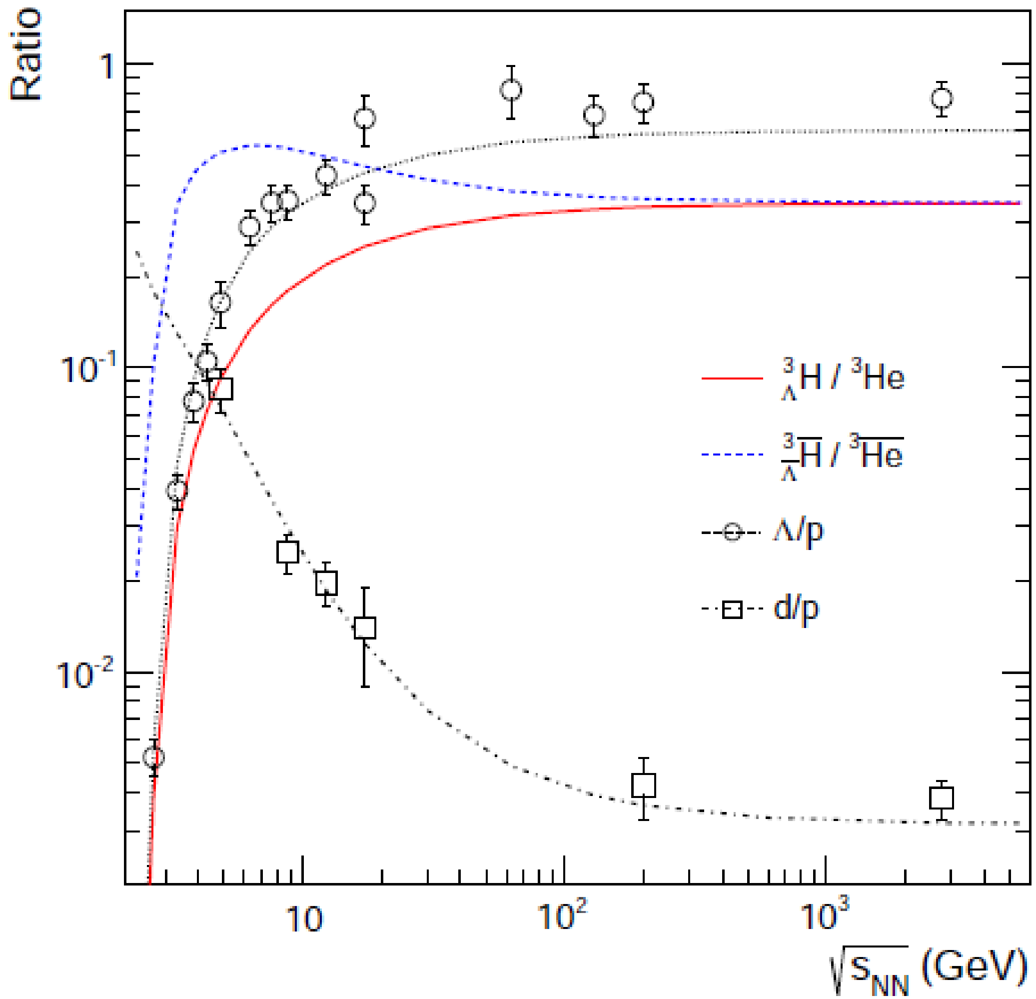

agreement between thermal model calculations and data from Bevalac/SIS18 to LHC energy

A. Andronic, P. Braun-Munzinger, J. Stachel, H. Stoecker, Phys. Lett. B697 (2011) 203, arXiv:1010.2995 [nucl-th].

ALICE TRD Detector complete Nov. 26, 2014

first fully operational barrel TRD
project coordination: Heidelberg

Quarkonia:

heavy quark bound states stable under strong decay

heavy: charm ($m_c \simeq 1.3$ GeV) or beauty ($m_b \simeq 4.7$ GeV)

stable: $M_{c\bar{c}} \leq 2M_D$ and $M_{b\bar{b}} \leq 2M_B$

heavy quarks $\Rightarrow$ quarkonium spectroscopy via non-relativistic potential theory

Schrödinger equation $\left\{2m_c - \frac{1}{m_c}\nabla^2 + V(r)\right\}\Phi_i(r) = M_i\Phi_i(r)$

confining ("Cornell") potential $V(r) = \sigma\ r - \frac{\alpha}{r}$

string tension $\sigma \simeq 0.2$ GeV^2, gauge coupling $\alpha \simeq \pi/12$

$\Rightarrow$ quarkonium masses M_i and radii r_i

Complete angular (pseudo-rapidity) distributions

complete angular distr. between 1 and 179 deg

excellent pseudo-rapidity coverage

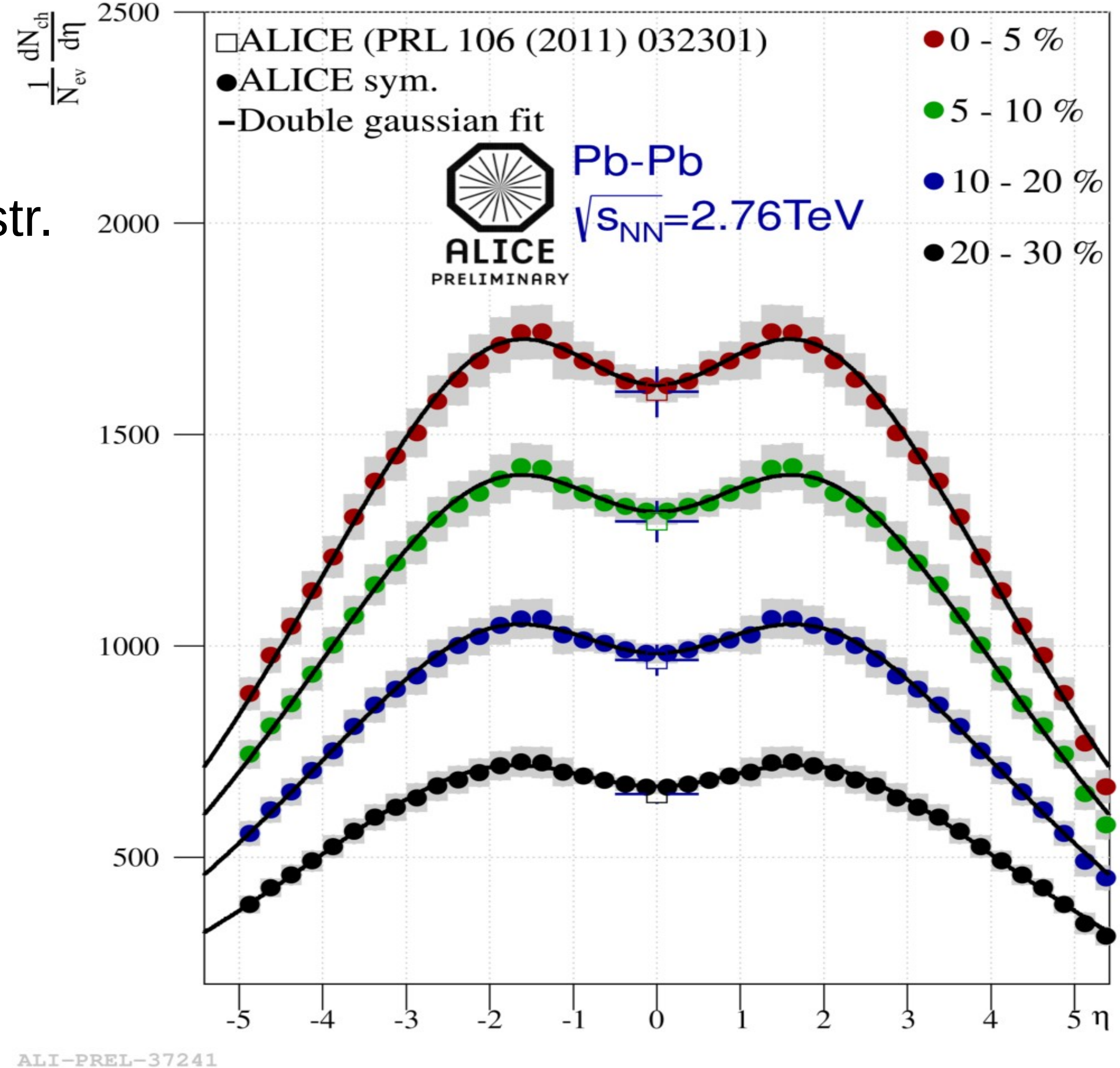

Charged particle multiplicity in pp, pPb and central PbPb collisions

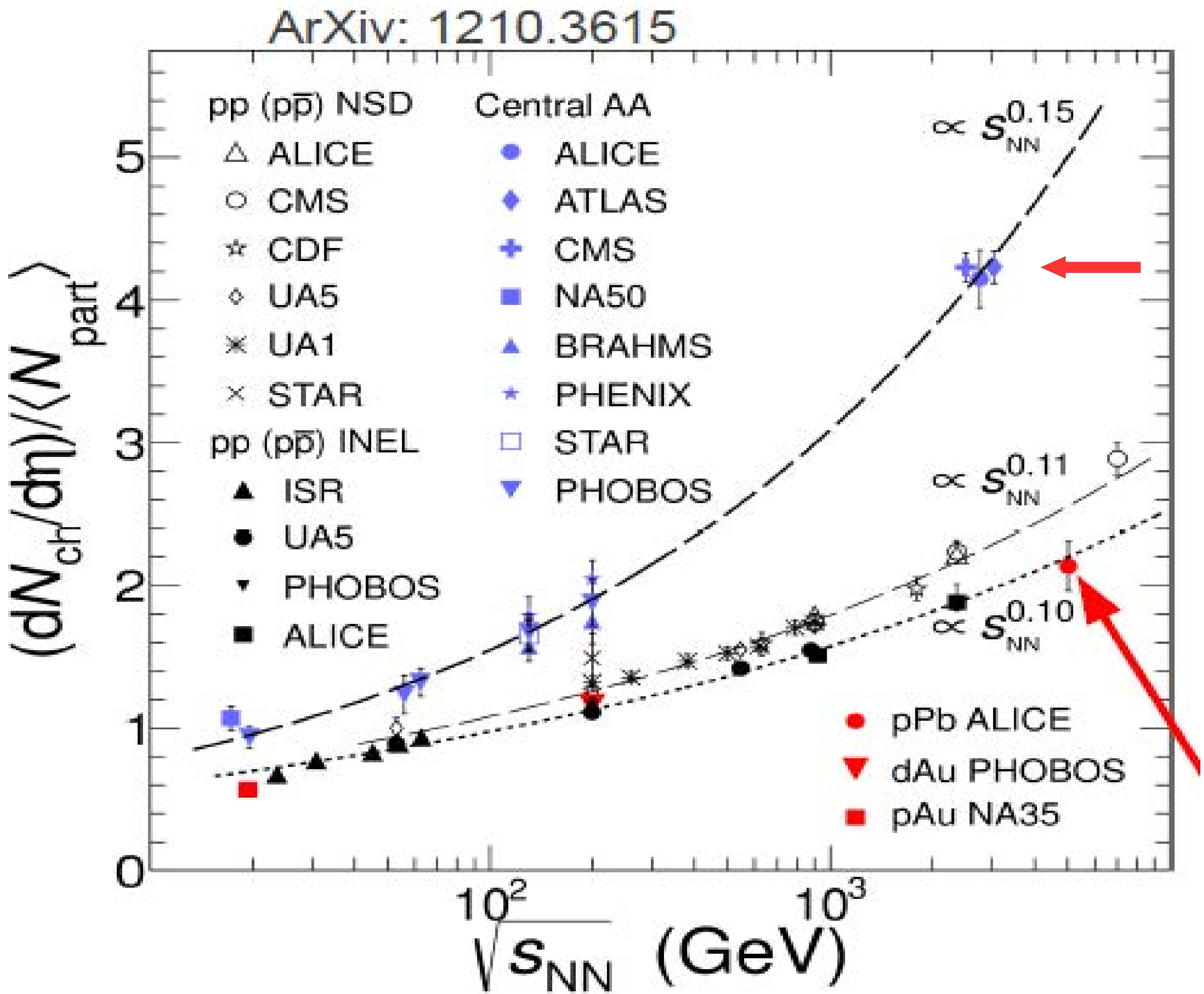

increase with beam energy significantly steeper than in pp

pPb similar to pp inelastic

can the fireball formed in central nuclear collisions be considered matter in equilibrium?

Phys. Rev. Lett. 105(2010)252301